Master's thesis

NTNU
Norwegian University of Science and Technology
Faculty of Natural Sciences
Department of Physics

Nora Sofie Thesen Laeskogen

Comparing Automatic Treatment Planning with Helical Tomotherapy and VMAT for Locally Advanced Cervical Cancer

Master's thesis in Applied Physics and Mathematics
Supervisor: Anne Beate Langeland Marthinsen
Co-supervisor: Josefine Ståhl-Kornerup
June 2023

NTNU
Norwegian University of Science and Technology

ST. OLAVS HOSPITAL
UNIVERSITETSSYKEHUSET I TRONDHEIM

Nora Sofie Thesen Laeskogen

Comparing Automatic Treatment Planning with Helical Tomotherapy and VMAT for Locally Advanced Cervical Cancer

Master's thesis in Applied Physics and Mathematics
Supervisor: Anne Beate Langeland Marthinsen
Co-supervisor: Josefine Ståhl-Kornerup
June 2023

Norwegian University of Science and Technology
Faculty of Natural Sciences
Department of Physics

NTNU
Norwegian University of
Science and Technology

Preface

This master thesis is written as a part of the study program Biophysics and medical technology at the Norwegian University of Science and Technology (NTNU) in Trondheim. It was carried out at the radiotherapy department at St. Olavs Hospital in Trondheim during the spring semester of 2023. This project thesis aimed to apply helical tomotherapy in an automatic treatment planning script developed for volumetric modulated arc therapy. Plans for locally advanced cervical cancer were used for plan quality comparison between the two treatment modalities. The motivation was to look into the HT as an alternative treatment option in the clinic for treatment of LACC patients.

I want to thank my supervisor at the Department of Physics, Adjunct Associate Professor and Medical Physicist Anne Beate Langeland Marthinsen for good theoretical discussions, guidance and feedback during the writing of the thesis, organising meetings, having patience and always believing in me.

Thanks to my supervisor at St. Olavs Hospital, Medical Physicist Josefine Ståhl-Kornerup, for her enthusiasm and being an instigator for the project, as well as wonderful guidance on treatment planning in RayStation, and valuable feedback and academic discussion throughout this whole project.

I also want to thank Medical Physicist Marit Funderud, at St. Olavs Hospital, for access to the automatic planning script, as well as guidance on scripting for RayStation.

Finally, thanks to my good friends at Physics and Mathematics and other studies at NTNU for for five unforgettable years and all the lunch breaks, and social and academic discussions. I want to thank my family for always supporting me, and their encouraging words.

Nora Sofie Thesen Laeskogen
June 2023

Abstract

Purpose: This project aimed to apply helical tomotherapy (HT) in an automatic treatment planning script used in the clinic for treatment planning with volumetric modulated arc therapy (VMAT) in the treatment planning system (TPS) RayStation at St. Olavs Hospital. Plans for locally advanced cervical cancer (LACC) were used for plan quality comparison between the two treatment modalities.

Materials and Method: Treatment plans were generated for 10 LACC patients. LACC was mainly chosen because of its often large and intricate shape of the target volume and often several dose levels, planned as simultaneously integrated boost (SIB) doses. Adjustments of the script were made to employ HT as an alternative delivery technique in the TPS. The structure of the treatment planning optimization was unaffected. By using the same planning script for both RT techniques, an unbiased method for dose planning comparison was ensured. Several HT treatment plans were made with different beam optimization parameters. The automatic HT plans were compared quantitatively to the reference plans through dose statistics extracted from RayStation. The plans were qualitatively compared by visual evaluation performed together with physicists in the clinic.

Results: Visual evaluation of the script-based treatment plans revealed that HT plans were generally of lower quality than those made for VMAT. By combining visual and quantitative evaluation of the treatment plans it was observed that HT plans had a lower boost dose conformity, the appearance of hot spots in organs at risk (OARs) overlapping with target volumes and extensive spread of lower dose levels outside of target volumes. Additionally, dose statistics revealed that for both treatment modalities, the dose coverage to target volumes were sufficient, while the portion of OAR located outside of the target volumes generally received higher doses in the HT plans. The dose distribution in main target volume was similar or less homogeneous than for the reference plans. The script-based HT plans failed to meet the necessary criteria for a clinically acceptable dose distribution when compared to the reference VMAT plans.

Conclusion: The automatic planning script is not suitable for generating clinical LACC plans for treatment with HT, without further adjustments.

Sammendrag

Hensikt: Dette prosjektet hadde til hensikt å anvende helikal tomoterapi (HT) i et automatisk skript for behandlingsplanlegging brukt i klinikken på St. Olavs Hospital for planlegging med volumetric modulated arc therapy (VMAT) i behandlingsplanleggingssystemet (TPS) RayStation. Behandlingsplaner for (lokalt avansert) livmorhalskreft (LACC) ble brukt for sammenligning av plankvalitet av de to behandlingsmodalitetene.

Materialer og metode: Behandlingsplaner ble generert for 10 LACC-pasienter. LACC ble valgt på grunnlag av den kompliserte formen og store størrelsen på målvolumet, og ofte med flere dosenivåer, behandlet som simultanintegrerte boostdoser (SIB). Justeringer av skriptet ble gjort for å kunne anvende HT som en alternativ behandlingsteknikk i TPS. Strukturen av skriptene for optimaliseringen av behandlingsplanene forble upåvirket. Ved å bruke samme planleggingsskript for begge RT-teknikkene, ble det sikret en objektiv metode for sammenligning av doseberegningene. Det ble laget HT-planer med ulike optimaliseringsparametere. De automatiske HT-planene ble sammenlignet kvantitativt med referanseplanene gjennom dosestatistikk hentet fra RayStation. Planene ble kvalitativt sammenlignet ved visuell evaluering utført sammen med fysikere i klinikken.

Resultater: En visuell evaluering av de skriptbaserte behandlingsplanene viste at HT-planene generelt var av dårligere kvalitet enn referanseplanene laget for VMAT. Ved å kombinere visuell og kvantitativ evaluering av behandlingsplanene ble det observert at HT-planer hadde en lavere boostdosekonformitet, høyere forekomst av hot spots i risikoorganer (OARs) som overlappet med målvolumer og omfattende spredning av lavere dosenivåer utenfor målvolumene. I tillegg viste dosestatistikken at dosedekningen til målvolumene var tilstrekkelig for begge behandlingsmodaliteter, mens andelen av OAR som lå utenfor målvolumene generelt fikk høyere doser i HT-planene. Dosefordelingen i hovedmålvolumene var lik eller mindre homogen enn for referanseplanene. De skriptbaserte HT-planene klarte ikke å oppfylle de nødvendige kriteriene for en klinisk akseptabel dosefordeling sammenlignet med VMAT-referanseplanene.

Konklusjon: Det automatiske planleggingsskriptet er ikke egnet for å generere kliniske planer for behandling av LACC-pasienter med HT, uten ytterligere justeringer for optimalisering.

Abbreviations

3D-CRT	3D Conformal Radiation Therapy
ADC	Adenocarcinoma
ADSC	Adenosquamos Carcinoma
AI	Artificial Intelligence
ART	Adaptive Radiation Therapy
BT	Brachytherapy
CBCT	Cone Beam Computed Tomography
CI	Conformity Index
CN	Conformation Number
CT	Computed Tomography
CTV	Clinical Target Volume
DHI	Dose Homogeneity Index
DSB	Double Strand Break
DTf	Delivery Time Factor
DVH	Dose-Volume Histogram
EBRT	External Beam Radiation Therapy
EUD	Equivalent Uniform Dose
FB	Fallback
FIGO	Inernational Federation of Gynecology and Obstetrics
FW	Field Width
GTV	Gross Tumor Volume
HFS	Head First Supine
HI	Homogeneity Index
HPV	Human Papillomavirus
IGABT	Image Guided Adaptive Brachytherapy
IGRT	Image Guided Radiation Therapy
IM	Internal Margin

IMRT	Intensity Modulated Radiation Therapy
ITV	Internal Target Volume
KB	Knowledge-Based
kV	Kilo Voltage
LACC	Locally Advanced Cervical Cancer
LINAC	Linear Accelerator
LN	Lymph Node
LQ	Linear-Quadratic Model
MF	Modulation Factor
MLC	Multileaf Collimator
MRI	Magnetic Resonance Imaging
MV	Mega Voltage
MVCT	Mega Voltage Computed Tomography
NTCP	Normal Tissue Complication Probability
OAR	Organ at Risk
PET	Positron Emission Tomography
PF	Pitch Factor
PTV	Planning Target Volume
RT	Radiation Therapy
SCC	Squamous Cell Carcinoma
SM	Set-Up Margin
SSB	Single Strand Break
TPS	Treatment Planning System
VMAT	Volumetric Modulated Arc Therapy

Table of Contents

1 Introduction

Radiation therapy (RT) is an essential modality in cancer treatment. RT treatment planning aims to deliver a high radiation dose to cancerous tissue while limiting the radiation dose to surrounding organs at risk (OARs). Its efficiency is dependent on the precision of the radiation delivery to achieve this aim [1]. A linear accelerator (linac) is the most commonly used radiation delivery system for external beam radiation therapy (EBRT) that uses high energy photon radiation that can be delivered form different angles around the patient adapted to actual target volume by multi-leaf collimators (MLCs). Intensity-modulated radiation therapy (IMRT) is a high precision technique that uses computer controlled linacs to deliver precise radiation doses to a tumor by modulating the intensity of the radiation with MLC positioning [2]. Volumetric modulated arc therapy (VMAT) is an advanced type of IMRT in which the gantry and the positioning of the MLCs are in continuous movement during irradiation. IMRT and VMAT are two modern RT techniques that allow complex treatment plans to be created by providing a set of objectives that a computer algorithm will attempt to fulfill by inverse optimization [3]. In such inverse planning, the input parameters are a set of dose objectives, while the output is the calculated photon-fluence, as well as MLC positions and movements required to meet the dose objectives [4]. This is a computationally heavy process that requires a computerized treatment planning system (TPS). Helical tomotherapy (HT) is a form of RT that combines the features of a linac and a helical computed tomography (CT) scanner. As a modality for delivering rotational therapy, HT system delivers intensity-modulated fan beams in a helical pattern while the couch is translated through a continuously rotating gantry [5]. While both the linac and the tomotherapy system aim to deliver radiation to the target tissue, they differ in their delivery methods, resulting in different treatment dose distributions.

RT using linacs and IMRT or VMAT techniques are considered standard treatment technology, but in recent years the development of tomotherapy machines has been documented to achieve satisfactory target dose coverage and conformity, as well as high-dose homogeneity, and has been reported to be comparable to VMAT for treatment of different cancer types [6, 7, 8, 9]. Due to different beam arrangement and considerations of tomo-specific parameters, treatment planning for tomotherapy differs from that of a treatment with a standard linac.

In recent years, automation of RT treatment planning has been seen due to the increase in use of advanced technology for automation of treatment planning, such as implementation involving the use of deep learning and artificial intelligence (AI) [10]. This progression been seen for both IMRT and VMAT different cancer types and localizations [11, 12, 13]. At St. Olavs Hospital, RT with VMAT is standard treatment for nearly all tumor localizations. These plans are generally made manually with various user-selected objectives set up by the treatment planner, in order to achieve the clinically defined OAR dose limits, i.e. clinical goals. In 2021, St. Olavs Hospital implemented an in-house-developed automatic

dose planner mimicking solution for breast and prostate cancer in the clinic. The automatic script based method was initiated and developed by Marit Funderud, Jomar Frengen and Sigrun Saur Almberg at the RT department. The automatically made VMAT plans for breast and prostate cancer were of similar or better quality as manually made VMAT plans and significantly reduced the planning time. The following year, the automatic planning script was adapted for cervical cancer in the master project of Ingvild Hoem with supervision from Marit Funderud [14]. Automatic script-based planning with VMAT is currently considered the "golden standard" for radiation treatment planning for locally advanced cervical cancer (LACC) patients at St. Olavs Hospital, which usually only requires the treatment planner to make some minor, if any, manual adjustments to the final script-based plan.

Cervical cancer is one of the most common cancer types among women worldwide and has an associated risk of spreading to nearby lymph nodes (LNs) in the pelvic area. Approximately 45 % of all cervical cancer patients are diagnosed with LN metastases, which is associated with a reduced probability of long-term survival [15]. The standard treatment procedure for LACC patients consists of EBRT, brachytherapy (BT) and chemotherapy. LN metastases should receive an additional external radiation boost. This boost was commonly given sequentially after the EBRT of the primary tumour, but, with modern techniques, EBRT of the primary tumour and the boost of LN may be given simultaneously [16]. Due to the many nearby OARs and different target dose levels for LN metastases, treatment planning for LACC patients is a complicated process. HT could be considered as an alternative RT technique for LACC patients as its enables for long target volumes without any junction [17].

Aim of project: This project aimed to apply an automatic planning script for treatment planning for LACC with HT, and analyse and compare the plan quality of reference plans and HT plans.

2 Theory

In this thesis, the term dose refers to absorbed dose and is defined as the amount of radiation energy absorbed per unit mass of an organ or tissue [18]. The unit of absorbed dose is Gray (Gy). The term tumor refer to malignant tumors that are cancerous and require treatment in order to avoid spread and increased severity of disease [19].

2.1 Biological Effect of Ionizing Photon Radiation

Photon radiation is used for cancer treatment due to its ability to induce DNA strand breaks which result in cell damage. If the damage to the DNA strands is irreparable, the cells lose their ability to proliferate, stop dividing, and die [20]. Ionising photon radiation can damage DNA strands through both direct action and indirect action. For the photon energies used in RT, both mechanisms include incident photons transferring parts of their energy to free electrons, mostly through Compton scattering [21]. Further, these electrons can interact either directly with the DNA or indirectly by first interacting with a water molecule producing a free radical, a water radical, that interacts with the DNA. Ionizing radiation can produce DNA lesions that have the potential of killing cells, i.e. lethal damage, such as single-strand breaks (SSB) and double-strand breaks (DSB). DNA lesions are usually repaired by copying the undamaged DNA strand, and most cells can rapidly repair most or all of them. Thus lethal lesions are most likely from unrepaired or misrepaired DSBs [22]. DSBs are induced by either single-hit events, α, or multiple-hit events, β. A single-hit event is when one ionisation damages both DNA strands, whilst multiple-hit event is when two SSBs occur on opposing DNA strands within a short distance from each other [23].

A variety of DNA damage assays have been applied in an effort to predict the sensitivity of cells to ionizing radiation [21]. The probability of these events to occur is described by a linear-quadratic relationship between cell survival and dose. The linear-quadratic (LQ) model describes the relationship between the two and is used extensively to analyse and predict responses to ionising radiation [23]. The relative biologic effectiveness of radiation is influenced by radiobiological determinants [24]. Radiosensitivity varies between normal cells and cancerous cells, mainly caused by the cells' ability to repair DNA damage. The difference in radiosensitivity can be characterised by the α/β-ratio. A low α/β-ratio is associated with cell types with a high repair capacity, such as many healthy cells. On the contrary, cancer cells are often characterised with a higher α/β-ratio as they tend to have lower repair capacity. This difference is exploited by fractionation in RT. Fractionation serves to decrease acute and late toxicity to surrounding normal tissue exposed to RT [24]. Thus, cells are irradiated with a dose that should be lethal to cancerous tissue and more tolerable for normal tissues since they are able to repair sub-lethal damage between fractions [23].

However, radiation to healthy tissue is inevitable. Thus, consideration of the effect of

photon radiation to normal tissue in vital organs is important. Organs differ in radiosensitivity depending on the distribution and amount of radiation dose received [25]. The effect of irradiation of normal tissue depends on the structure of the organs' functional sub-volumes, the parts of an organ related to the function of the organ. Sub-volumes are arranged in parallel or serial structures, or somewhere in between [26]. In parallel organs, radiation-induced complications only occur when a critical volume of the organ is damaged [25]. Therefore, parallel organs have a significant volume effect, meaning that the tolerance dose of the organ is related to the irradiated organ volume and the mean radiation can predict the normal tissue complication probability (NTCP). The kidneys are an example of a parallel organ. In serial organs, damage to any one sub-volume cause the entire organ to fail. Serial complications are most affected by the highest dose received by the organ, and the maximum radiation dose gives predictions of the NTCP. The rectum, bowel, bladder and spinal cord are examples of serial organs [25]. Parallel organs can tolerate high doses to a small volume better than low doses to the whole organ. Serial structures can tolerate low doses to the whole organ, but cannot tolerate high doses to a small volume [27]. Hence, consideration of the dose distribution to nearby OARs is an important part of RT treatment planning.

2.2 External Beam Radiation

Therapeutic use of radiation is a well established method of treating malignant tumor. RT, also known as radiotherapy, is a local cancer treatment that uses high doses of ionizing radiation to kill cancer cells and shrink tumors. EBRT is the use of radiation from outside of the body and is a local type of treatment. At high doses, radiation therapy kills cancer cells or slow down their growth by damaging their DNA [28]. EBRT is most commonly delivered by a medical linac that produces high energy electrons or photons focused towards cancerous tissue in the patient. In addition, EBRT with the use of protons for RT is subject to recent reviews [29]. However, photon beams are mostly used. For the photon energies used in RT, the incident photons transfer parts of their energy to free electrons, mostly through Compton scattering [21].

2.2.1 The Radiation Treatment Workflow

The RT workflow in the clinic can be divided into five steps; (1) consulting of patient and diagnosis, (2) image acquisition, (3) treatment planning, (4) delivery, and (5) follow-up. RT is a resource demanding treatment.

Before RT is carried out, a treatment plan is worked out considering the chosen treatment technique and the radiation dose needed for best possible treatment outcome. A set of 3D CT images are acquired of the treatment site. In a CT image, the voxel intensity is proportional to the tissue's electron density, which is proportional to the dose. CT scanners have been used for planning external radiation treatment for many years due of

their ability to image patient anatomy and gross tumor, slice by slice. Thus, the CT images of the patient are used in conjunction with computerized dose calculations to determine the dose intensity pattern that will best conform to the tumor shape, as well as limiting dose to healthy tissue [30]. In addition to CT images, positron emission tomography images (PET) or magnetic resonance images (MRI) can provide additional information about the tissue characteristics to obtain more accurate volume delineations [31].

Treatment planning is the process of determining the most appropriate way to irradiate the patient, after the time consuming process of delineating target volumes and all relevant OARs. During this stage the shape and location of the tumor and of the neighbouring risk organs are identified and assigned dosimetric planning goals. A suitable beam arrangement has to be selected and the resulting dose distribution is evaluated to deliver the required absolute dose [1]. A team of specifically trained treatment planners modifies the radiation beams and weights of the planning goals in the TPS to generate an optimal treatment plan, ensuring the goals are achieved. The process of treatment planning always involves a compromise between delivering high doses to target volumes while minimizing doses to OARs. The final treatment plan undergoes a thorough review by a physician and a physicist, and may undergo quality assurance testing on the linac. During the treatment delivery stage, daily cone beam CT (CBCT) images are frequently taken to ensure accurate patient positioning in relation to the treatment plan. Once the RT is completed, the patient will receive follow-up care from a physician [1].

2.2.2 The Linear Accelerator

The linac is the primary equipment of generating mega-voltage (MV) beams, with the ultimate goal to deliver high energy radiation to tumor tissue, while minimizing radiation to healthy tissue. Compared to kilovoltage (kV) beams, a major benefit of using MV beams is that the maximum dose being delivered below the skin surface. In addition, due to the Compton scattering being the main interaction with tissue at the clinical energy range, $6\,\mathrm{MV} - 20\,\mathrm{MV}$, the locally absorbed dose is not atomic number dependent. Thus, the actual dose to the bone is not enhanced compared to soft tissue [1].

Figure 1 shows a schematic illustration of a linac. In the linac, electrons gain energy by interacting with synchronised radio-frequency electromagnetic field and are further accelerated through an accelerating wave guide. The beam has to be bent in order for the radiation beam to be able to irradiate the patient. Electrons are easily deflected in a magnetic field, and is conveniently bent through 90°. In the linac, the electron beams can be used directly or be converted to photons for patient treatment [1].

High energy electron beams, 6 MeV or higher, can be directly used to treat tumors close to skin surface. For more deep-seated tumors, photons are used. This is due to the depth-dose-curves characterised by initial skin sparing followed by several centimetres of uniform dose and a rapid fall-off in dose. Photons can be made by focusing electrons onto a target, typically made of a high-atomic-number material like tungsten. Their energy losses

are converted into bremsstrahlung radiation. At MV energies, the primary direction of bremsstrahlung emission is forward. Collimators are used to shape the radiation field. Conventional collimators only constrain the radiation in a rectangular shape. MLCs, together with backup collimators, provide field shaping as well as shielding. MLCs can be up to 80 pairs of leaves that move independently, allowing all beam shapes to be produced accordingly to the width of the leaves. This allows for optimization of the radiation treatment [1].

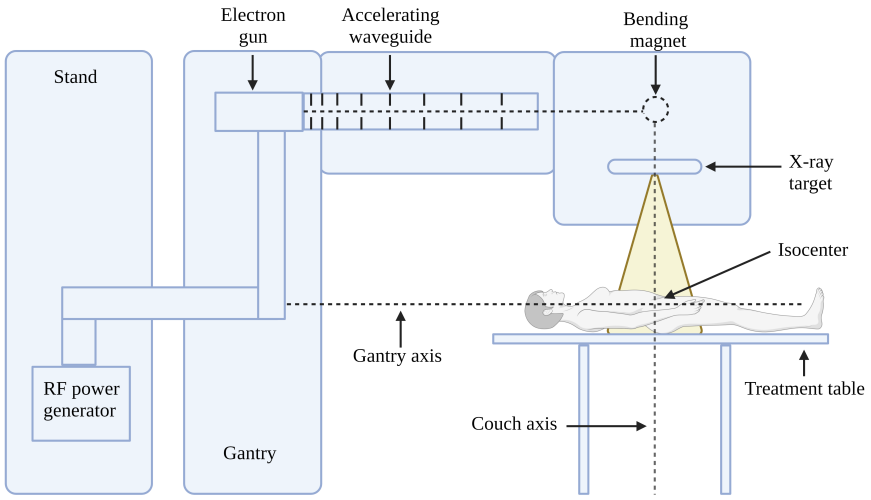

Figure 1: Schematic diagram of a linac including the RF power generator, electron gun, accelerating waveguide, the bending magnet and the x-ray target. Figure adapted from [32] and created in Biorender.

2.3 Treatment Planning

Treatment planning is the process of determining the most appropriate way to irradiate a patient. First an appropriate patient position and fixation is chosen so that treatments will be reproducible. Followed by identifying the shape and the location of the tumor and of the neighbouring risk organs on CT images for delineation of target volumes and OARs. Further, a suitable beam arrangement has to be selected. Finally, the resulting dose distribution has to be evaluated and calculate the treatment machine settings to deliver the required absolute dose [1]. The main objective of treatment planning is to deliver the prescribed dose accurately to the target volumes, keeping the dose to OAR below the set acceptable limits and minimizing dose to surrounding, healthy tissue. A set of dose-constraints are defined for targets, OARs and other regions of interest, typically dose-volume relations, stating the minimum or maximum dose that is allowed to a given region [4]. In RayStation these constraints are referred to as clinical goals.

2.3.1 Treatment Plan Volume Definitions

EBRT is usually carried out with multiple radiation beams in order to provide a uniform dose distribution inside the target volume, as well as minimizing the dose delivered to healthy tissues surrounding the target [20]. In the context of RT treatment planning, target volumes are defined as volumes to which a prescribed high dose is delivered, whereas OARs are volumes that should receive as little radiation as possible [33]. Definition of the tumour, adjacent OAR, and other anatomical structures are an essential part of the treatment planning process to ensure optimization of the beam size, number, trajectory and weighting in relation to these structures [1]. In the CT images, the external shape of the patient is outlined in all areas where the beams enter and exit for contour corrections, and in the adjacent areas to account for scattered radiation. The target volumes and other internal structures are outlined in order to determine their shape and volume for dose calculation. The electron densities for each volume element in the dose calculation matrix must be determined if a correction for heterogeneities is to be applied. The attenuation characteristics of each volume element are required for image processing [20].

The principal volumes related to 3D-treatment planning are gross tumor volume (GTV), clinical target volume (CTV), internal target volume (ITV) and planning target volume (PTV) [20]. A schematic representation of the relationship between the different volume definitions is shown in Figure 2.

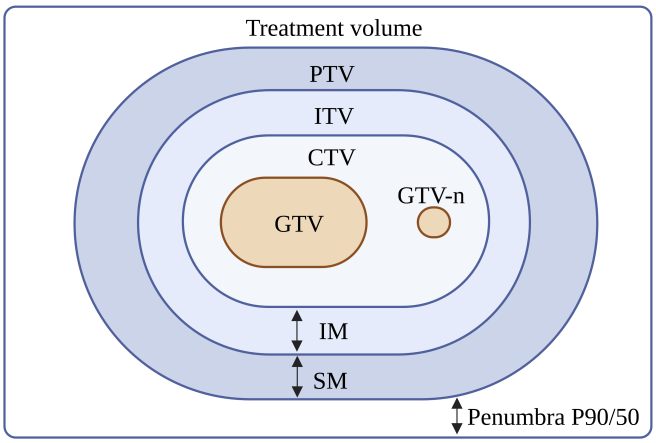

Figure 2: Schematic representation of the volumes and margins demonstrating the relationship between different volumes: GTV, gross tumour volume; ITV, internal target volume; CTV, clinical target volume; PTV, planning target volume; GTV-n, lymph node; Treatment volume, irradiated volume. The internal margin (IM) and setup margin (SM) is also included. Figure is adapted from [33].

The GTV is the visible extension of the malignant growth in diagnostic images, and in some cases, it may be necessary to subdivide the GTV into primary tumor (GTVp), lymph nodes (GTVn), and other metastases (GTVm). The CTV includes the GTV and areas with subclinical malignant disease that are difficult to identify and thus often defined based on discretion. The ITV includes the CTV and an internal margin (IM) to encompass potential volume changes of the CTV and physiological movements, such as breathing. The ITV, or the CTV, is the volume that should receive the prescribed dose. The PTV is a geometric volume that must ensure that the requested dose is given with an acceptable probability to all parts of the CTV when geometric uncertainties included in the total margin, TM, are taken into account. PTV is defined based on the treatment device's coordinate system and therefore independent of the patient's anatomy [33].

The definitions of GTV, CTV, and ITV remain similar for all treatment techniques, including EBRT and BT. The PTV includes the ITV and a setup margin (SM) that accounts for patient movements during irradiation and uncertainties due to patient positioning and field settings for each treatment. The sizes of IM and SM may vary in different directions, depending on the specific treatment approach. In some cases, PTV will overlap OARs and margins around them. In the event of such an overlap, prioritization rules must be determined during optimization of treatment plans [33]. In some cases, boost volumes are also defined. These volumes are partial volumes for high dose and usually defined on the basis of the original GTV with justified margins and indexation [33].

Furthermore, OARs are defined through contouring the visible extension of the OAR in the diagnostic images, followed by adding margins to account for uncertainties. OARs located close to target volumes receive a relatively high radiation dose and are of great interest due to their structure and sensitivity of the OARs' functional sub-units, different OARs have different tolerance doses. Actual OARs, and how these are to be defined, should be indicated in the clinical recommendations for current diagnoses [33]. The complexity of the treatment plans is related to the location of the tumor and the surrounding OARs.

2.3.2 Modern Treatment Planning

The planning and delivery of modern radiation therapy treatment is a complex process that relies on advanced imaging and computational technology in the TPSs, in addition to the expertise of the medical team [34].

Over time, RT evolved from manual planning to conformal therapy. In the 1990s, 3D conformal radiation therapy (3D-CRT) gained popularity as improvements in computing and imaging allowed for dose calculations on 3D image sets [35]. MLCs have replaced the use of wedges and other compensators, and hence simplified radiation delivery by better conforming the tumors [36]. MLCs are positioned independently to arrange the beams and the dose is calculated to obtain the desired dose distribution in the target volume. This method of planning is called forward planning because the beams are arranged prior to calculating the dose distribution [35]. The TPS uses desired beam characteristics and

calculates the dose distribution, combining radiation beams of varying weights aimed from different angles towards the target volume. As an interactive approach, it heavily depends on the planner's experience and knowledge. The shift from forward to inverse planning has been a significant development in modern RT [36]. As opposed to forward planning, inverse planning starts with the desired dose result, the dose objectives, and works backwards to achieve best possible beam shape and fluence pattern [36]. The required radiation beam setup for achieving the desired dose distribution is then the output. The inverse TPS utilises iterative algorithms to optimise radiation delivery to meet the dose objectives. The input parameters can be adjusted to obtain an optimal treatment plan for each patient [36]. Two modern RT techniques are IMRT and VMAT, which are both based on inverse planning [36].

2.3.3 IMRT and VMAT

IMRT and VMAT both improve target volume conformity and normal tissue sparing, resulting in reduced acute and late toxicities [3]. IMRT is a high precision RT that uses computer controlled linacs to deliver precise radiation doses to a tumor. The modulation of the intensities is achieved through MLC positioning for step-and-shoot or segmental IMRT, and MLC position and speed variation for sliding window IMRT. Modulated beams from IMRT allows for the radiation dose to conform more precisely to the 3D shape of the tumor. This is done by modulating the intensity of the radiation beam in several small volumes [2]. VMAT is an advanced type of IMRT in which the gantry and the positioning of the MLCs are in continuous movement during irradiation. As the gantry rotates around the patient, there is simultaneous change in dose rate, gantry speed, and collimator system. Compared to IMRT, the continuous delivery of dose improves conformity and significantly shortens treatment time [36]. For VMAT, modulation of the intensities is achieved through the rotation speed of the gantry and the dose rate variations [2]. IMRT and VMAT allow the treatment planner to create complex treatment plans by providing a set of objectives that an algorithm attempts to fulfill by inverse optimization [4].

2.4 Automatic Treatment Planning

Modern RT treatment planning is a complex and time-consuming process that requires the skills of experienced users to obtain quality plans [37]. To increase the effectiveness of the treatment planning process, manual VMAT planning can be automated. The working procedure of manual VMAT planning includes definition of optimisation functions, TPS optimisation and plan evaluation [37, 4], a procedure which is repeated until the plan is clinically acceptable. Objectives and constraints for the desired dose are defined, and the system creates a plan that matches these criteria as closely as possible within the limitations of the treatment machine. The optimized plan is directly deliverable, without the need for post-processing that might degrade quality [38].

In recent years, various methods for automation of treatment planning, both IMRT and VMAT, for different cancer types and localization have been proposed. Reviews of clinical applications and future prospects for fully automated workflows and artificial intelligence (AI) in radiotherapy treatment planning have been conducted [37, 39]. These algorithms focus on automating the planning process and optimizing dosimetric compromises. Studies reporting the use of the RayStation TPS (RaySearch Laboratories, Stockholm, Sweden) for automatic planning have also been published [40, 11]. Automatic planning of modern breast techniques has been successfully introduced using a commercial planning system with the purpose of creating plans similar to manual plans while requiring little manual interaction [11]. Other TPSs have been also reported. For cervical cancer, the status of automated VMAT planning was reviewed in 2020 by Rhee et al. who employed knowledge-based VMAT planning with Rapid Plan (Varian Medical Systems) and Erasmus-iCycle (Elekta AB) [12]. Automatic IMRT treatment planning for cervical cancer using direct 3D patient anatomy match [41] and convolution neural network successfully achieving superior dose sparing without compromising of target dose [42] was published in 2022 and 2020, respectively. All studies proven to significantly reduce the treatment planning time. In 2022, Yuan et al. employed deep learning generated fluence maps for cervical cancer. IMRT have been shown to accelerate the treatment planning process by skipping the inverse plan optimization process [13]. Additionally, a study evaluating lexicographic optimization-based planning for cervical cancer was recently published (2022) showing a comparable OAR sparing while increasing target volume coverage [43].

Moreover, several studies addressing risk assessments of automated treatment planning and recommendations for clinical deployment have been taken into account to reduce the risk associated with the utilization of automated planning tools in clinical practice [44, 45, 46, 47].

2.4.1 Automatic Planning Script

The automatic planning script developed for cervical cancer at St. Olavs Hospital last year for the master and project thesis of Ingvild Hoem under supervision of Marit Funderud is the basis of this master project. The treatment planning software used was RayStation 11A SP1 (RaySearch Laboratories, Stockholm, Sweden) [14].

The main design idea of the autoscript was to deliver just enough dose to target volumes while reducing dose to OARs as much as possible. Only optimisation functions that supported this design were included in the script [14]. The automatic VMAT planning script was divided into two phases which automatically modified and re-optimised the optimisation functions in RayStation [14]. A flowchart of the script is provided in Figure 3.

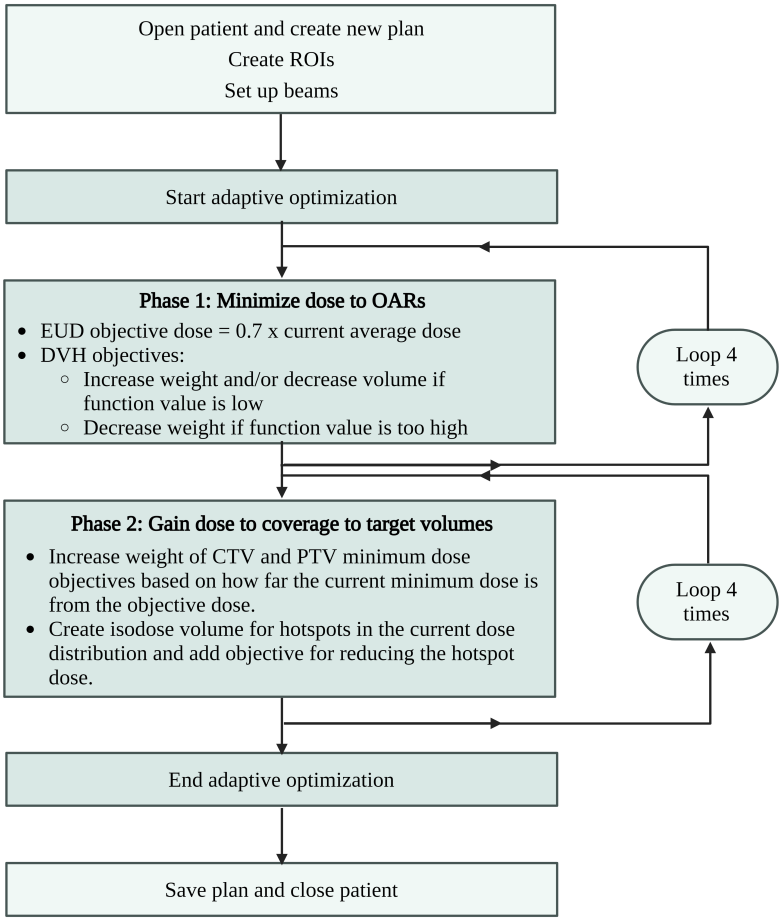

Figure 3: Flowchart of the automatic VMAT planning script. The script include entrance procedures, phase 1 that works to minimise dose to OARs, phase 2 that works to gain dose coverage to target volumes, and exit procedures. Figure is adapted from [14] and is created in Biorender.

The first phase of the optimization process focuses on minimizing the dose to OARs and comprises four steps, each consisting of 40 or 100 iterations that works with the optimisation functions. Before each new step, adaptive changes are made to the max equivalent uniform dose (EUD) and max dose volume histogram (DVH) optimization functions. An optimization function is considered adaptive if its input parameters are dynamically adjusted based on the dose distribution during the script's execution. Consequently, adaptive optimization functions are tailored to the specific characteristics of each patient, thereby facilitating the generation of high-quality VMAT plans [14]. The adaptive weight adjustments prevent the max DVH functions from acquiring excessively high function values that would lead them to dominate in the next phase. It is important to achieve a evenly distribution of function values in order to prioritize all optimization functions and effect-

ively suffice as objectives as possible [14]. Additionally, to improve homogeneity of the dose distribution, isodose help volumes are created. For each iteration, if hot spots (unwanted high dose levels) are detected, help-structures around the hot spots are created to adjust the dose value down. For some isodoses outside of the target volumes help improve conformity of the target volumes.Further, OAR volumes that do not intersect with PTVn, with a 15 mm margin, xOAR-PTVn, are used to assess max doses within the OARs while allowing relatively high doses in the parts of the OARs that do overlap with the PTVs.

Further, the second phase of aims to achieve adequate coverage of the target volumes and consists of four steps, each with 50 iterations. To emphasize the importance of delivering a high homogeneous dose to the CTV, the function weight of the uniform dose functions is increased to 50 before the first step. By employing minimum dose functions on the target volumes, the script ensures that the target dose remains within the specified hard dose constraints, in line with the main design idea [14]. To increase conformity of the dose distribution in target volumes, adaptive changes were made to optimisation functions. Depending on the deviation from the objective dose, the function weight of the min dose functions to CTV and PTV were changed [14].

The RayStation settings presented in Table 1 are the basis for generating VMAT plans with the automatic VMAT planning script for LACC.

Table 1: RayStation settings for automatic VMAT plans [14].

Settings	**Parameter**
VMAT Technique	Dual arc
Energy	6 MV
Max gantry spacing	2 degrees
Start/stop angle of 1st. arc	178/182 degrees
Start/stop angle of 2nd. arc	178/182 degrees
Collimator angle	25 degrees
Leaf motion constraint	0.5 cm

2.5 Tomotherapy

Tomotherapy is a different method of delivering radiation in EBRT. The tomotherapy system is a RT delivery machine that combines the features of a linac and a helical CT scanner to provide IMRT by using a fan beam where the target is treated slice by slice [48]. The beam delivery can be of either a serial or a helical type. Serial tomotherapy was the first form of tomotherapy clinical use where a normal linear accelerator was modified to deliver tomotherapy. The serial tomotherapy was one of the earliest forms of IMRT. A

disadvantage of the serial tomotherapy was uncertainty with junctions between the fields as the couch moves for treatment. This has led to the development of the HT where the radiation is delivered in a helical manner, thereby avoiding junctions [36]. Serial tomotherapy will not be discussed further in this project. HT is a RT concept that offers an innovative approach to delivering radiotherapy [48].

2.5.1 Helical Tomotherapy

HT is a method of delivering IMRT that combines the functions of a linear accelerator and a helical CT scanner into one system [49]. The radiation treatment is delivered with a 6 MV linac that is mounted on a gantry ring, similar to that of a CT scanner, allowing the linac to rotate around the patient. The fan beam collimation is accomplished with a binary MLCs, also mounted on the rotating gantry. The intensity modulation is provided by a set of binary MLCs that rapidly transition between open (leaf retracted) and closed (leaf blocking) states [48]. Two sets of interlaced leaves move as the linac rotates around the patient [20]. During treatment, the couch advances the patient through the gantry bore, in the y-direction, so that the radiation is delivered in a helical geometry around the target volume as shown i Figure 4. Intensity modulation is accomplished by varying the fraction of time that individual leaves are opened. During treatment the beam projection and delivery is characterized by a number of beam optimization parameters specific for HT treatment to be specified by the treatment planner. These parameters are further explained in Section 2.5.2. In addition, one of the key advantages of HT is its ability to acquire CT images of the patient in the treatment position, which can then be used for image guidance during treatment [48]. When operating as an MVCT imaging system the leaves are retracted to the open state [48].

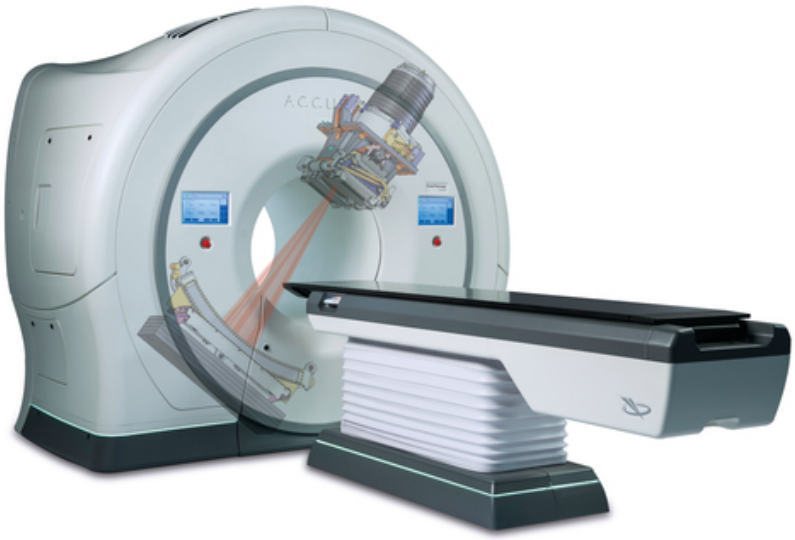

Figure 4: Image of a HT system, Accuracy, illustrating the radiation source, as linac, mounted onto the gantry ring. Figure adapted from [50].

2.5.2 TomoHelical-Specific Beam Optimization Parameters

Depending on a set of parameters, the beam technique "TomoHelical" forms beams with different treatment delivery characteristics. In RayStation these parameters are jaw mode, field width, pitch factor, delivery time factor, delivery time and gantry period.

Jaw mode determines if the jaws are allowed to move (dynamic) or not (fixed) and only refer to movement in the outer areas of the target volumes [51]. Dynamic mode is used in this project. *Field width* (FW) [cm] is the longitudinal distance thickness, in y-direction, of the treatment field at the machine isocenter. *Pitch factor* (PF) is a variable that determines the distance the couch moves each gantry rotation. The couch moves a distance which is determined by the FW times the PF [51]. If the couch moves 2 cm per gantry rotation and the FW is 5 cm the related PF is 0.4. The rotation is oriented about the patient right-left axis. For a head first-supine (HFS) patient, a positive pitch angle corresponds to a clockwise rotation when observed from the right. PF is typically a value between 0.2 and 0.5 [51]. Delivery time is limited by the shortest possible delivery time multiplied by the *delivery time factor* (DTf). There is a possibility to set an upper limit for the delivery time directly by determining a maximum delivery time [51]. The parameter *gantry period* [sec] is defined as an upper limit for the gantry period, which is the time for the gantry to rotate one time. A minimum value of $11.8s$ is determined by RayStation [51]. The gantry period normally ranges between 10 and 60 s per rotation. However, the velocity of the gantry rotation is constant throughout the treatment delivery [52].

Additionally, the *modulation factor* (MF) is defined as the ratio of the maximum leaf open time to the average leaf open time for the beam projection. The extent to which a treatment beam projection is modulated is characterized by this factor. In RayStation, a default value is set for this factor.

2.5.3 Tomotherapy for Adaptive Radiation Therapy

Adaptive therapy (ART) is a separate feature of the HT system. In general, ART can be used to address deformation of a patient's anatomy, such as tumor volume and positional changes, and also can be used to achieve smaller SM by continuously adjusting the parameters based on the information obtained from imaging [53]. The dose delivery for subsequent treatment fractions of a treatment course can be modified to compensate for such inaccuracies in the dose delivery [20]. In HT, the CT component of this delivery system enables the visualization of targeted regions before, during, and after each treatment, and provides anatomical detail through megavoltage CT (MVCT) images. The 3D imaging is utilized to generate an optimized intensity-modulated treatment plan, set-up verification via MVCT, delivery modification, treatment delivery and dose reconstruction. ART is therefore able to use information obtained during previous fractions, to correct or modify an ongoing treatment [48].

2.6 Treatment Planning Evaluation Tools

Dose statistics, DVH, the conformity index and the homogeneity index are statistical tools that can be used to evaluate and compare plan quality.

2.6.1 Clinical Goals

In RayStation, the dose constraints are referred to as clinical goals. These goals are upper or lower limits for the desired dose in a certain volume. Set of clinical goals is presented in Figure A.1-A.3 for plans with prescribed SIB of 55 Gy, 57.5 Gy and both dose levels, respectively, in Appendix A. Objective functions are used in optimization process to fulfill the clinical goals. A set of objective functions is presented in Figure B.1 Appendix B.

2.6.2 Dose Volume Histograms

Cumulative DVHs are graphical illustrations of the radiation dose delivered to a specific volume, and can be used to compare dose distributions in different treatment plans. The height, in the y-axis, of a DVH curve at any given dose corresponds to the percentage of the volume that receives a dose equal to or higher than that particular dose. For target volumes, PTV and CTV, an ideal DVH curve would stay at 100 % until the limit set by dose restrictions is reached [54]. Parameters in that are associated with DVHs are D_{max}, D_{min} and V_{dose}. The maximum dose, D_{max}, and minimum dose, D_{min}, are respectively the highest and lowest dose received by a specified volume and are often referred to as D_{98} and D_2. D_{98} and D_{50} defined as the minimum dose received by the hottest 98 % and 50 % of the volume, respectively. V_{dose} indicates a percentage of the volume that receives a particular dose. For instance, $V_{45\,\mathrm{Gy}}$ represents the volume percentage receiving at least 45 Gy, and $V_{95\%}$ represents the volume percentage receiving 95 %, of the prescribed dose or more [54].

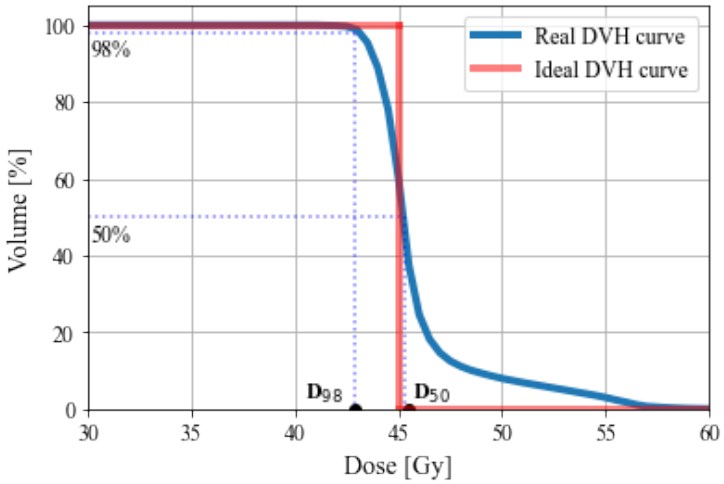

Figure 5: Cumulative DVH showing the portion of a specific volume that receive a specific dose or higher, in percentage. The blue curve represents a real DVH curve, and the red curve represents the ideal DVH curve for a target volume with a prescribed homogeneous dose of 45 Gy. D_{98} and D_{50} is the dose received by 98 % and 50 % of the volume, respectively. Figure is adapted from [14].

2.6.3 Conformity Index

The conformity of a treatment plan indicates the degree to which the prescribed dose is accurately and precisely delivered within a specific target volume. The CI is calculated from a reference isodose around a specific target volume. The reference isodose is defined as the volume that receives the reference dose or higher, as expressed by the isodose. Different definitions of the CI are published of which some provides more, or different, information about the treatment plan than others [55]. Taking into account irradiation to both target volume and surrounding healthy tissue van't Riet et al. defined the conformation index as the conformation number (CN) by,

$$CN = \frac{TV_{RI}}{TV} \times \frac{TV_{RI}}{V_{RI}}, \tag{1}$$

where TV_{RI} is the volume of target receiving a dose equal to or greater than the reference dose, TV is the volume of the target, V_{RI} is the volume receiving a dose equal to or greater than the reference dose. The first term of Equation (1) represents the coverage of the target volume, while the second term refers to the volume of healthy tissue receiving dose equal to or greater than the reference dose [56]. The CN is quantified by a value between 0 and 1 and is easily interpreted. A CN equal to 1 corresponds to high conformity, ideal dose coverage of the reference isodose without irradiation of healthy tissue. Treatments with a CN greater than 0.60 might be considered conformal RT [56].

2.6.4 Homogeneity Index

Homogeneity index (HI) is an objective tool to analyse the uniformity of dose distribution in a target volume. In RT the objective is to deliver maximum dose to the target volume homogeneously, while avoiding dose to healthy surrounding structures [57]. Different definitions for the HI are proposed in literature [58]. A standard definition of the homogeneity is the ratio between the maximum isodose and the reference isodose. The dose homogeneity index (DHI) can be defined as,

$$DHI = \frac{D_{\geq 95}}{D_{\geq 5}}, \tag{2}$$

which represent the relationship between the dose reached by 95 % of a selected volume and the dose reached by 5 % of the same volume [59]. A DHI-value close to 1 would represent an homogeneous dose distribution, while a lower value implies that the dose distribution is less homogeneous.

2.7 Statistical Analysis

Statistical tests for paired data are used in hypothesis testing for determining whether there is statistically significant differences between the two sets of data.

2.7.1 Wilcoxon Signed-Rank Test

Wilcoxon signed-rank test is a non-parametric statistical hypothesis test comparing the medians of the differences between the paired observations. A non-parametric test implies that there no assumptions about the distribution or variability of the data being analysed. The Wilcoxon signed-rank test is considered the non-parametric equivalent of the parametric paired t-test, and appropriate to when the distribution is known to not have a normal distribution. The null hypothesis (H0) is that the difference between the paired observations in the population is zero. The alternative hypothesis (H1) is that the difference between the paired observations is not equal to zero. The Wilcoxon signed-rank test compares the sample median against a hypothetical median [60]. The p-value represents the probability that the results from the paired data sets occurred by chance, and if the obtained p-value is ≤ 0.05 there is sufficient evidence to reject the null hypothesis end there there is statistical significance.

2.8 Cervical Cancer

Cervical cancer is the fourth most common malignancy diagnosed in females worldwide [61]. In developed countries, early detection and prevention through screening and vaccination are available. However, in countries with limited resources there is still a lack of

comprehensive programs [15]. Cervical cancer is the pathological condition characterized by abnormal cell growth in the lining of the cervix, the lower and inferior part of the uterus. This is an essential organ of the female reproductive tract illustrated in Figure 6. The endocervix, the upper part of the cervix, consists of mostly glandular cells and forms the cervical channel connecting the vagina to the lower inner part of the uterus. The lower and outer part of the cervix which faces the inner lumen of the vagina consists of mostly squamous cells. The most frequent abnormal cell development occurs in the transition in the mucous membrane between the two cervical regions, also known as the transition zone. Thus, most cancer of the cervix and vagina are squamous cell carcinomas [62].

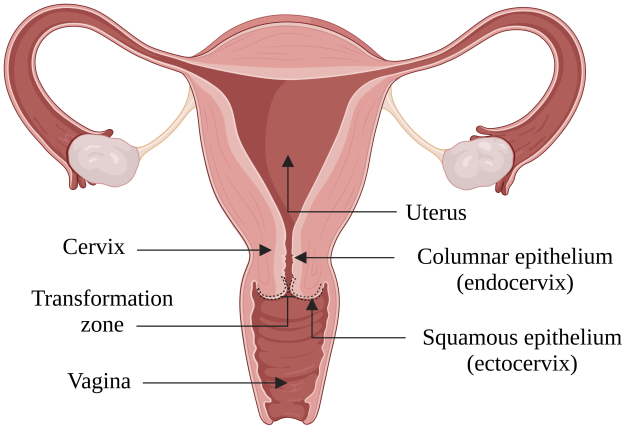

Figure 6: Illustration of the anatomy of the female reproductive tract, including the cervix, the uterus, the vagina, and the transformation zone connecting the endocervix and ectocervix. Figure adapted from [63] and created in Biorender.

Cervical cancer is primarily caused by human papillomavirus (HPV), which encodes for proteins necessary for viral replication, such as E6. E6 targets the tumour suppressor gene p53 and the cell cycle checkpoints, leading to the development of cervical cancer [64]. HPV type 16 is responsible for 60% of cervical cancer cases and encodes this specific protein [65]. Squamous cell carcinoma is the most common type of cervical cancer, with HPV DNA found in 90% of cases. In some cases, adenocarcinoma can occur, which develops in glandular cells in the endocervix. Squamous cell carcinoma (SCC), adenocarcinoma (ADC), and adenosquamous carcinoma (ADSC) are the three most common histological subtypes of cervical cancer, accounting for 70%, 25% and 5% of cases, respectively. In recent decades, SCC has experienced a progressive decrease in incidence and mortality. On the other hand, the incidence and mortality of ADC has increased during the same time frame. This evolution has been attributed to the Pap test and its ability to more efficiently detect squamous, rather than glandular, neoplasia [63].

2.8.1 Locally Advanced Cervical Cancer

Metastasis is a term used for the spread of cancer cell from the primary tumor to a secondary location. LNs are located at several locations in the body, such as the armpits, neck, chest and belly, and work as filters for foreign and unwanted substances such as infections and cancer cells. Cervical cancer cells can break loose from the cervix and spread to the lymphatic system and form metastases at LNs [14].

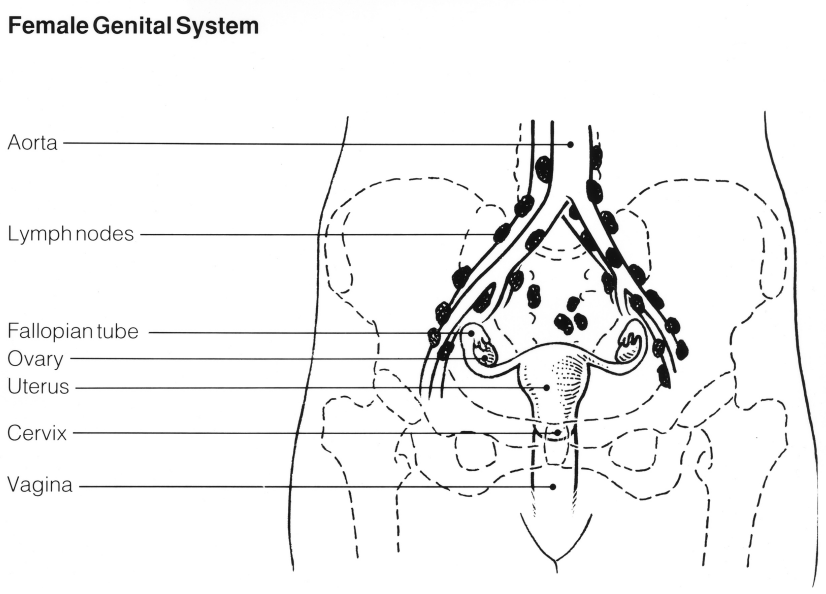

Figure 7: Lymph node location in the pelvis illustrated with the larger black dots. Figure adapted from [63].

LACC includes a heterogeneous group of diseases [66]. The standard treatment of LACC is radio-chemotherapy including EBRT, BT and chemotherapy. However, image guided adaptive brachytherapy (IGABT), with repetitive MRI is regarded as a gold standard and is increasingly recognized as the new paradigm replacing 2D BT and spreading throughout the world [67].

Overall survival rate at 5 years is approximately 92%, 65% and 17% for early-stage, locally advanced and metastatic disease, respectively. The prognosis of patients with recurrent disease remains very poor, except in cases of local recurrence accessible to curative treatment [66]. Major advances have occurred in the treatment of LACC over the past two decades, including the emergence of the crucial role of imaging in RT planning with the implementation of conformal techniques, such as IMRT and VMAT, image-guided radiation therapy (IGRT) and IGABT, sparing the OAR and concentrating the therapeutic dose to the primary disease. Furthermore, the addition of chemotherapy to RT has resulted in a significant improvement in local, regional and distant control rates [66].

2.8.2 FIGO Staging of Cervical Cancer

The staging system for cervical cancer was initially introduced by the International Federation of Gynecology and Obstetrics (FIGO) in 1929 to assess the severity of the disease. Since then, it has undergone several revisions, with the most recent update occurring in 2018 [16]. Staging plays a crucial role in ensuring that patients with similar cancer profiles receive consistent treatment. Cervical cancer is classified into four stages, denoted as I-IV, where higher stages indicate a larger tumor volume and increased spread of the disease. Each stage is further divided into subgroups, designated by a letter (IA, IB) providing a more detailed description of the disease. Additionally, a subgroup can be assigned a number (e.g. IB2), which corresponds to the size of the tumor [16]. An overview of the four FIGO stages for cervical cancer with associated subgroups of is presented in Table 2.

Table 2: Description of the FIGO stages (I-IV) and subgroups (A, B) [16].

Stage	**Description**
I	Tumor spread limited to the cervix
IA	Invasive tumor depth $< 5\,\text{mm}$, only diagnosed by microscopy.
IB	Clinically visible lesion confined to the cervix, invasion depth $> 5\,\text{mm}$.
II	Cervix cancer that grows beyond the uterus, but not to the pelvic wall or to the lower third of the vagina.
IIA	Tumor without parametrial infiltration, limited to the upper 2/3 of the vagina.
IIB	Tumor with parametrial infiltration, but not reaching the pelvic wall.
III	Tumors that grow to the pelvic wall and/or to the lower third of the vagina and/or pelvic and/or para-aortic lymph nodes.
IIIA	Growth to the outer third of the vagina, but not extended to the pelvic wall.
IIIB	Growth to the pelvic wall and/or causes hydronephrosis or a non-functioning kidney.
IV	Extensions beyond the true pelvis or has involved the mucosa of the bladder or rectum.
IVA	Spread of growth to adjacent organs.
IVB	Spread to distant organs/ distant metastasis.

2.8.3 Treatment Planning of Cervical Cancer

Treatment planning for LACC patients is complicated due to the many nearby OARs and different target dose levels for cases with LN metastases. These difficulties also make manual VMAT planning of LACC patients particularly complicated. From the dose coverage for target volumes and dose restrictions to OARs set by the standard protocol for cervical cancer treatment plans can be optimized to give the optimal treatment [16]. In this project, tomotherapy is explored as a possible alternative treatment technique to linac treatment for LACC patients.

Target volumes for LACC

Figure 8 shows the target volumes for a LACC patient with 2 LN metastases including GTVp, CTVp, PTVp, GTVn, CTVn and PTVn. For the purpose of planning target volumes are labelled with its associated prescribed physical dose, i.e. PTV_45.

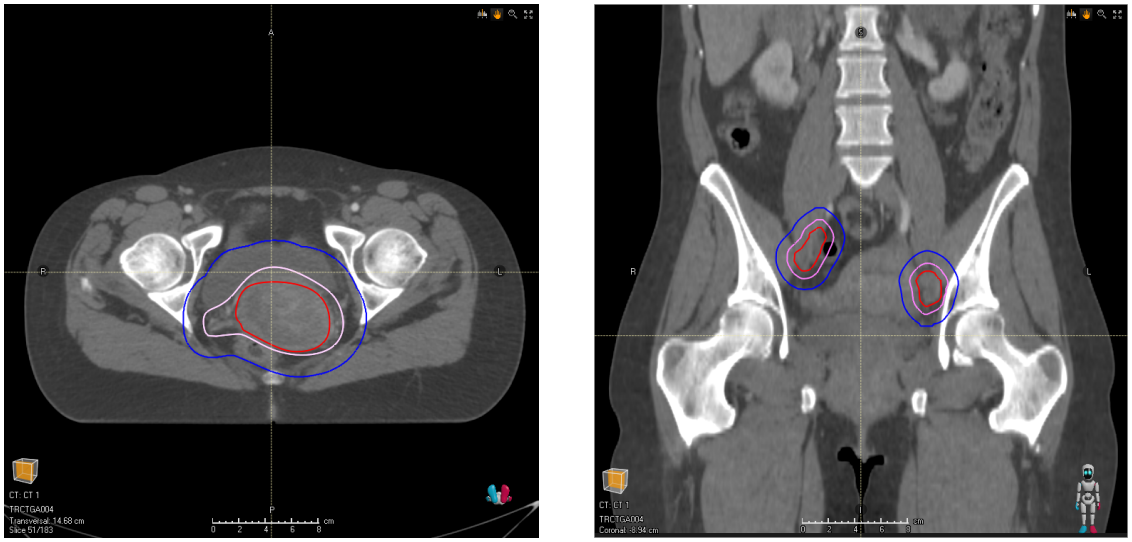

Figure 8: Left: delineations of the primary target volumes GTVp (red), CTVp (pink) and PTVp (blue) of a LACC patient, viewed in the transverse plane. Right: delineations of the target volumes GTVn (red), CTVn (pink) and PTVn (blue) of the lymph node metastases of a LACC patient, viewed in the coronal plane.

Risk organs for LACC

The organs at highest risk for LACC patients are the rectum, bladder, sigmoideum, bowel, kidneys and femoral heads. The image to the left in Figure 9 shows the location of a selection of the OARs and their proximity to GTVp, while image to the right shows the selected xOARs, being the volumes of OARs that do not intersect with PTV.

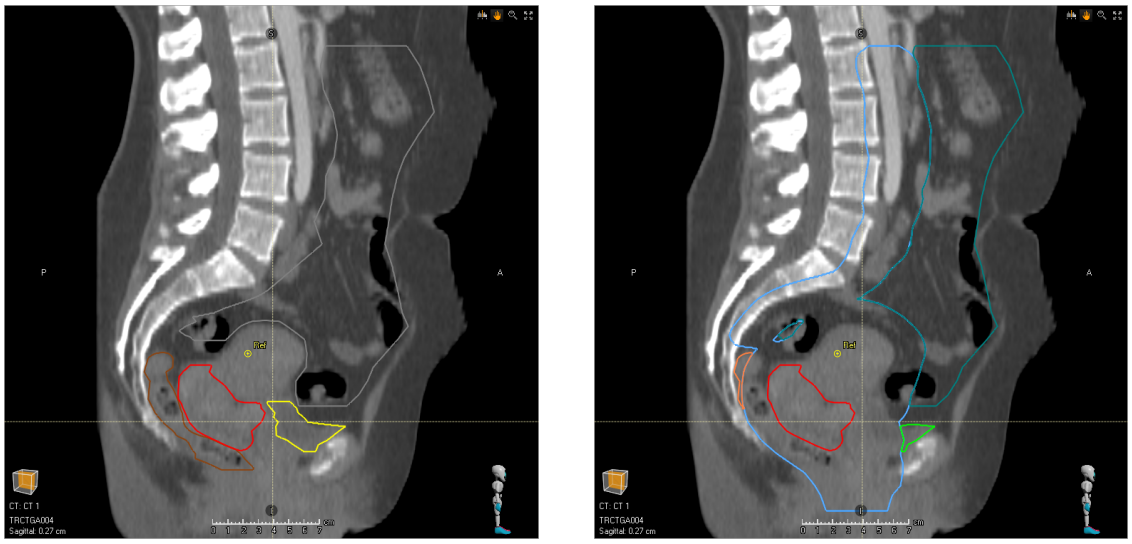

Figure 9: Left: delineations of OARs on a LACC one patient showing the bladder (yellow), rectum (brown), bowel (grey), as well as GTVp (red), viewed in the sagittal plane. Right: delineations of xOARs, excluding PTV with zero margin showing the xBladder (green), xRectum (orange), xBowelBag (dark green), as well as PTV (blue), viewed in the sagittal plane.

3 Materials and Method

The basis of this master project is the automatic script-based treatment planning for cervical cancer, developed at St. Olavs Hospital for the master and project thesis of Ingvild Hoem under supervision of Marit Funderud during the academic year of 2021/2022. The treatment planning software used in the current work was RayStation 12A SP1 (RaySearch Laboratories, Stockholm, Sweden).

3.1 Patient Group

This project included 10 patients diagnosed and treated for LACC at St. Olavs Hospital between December 2019 and December 2021. The patients had 1-4 positive LNs inside the true pelvis and/or 1-5 positive LNs outside the true pelvis. While in treatment, all patients were treated with a combination of VMAT and BT with manually made VMAT plans uniquely designed for each patient. An overview of the number of positive LNs inside and outside true pelvis for the patients in the study is presented in Table 3. Additionally, all 10 patients were used in the previous masters' study comparing manual and automated VMAT planning [14]. All patients were anonymised before being used in this project.

Table 3: An overview of number of positive LNs inside and outside true pelvis for the patients in the study.

Patient	**Number of LN inside true pelvis**	**Number of LN outside true pelvis**
1	-	3
2	-	5
3	2	2
4	3	-
5	4	2
6	-	3
7	-	2
8	2	1
9	-	1
10	-	2

3.2 Adjustments of the Automatic Planning Script for Helical Tomotherapy

The initial phase of this project required comprehending and becoming acquainted with the intricate structure of the scripts by understanding the diverse components and functionalities, as well as the scripting environment. The automatic planning scripts has a complex structure, incorporating numerous sub-scripts in the form of functions, classes and TPS-specific features, which made this a time-consuming part of the project.

Adapting the scripts for tomotherapy planning commenced by identifying the areas in need of adjustments. Firstly, the tomotherapy system had to be included in the script. "TomoHelical" was chosen as the delivery technique, along with "tomomachine" as the delivery machine. Further, new definitions and parameter settings were required due to a different beam settings for the tomotherapy system than for the standard linac. A specific tomobeam was created, as a new beam definition, among the beams set functions that would be employed when "TomoHelical" was the selected treatment technique. Different parameter combinations were applied to see the effect of the variations on the plan quality as well at the treatment delivery time. It was decided to look into the effect of varying the pitch factor, the delivery time factor and the field width. In addition, the minimum treatment time for each patient was determined. To keep a comparative basis, the number of loops and iterations of the optimization part of the script was kept unaffected. No adjustments were made to enhance the optimization process to further improve overall dose distribution. However, changes were made to ensure correct computation of final dose and the appropriate number of iterations in preparation phase for the techniques. The adjustments were made to ensure correctly generation of treatment plans for HT with the automatic planning script.

3.3 Creation of Treatment Plans

Treatment plans for tomotherapy (HT plans) and automatic VMAT plans (reference plans) were made for all 10 patients. The same target volumes and risk organ delineations, with equal margins, were used for corresponding plans. The treatment planning objectives follow the dose constraints in the clinical procedures at St. Olavs Hospital, which are based on recommendations from the the Norwegian Directory of Health [16] and the EMBRACE II protocol [67].

3.3.1 Reference Plans

New VMAT plans were generated with the automatic script for all 10 patients to include the latest linac and beam model in the clinic. This planning technique is considered the golden standard in the clinic, and are considered reference plans in this study. The plans were made by running the script in the scripting environment in RayStation 12A Clinical.

3.3.2 Tomotherapy Plans

Due to tomotherapy not being implemented in the clinic at St. Olavs Hospital a machine model in RayStation 12A Evaluation is used for the planning for tomotherapy. The automatic script with the tomo-specific modifications was applied for all patients and several plans were made with different parameter settings. A PF of 0.15, 0.20, 0.25 and 0.30 was applied, DTf was either set to 1.0 or 1.5, and FW was either 2.51 cm or 5.05 cm. Additionally, time pressed plans were made by manually setting the maximum allowed delivery time as the shortest possible delivery time, while leaving all other parameters non-predefined. Each patient had an individual minimum delivery time for each of the FWs which is set by the TPS. For these plans the PF is automatically set to 0.43 and the DTf to 1.5.

A total of 18 plans were made for each patient and used for further evaluation. The plans were named equally for each patient depending on the parameter combination used while generating the plan. An overview of the plan names are presented in Table 4. The runtime of the automatic script varied for the different patients between 30 - 60 minutes per plan.

Table 4: Overview of plan names for the HT plans made with field width 2.51 cm and 5.05 cm according to the combination of the parameters: FW, DTf and PF.

Plan name		**DTf**	**PF**
FW 2.51 cm	**FW** 5.05 cm		
Plan 1	Plan 11	1.0	0.15
Plan 2	Plan 12		0.20
Plan 3	Plan 13		0.25
Plan 4	Plan 14		0.30
Plan 5	Plan 15	1.5	0.15
Plan 6	Plan 16		0.20
Plan 7	Plan 17		0.25
Plan 8	Plan 18		0.30
Plan 10 (min)	Plan 20 (min)	1.5	0.43

3.4 Plan Comparison and Statistical Analysis of Plan Quality

The plan quality of the HT plans was compared against the reference plans for the same patients both quantitatively and qualitatively. Quantitative comparison was performed through analysing dose statistics from RayStation. Qualitative comparisons were performed through a visual evaluation together with physicists at St. Olavs Hospital.

3.4.1 Selection of Plans

By the use of the dose statistics related to the clinical goals as well as a visual evaluation of the HT plans, the selected best and worst plans were determined for both FWs for all patients. These evaluations focused on identifying strengths and weaknesses of each HT plan and comparing the different plans with the same FW generated for each patient, as well as with the reference VMAT plans.

Several key considerations were assessed during the evaluation, including dose distribution to OARs, target volumes and to the patient's overall body volume. The conformity of the dose distribution to the target volumes and boost volumes was assessed. For the boost volumes the objective was to ensure that the 90 % isodose lines of the prescription doses of 55 Gy and 57.5 Gy, i.e. 49.5 Gy and 51.75 Gy respectively, encompassed the PTVn, while also assessing any potential dose distribution beyond the boundaries of PTVn. While for the primary dose conformity, the objective is to ensure that the 95 % of 45 Gy (42.75 Gy) followed the PTVp and PTVe. Additionally, the evaluation took into account other factors such as the occurrence and placement of hotspots within target volumes and OARs, spreading of lower dose levels, location and value of the maximum dose and sparing of OARs. Other relevant effects, such as the thread effect, was observed. The observations were made to identify which plans had clinically unacceptable dose distribution and which plans were considered the best and most favorable for both FWs for each patient.

Moreover, the dose statistics related to the clinical goals set for each patient were used for and making final decisions of the best plans, especially when deciding between plans that were evaluated as equally good through visual evaluation. Both statistics for target volumes and OARs were considered. The D_{max}, defined as the dose to 0.03 cm^3 of the volume, for xRectum-PTVn, xBowelBag-PTVn, xBladder-PTV and xBody-PTVn were used for the plan analysis. The upper limits are set to 105 % (47.3 Gy) for rectum, bowel and bladder, and 107 % (48.2 Gy) for body of the reference isodose in PTV_45 at 45 Gy. Additionally, new partial volumes were defined for a selection of the OARs. These were defined as the volume of the OAR that does not overlap with the PTV, an xOAR. Such volumes were created for rectum, bowel, bladder and body, namely xRectum, xBowelBag, xBladder and xBody. The average dose to the volume, D_{mean}, was compared for these xOARs to get a measure of dose distributed to the part of the OARs that does not intersect with the PTV.

Combining observations from visual evaluation and analysis of the dose statistics in relation to the clinical goals the best plans for all patients were determined. A selected worst plans is also included for comparison, but due to challenge in choosing between plans of bad quality the worst selected plan is more randomly selected. The selected plans are used for further comparison with the reference plans.

3.4.2 Dose Statistics and Statistical Analysis

The selected HT plans were compared to the reference plans quantitatively with DVHs, CNs and DHIs. Statistical significance of the differences was evaluated using the Wilcoxon signed-rank test.

DVH

The data for the DVHs were retrieved from RayStation with a Python script. All DVHs were plotted for a selection of xVolumes with matplotlib version 3.5.1. DVH curves were plotted for the mean cumulative dose for xRectum, xBowelBag, xBladder and xBody with data from the reference plans and the best HT plans with field width 2.51 cm and 5.05 cm. The plots include the minimum and maximum dose values, as well as the standard deviations.

CN

CNs were calculated according to Equation (1) using Python, and were used to compare the quality of the dose distributions in the reference plans and the selected HT plans. The CNs were calculated for the isodoses at 90 % of the prescribed dose to the boost volumes, PTVn_55 (49.50 Gy) and PTVn_57.5 (51.75 Gy).

DHI

DHIs were calculated according to Equation (2) using Python, and were used to compare the quality of the dose distributions in the reference plans and the selected HT plans. The DHI represents the ratio between the dose that is reached by 95 % of the volume, $D_{\geq 95\%}$, and the dose that is reached by 5 % of the volume, $D_{\geq 5\%}$. The DHIs were calculated for volume xPTV_45!, which is a volume of PTV_45 excluding PTVn, with a margin of 10 mm.

Wilcoxon Signed-Rank test

A paired Student t-test was considered for statistical analysing the data. However, this t-test assumes normal distribution of the data being analysed. A *Shapiro-Wilk* test for normality to was done for all sets of data. Measured average dose data to xBowelBag for reference plans and HT plans was not normally distributed, and it was chosen to do a non parametric test called the Wilcoxon signed-rank test, which does not assume a normal distribution and is suitable for analyzing paired data. The Wilcoxon SR-test was performed to conclude whether the median of a dose parameter deviated between the reference plans and HT plans. The p-values were evaluated for a significance level of 0.5 to determine if there is statistically significant differences in the dose distribution between

the different plan types. This test was done for the measurements of the average dose to the xOARs in reference plans and the selected best HT plans. Additionally, p-values were calculated for the mean values of corresponding the conformity indices and dose homogeneity indices. The p-values from the Wilcoxon SR-test were calculated using scipy version 1.7.3.

4 Results

4.1 Plan Evaluation

All plans were assessed both quantitatively and qualitatively, through analyzing dose statistics and visual evaluation, respectively. This section presents results relevant for the plan selection, thus the further comparison of the treatment modalities.

Quantitative analysis was performed for target volumes and OARs. Dose coverage to target volumes was sufficient for all plans regardless of treatment technique, and parameter settings for HT plans. Dose constraints for the target volumes are evaluated for percentage of volume receiving 95 % of prescribed dose to CTV_45 and PTV_45, 100 % to all CTVns and 90 % to PTVn_55 and PTVn_57.5. In the dose constraints, the accepted volume percentage is set to 99.5 % for CTV_45 and 98 % for the remaining target volumes. This was set as a requirement for clinically acceptable plans and fulfilment of dose constraints for target volumes were not analyzed further. An overview of the dose statistics for the target volumes are presented in Table C.1-C.10 in Appendix C. The dose distributed to the OARs is presented in Tables 5-14 for patient 1-10. Mean cumulative dose, D_{mean}, and max dose, defined as $D_{0.03}$, in rectum, bowel bag, bladder and body are presented in the tables for the two different volume definitions for the OARs. Depending on the patient, D_{mean} in the xOARs is generally low for the reference plans, but not consistently lower than the HT plans. The HT plans has consistently higher doses to the xOAR-PTVn volumes than the reference plan, with a very few some exceptions. The highest max doses are found for plans with lowest PF (0.15), consequently Plan 1, 5, 11, and 15. In addition, the total treatment delivery time for each plan is displayed, in minutes and seconds. The treatment delivery time for reference planning is always lower than the HT plans, and in HT planning the delivery time is dependent on parameter combination. Delivery time decreases with increasing PF and FW, and is longer for DTf 1.5 than 1. The selected best plan is marked with green ** and worst plan with red **.

The qualitatively assessment was performed by visual evaluation of the 10 patients performed together with physicists in the clinic. A selection of the plans for each patient is presented in this section due to being an essential part of the evaluation and plan comparison. Figures 9 - 28 shows screenshots of the dose distribution in the transversal plane for the reference plans and HT plans made for all patients with FW 2.51 cm and 5.05 cm, respectively. The figures present two slices in the transversal plane for the reference plan, selected best and worst HT plans, as well as HT plan with the shortest delivery time, respectively. The images are selected to give the best impression of the dose distribution and presents interesting findings for all patients. The bar to the right in each screenshot shows the color coding for the dose distribution for each dose level. The pink volume represents the 42.75 Gy reference isodose to the PTV_45. Low dose levels refer to the doses below the reference isodose for PTV_45.

4.1.1 Patients

Patient 1

Table 5 shows that mean dose to xOAR are lower for FW 2.51 cm than for FW 5.05 cm. Figure 11 and 12 shows dose distribution for FW 2.51 cm and 5.05 cm, respectively. The dose distribution of lower dose levels is isotropic throughout the body volume. Selected best HT plan for FW 5.05 cm, Plan 18, has max doses to xOAR-PTVs below 50 Gy.

Selected best and worst HT plans for patient 1 were determined to be Plan 4 and Plan 5 for FW 2.51 cm, respectively, and Plan 18 and Plan 11 for FW 5.05 cm, respectively.

Table 5: Mean cumulative dose [Gy] and max dose [Gy] in selected OARs and plan delivery times for patient 1. The xOARs are color coded from lowest (green) to highest (red) dose. For the xOAR-PTVns the colors represents whether the dose constraint set to avoid hot spots in the volume is fulfilled or not, orange if it exceeds the constraint, red if it is greater than 50 Gy. Selected best plan is marked with ** and worst plan with **.

Patient 1	**Mean cumulative dose, Dmean [Gy]**				**Max dose, D0.03 [Gy]**				**Delivery time**
Plan name	xRectum	xBowelBag	xBladder	xBody	xRectum-PTVn	xBowelBag-PTVn	xBladder-PTVn	xBody-PTVn	
Reference plan	40,95	18,81	33,74	10,30	46,94	47,11	46,48	47,59	2 min 2 s
Plan 1	40,34	21,11	34,33	11,32	48,86	52,96	51,07	55,64	17 min 38 s
Plan 2	40,90	20,80	35,19	10,95	47,60	49,83	55,13	55,47	13 min 14 s
Plan 3	40,79	20,79	36,25	10,87	47,27	49,32	53,36	53,36	10 min 35 s
Plan 4**	40,64	20,50	36,75	10,76	47,15	48,91	52,81	52,81	8 min 49 s
Plan 5**	40,15	21,14	34,00	11,36	48,59	54,12	50,28	56,55	26 min 15 s
Plan 6	40,92	20,66	34,43	10,94	47,77	50,05	52,62	53,20	19 min 42 s
Plan 7	40,79	20,56	35,16	10,87	47,26	48,56	53,20	53,20	15 min 51 s
Plan 8	40,99	20,53	36,53	10,79	47,40	48,32	52,41	53,73	13 min 15 s
Plan 10 min	40,95	20,98	34,74	10,97	48,02	48,81	49,66	52,72	6 min 11 s
Plan 11**	41,26	20,82	33,09	11,47	48,34	49,84	49,74	53,90	9 min 27 s
Plan 12	40,92	20,74	34,79	11,37	47,66	51,46	48,66	52,27	7 min 6 s
Plan 13	41,32	20,95	36,19	11,39	47,94	48,37	48,34	50,90	5 min 39 s
Plan 14	41,00	21,01	35,34	11,38	47,36	48,28	48,32	51,89	4 min 44 s
Plan 15	41,15	20,74	34,10	11,46	48,33	49,80	60,56	60,56	14 min 14 s
Plan 16	40,90	20,75	35,75	11,40	47,35	49,52	53,26	53,26	10 min 39 s
Plan 17	40,90	21,00	35,49	11,38	47,55	49,28	53,14	53,14	8 min 31 s
Plan 18**	40,72	20,80	35,47	11,24	47,34	48,22	48,84	49,15	7 min 5 s
Plan 20 min	41,74	21,54	35,51	11,55	48,66	48,37	47,84	52,19	3 min 19 s

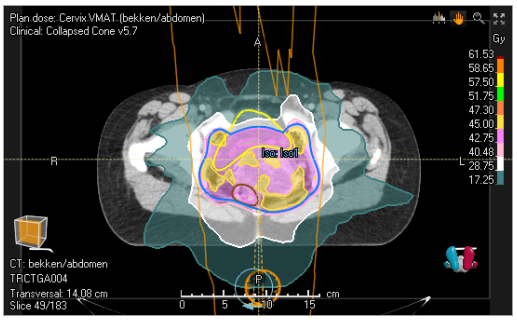

(a) Reference plan, slice 49.

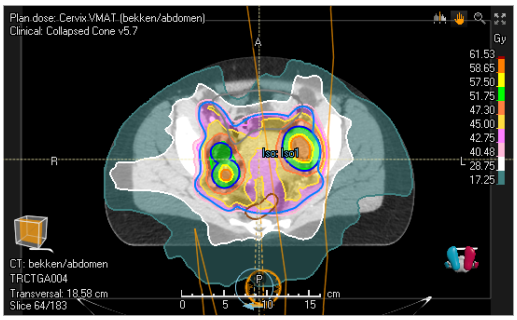

(b) Reference plan, slice 64.

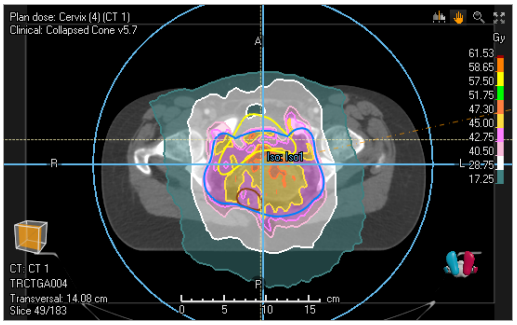

(c) Plan 4, slice 49.

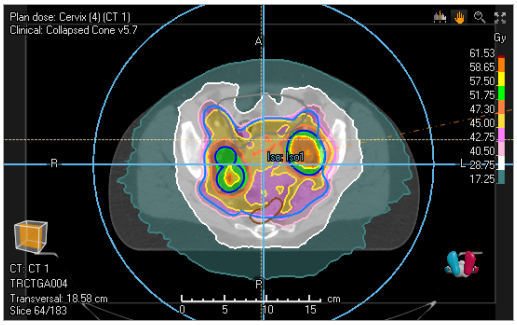

(d) Plan 4, slice 64.

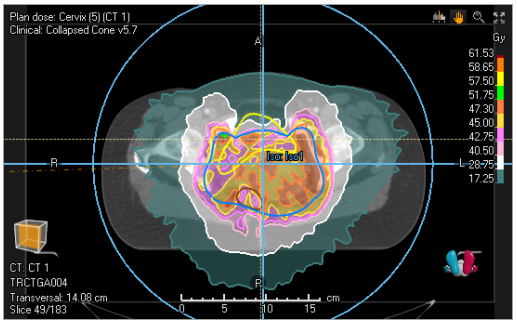

(e) Plan 5, slice 49.

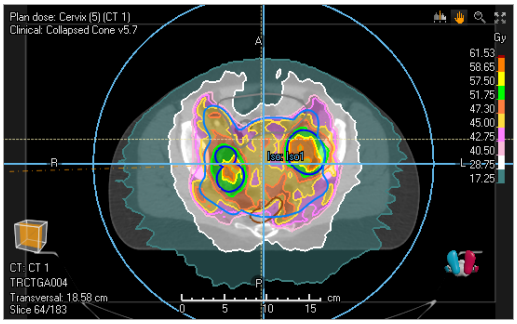

(f) Plan 5, slice 64.

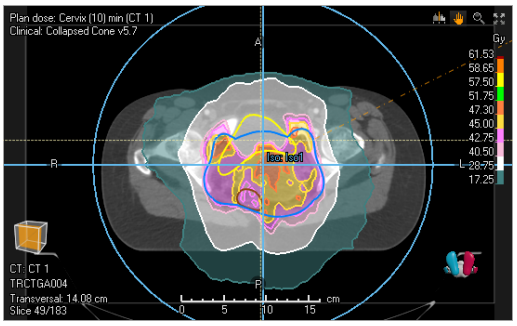

(g) Plan 10 min, slice 49.

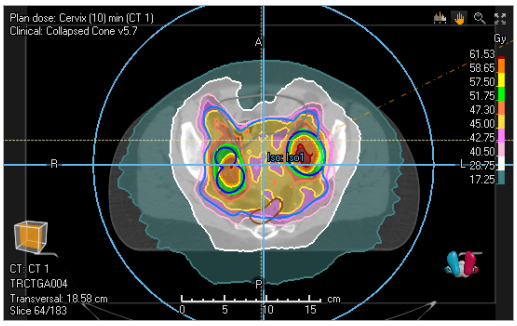

(h) Plan 10 min, slice 64.

Figure 9: Images of treatment plans made for patient 1 with FW 2.51 cm. Two slices for each row, 49 and 64: reference plan (a, b), the best HT plan (4) (c, d), worst HT plan (5) (e, f) and HT plan with minimum delivery time (10) (g, h). Isotropic distribution of lower dose levels to the body volume and horn formation in all HT plans. High conformity, comparable to reference plan, for boost volumes (PTVn_57.5) in best HT plan (d). All HT plans lack dose coverage of 95 % reference isodose (pink) to part of PTV_45 (blue) that overlaps with bladder (yellow).

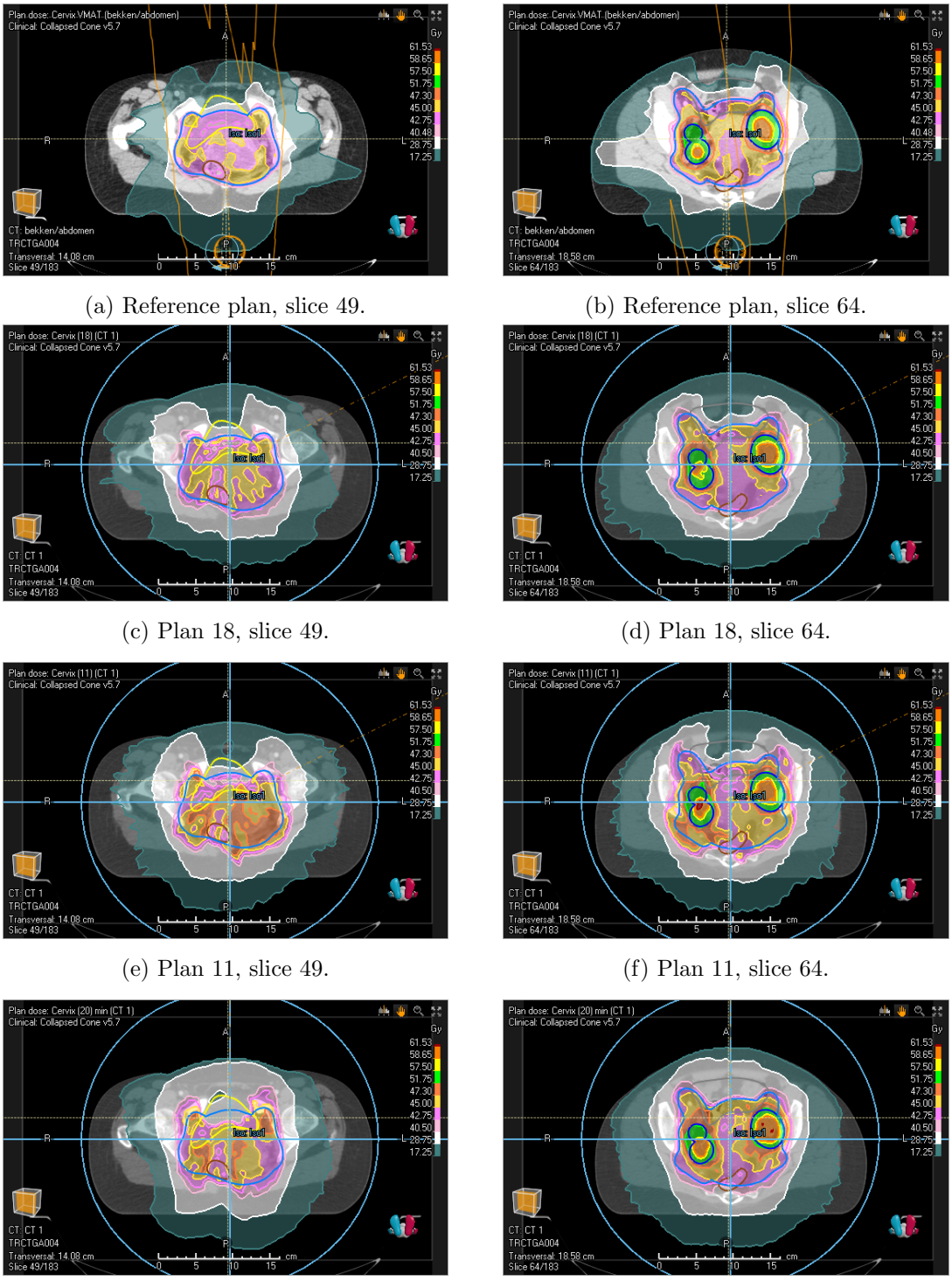

(a) Reference plan, slice 49.

(b) Reference plan, slice 64.

(c) Plan 18, slice 49.

(d) Plan 18, slice 64.

(e) Plan 11, slice 49.

(f) Plan 11, slice 64.

(g) Plan 20 min, slice 49.

(h) Plan 20 min, slice 64.

Figure 10: Images of treatment plans made for patient 1 with FW 5.05 cm. Two slices for each row, 49 and 64: reference plan (a, b), the best HT plan (18) (c, d), worst HT plan (11) (e, f) and HT plan with minimum delivery time (20) (g, h). Isotropic distribution of lower dose levels to the body volume and horn formation in all HT plans. High conformity, comparable to reference plan, for boost volumes (PTVn_57.5) in best HT plan (d). All HT plans lack dose coverage of 95 % reference isodose (pink) to part of PTV_45 (blue) that overlaps with bladder (yellow).

Patient 2

Table 6 shows that mean dose to xOAR are lower for FW 2.51 cm than for FW 5.05 cm. Max doses to xBladder-PTVn and xBody-PTVn are 56.21 Gy and 56.22 Gy respectivley, for Plan 8 although selected best plan. Figure 11 and 12 shows dose distribution for FW 2.51 cm and 5.05 cm, respectively. The dose distribution of lower dose levels is isotropic throughout the body volume. The best HT plans have high conformity, comparable to reference plan, for PTV_45 and boost volumes (PTVn_57.5).

Selected best and worst HT plans for patient 2 were determined to be Plan 8 and Plan 5 for FW 2.51 cm, respectively, and Plan 18 and Plan 11 for FW 5.05 cm, respectively.

Table 6: Mean cumulative dose [Gy] and max dose [Gy] in selected OARs and plan delivery times for patient 2. The xOARs are color coded from lowest (green) to highest (red) dose. For the xOAR-PTVns the colors represents whether the dose constraint set to avoid hot spots in the volume is fulfilled or not, orange if it exceeds the constraint, red if it is greater than 50 Gy. Selected best plan is marked with ** and worst plan with **.

Patient 2	**Mean cumulative dose, Dmean [Gy]**				**Max dose, D0.03 [Gy]**				**Delivery time**
Plan name	xRectum	xBowelBag	xBladder	xBody	xRectum-PTVn	xBowelBag-PTVn	xBladder-PTVn	xBody-PTVn	
Reference plan	31,66	23,57	34,53	14,29	46,27	47,09	47,12	47,56	2 min 3 s
Plan 1**	35,35	24,07	30,89	15,56	51,48	55,95	58,73	63,17	17 min 1 s
Plan 2	34,78	24,02	32,23	15,05	49,06	50,39	52,91	57,85	12 min 46 s
Plan 3	33,37	24,03	32,78	14,73	48,31	49,23	53,82	53,82	10 min 9 s
Plan 4	32,80	24,29	32,61	14,62	47,85	48,6	50,65	50,73	8 min 29 s
Plan 5	35,29	23,94	31,50	15,51	50,44	54,66	55,01	65,85	25 min 29 s
Plan 6	33,12	23,97	33,17	14,99	49,25	50,76	55,45	55,93	19 min 8 s
Plan 7	33,73	24,05	34,68	14,61	48,34	52,05	51,75	52,59	15 min 14 s
Plan 8**	33,53	23,99	34,96	14,46	47,66	52,6	56,21	56,22	12 min 45 s
Plan 10 min	33,75	25,01	32,71	14,69	48,36	48,73	51,05	51,79	5 min 57 s
Plan 11**	37,43	24,58	33,63	15,89	50,60	54,06	56,09	64,12	9 min 8 s
Plan 12	37,18	25,01	33,80	15,63	49,33	50,85	53,71	56,70	6 min 50 s
Plan 13	37,36	25,14	33,95	15,53	48,43	49,87	51,73	54,03	5 min 28 s
Plan 14	36,55	25,40	34,04	15,44	48,09	49,37	52,13	52,48	4 min 34 s
Plan 15	37,18	24,77	33,62	15,81	50,18	52,66	54,56	62,15	13 min 40 s
Plan 16	36,94	24,92	34,40	15,59	49,09	50,62	51,31	55,69	10 min 16 s
Plan 17	37,18	24,47	35,41	15,42	49,06	49,4	50,64	52,46	8 min 11 s
Plan 18**	36,50	24,70	35,52	15,18	47,49	48,47	49,49	50,10	6 min 51 s
Plan 20 min	37,11	26,15	33,81	15,72	48,99	49,41	52,02	52,44	3 min 13 s

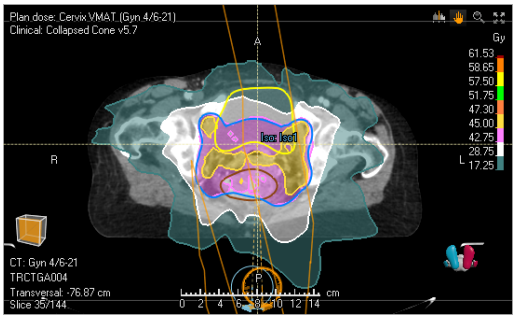

(a) Reference plan, slice 35.

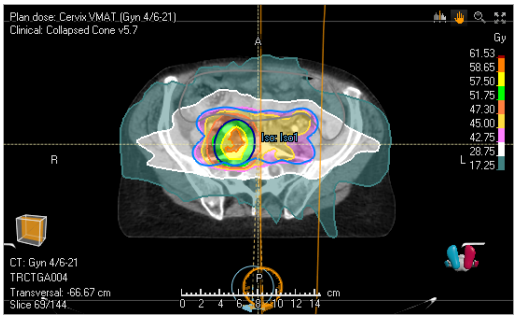

(b) Reference plan, slice 69.

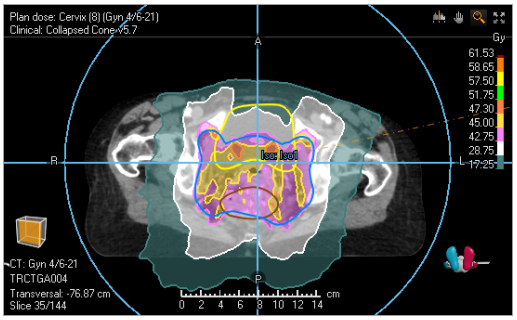

(c) Plan 8, slice 35.

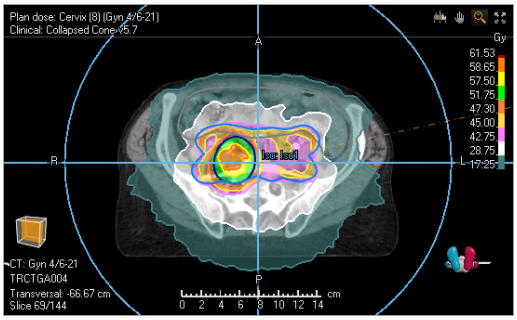

(d) Plan 8, slice 69.

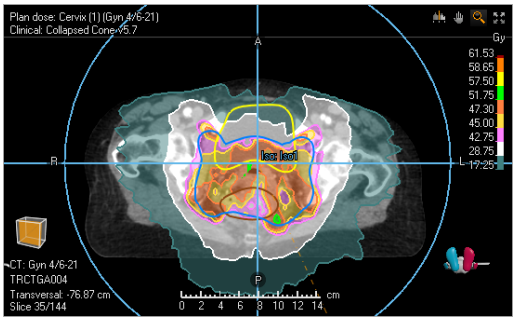

(e) Plan 5, slice 35.

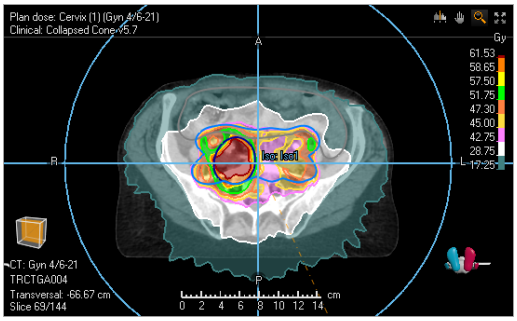

(f) Plan 5, slice 69.

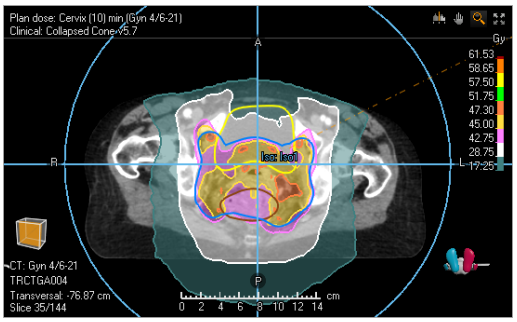

(g) Plan 10 min, slice 33.

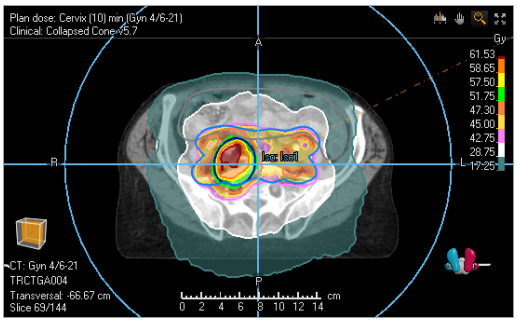

(h) Plan 10 min, slice 50.

Figure 11: Images of treatment plans made for patient 2 with FW 2.51 cm. Two slices for each row, 35 and 69: reference plan (a, b), the best HT plan (8) (c, d), worst HT plan (1) (e, f) and HT plan with minimum delivery time (10) (g, h). Isotropic distribution of lower dose levels to the body volume and horn formation in all HT plans. High conformity, comparable to reference plan, for PTV_45 and boost volumes (PTVn_57.5) in best HT plan (d). In the best hT, plan hot spots are placed with in bladder (yellow) volume.

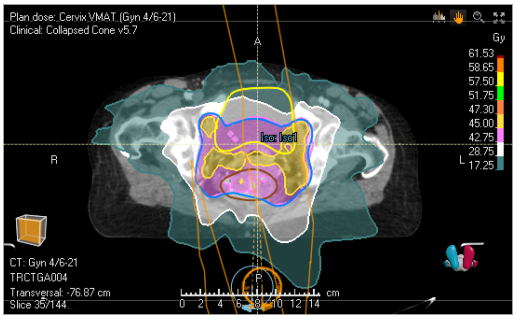

(a) Reference plan, slice 35.

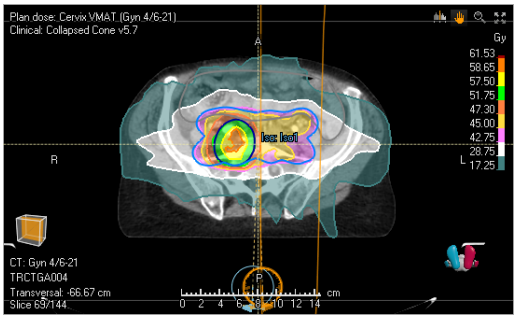

(b) Reference plan, slice 69.

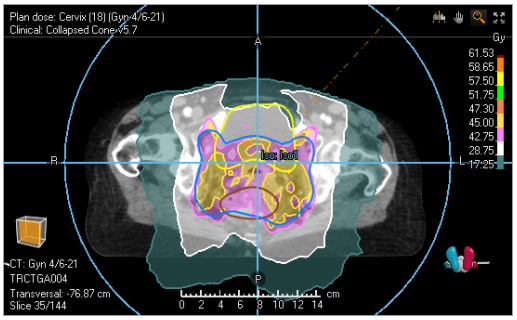

(c) Plan 18, slice 49.

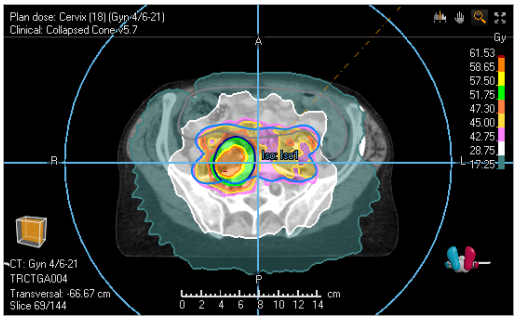

(d) Plan 18, slice 69.

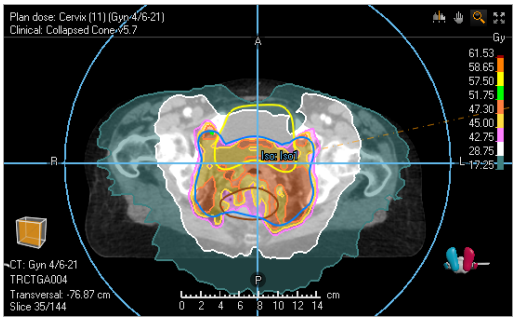

(e) Plan 11, slice 35.

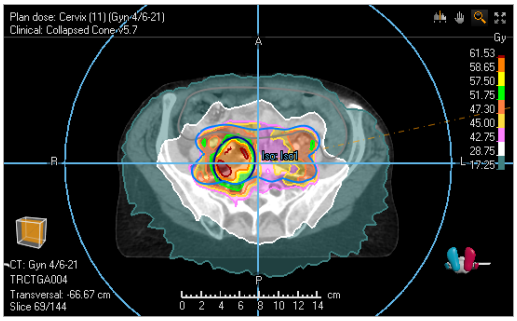

(f) Plan 11, slice 69.

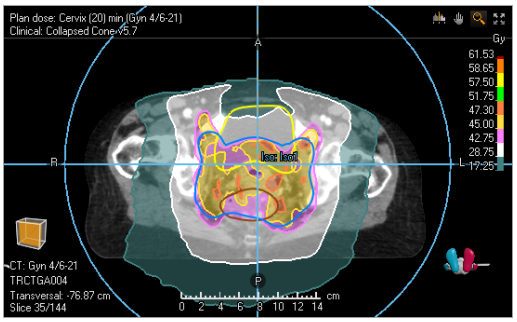

(g) Plan 20 min, slice 35.

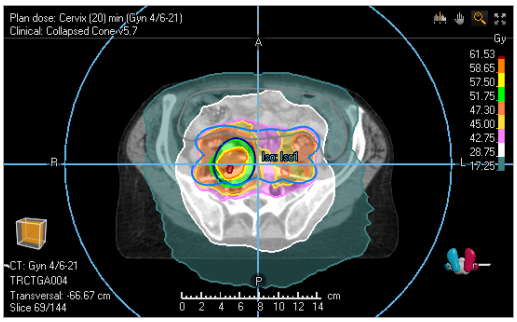

(h) Plan 20 min, slice 69.

Figure 12: Images of treatment plans made for patient 2 with FW 5.05 cm. Two slices for each row, 35 and 69: reference plan (a, b), the best HT plan (18) (c, d), worst HT plan (11) (e, f) and HT plan with minimum delivery time (20) (g, h). Isotropic distribution of lower dose levels to the body volume and horn formation in all HT plans. High conformity, comparable to reference plan, for PTV_45 and boost volumes (PTVn_57.5) in best HT plan (d).

Patient 3

Table 7 shows that mean dose to xOAR are lower for FW 2.51 cm than for FW 5.05 cm. Figure 13 and 14 shows dose distribution for FW 2.51 cm and 5.05 cm, respectively. The dose distribution of lower dose levels is isotropic throughout the body volume.

Selected best and worst HT plans for patient 3 were determined to be Plan 8 and Plan 5 for FW 2.51 cm, respectively, and Plan 14 and Plan 11 for FW 5.05 cm, respectively.

Table 7: Mean cumulative dose [Gy] and max dose [Gy] in selected OARs and plan delivery times for patient 3. The xOARs are color coded from lowest (green) to highest (red) dose. For the xOAR-PTVns the colors represents whether the dose constraint set to avoid hot spots in the volume is fulfilled or not, orange if it exceeds the constraint, red if it is greater than 50 Gy. Selected best plan is marked with ** and worst plan with **.

Patient 3	**Mean cumulative dose, Dmean [Gy]**				**Max dose, D0.03 [Gy]**				**Delivery time**
Plan name	xRectum	xBowelBag	xBladder	xBody	xRectum-PTVn	xBowelBag-PTVn	xBladder-PTVn	xBody-PTVn	
Reference plan	40,66	19,40	37,66	15,05	47,05	47,24	47,05	48,11	2 min 4 s
Plan 1**	39,65	20,74	38,00	16,64	54,23	55,09	54,23	58,93	17 min 28 s
Plan 2	40,94	20,62	37,92	16,04	52,87	50,37	52,87	53,25	13 min 12 s
Plan 3	41,04	20,60	38,00	15,80	51,96	52,58	51,96	52,96	10 min 37 s
Plan 4	40,97	20,58	38,00	15,67	51,91	52,25	51,91	52,54	8 min 50 s
Plan 5	39,55	20,78	37,38	16,77	52,94	54,75	52,94	58,98	26 min 21 s
Plan 6	41,08	20,58	38,49	16,13	53,29	49,58	53,29	53,30	19 min 51 s
Plan 7	41,18	20,63	38,09	15,91	52,13	50,56	52,13	52,13	15 min 54 s
Plan 8**	40,89	20,51	37,92	15,69	52,05	51,78	52,05	52,05	13 min 15 s
Plan 10 min	41,10	20,59	38,08	15,77	50,31	49,41	50,31	50,50	6 in 12 s
Plan 11**	41,08	20,84	37,77	16,74	50,96	51,73	50,96	56,61	9 min 21 s
Plan 12	41,64	20,97	37,96	16,60	50,97	51,07	50,97	53,29	7 min 3 s
Plan 13	41,52	21,02	38,32	16,54	49,03	49,76	49,03	51,84	5 min 39 s
Plan 14**	41,24	21,12	38,24	16,48	49,73	49,00	49,73	52,48	4 min 39 s
Plan 15	40,84	20,78	38,30	16,65	58,01	51,92	58,01	58,01	14 min 0 s
Plan 16	41,38	20,94	38,65	16,54	52,88	49,67	52,88	52,88	10 min 33 s
Plan 17	41,57	20,97	39,26	16,51	52,01	48,62	52,01	52,01	8 min 28 s
Plan 18	41,14	20,95	39,51	16,36	52,99	47,98	52,99	52,99	7 min 2 s
Plan 20 min	42,06	21,44	37,18	16,79	50,50	48,84	50,50	51,73	3 min 21 s

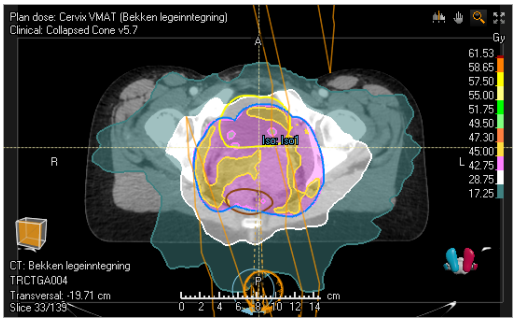

(a) Reference plan, slice 33.

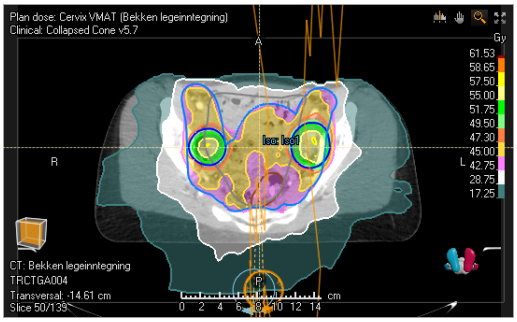

(b) Reference plan, slice 50.

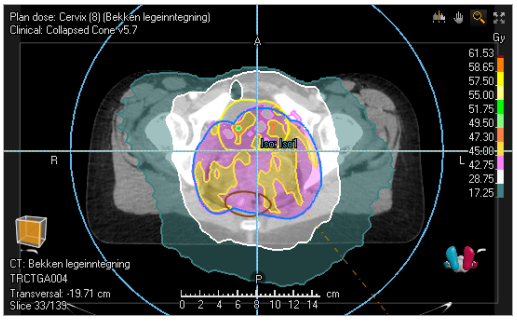

(c) Plan 8, slice 33.

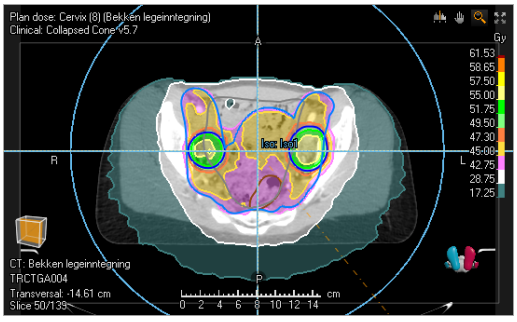

(d) Plan 8, slice 50.

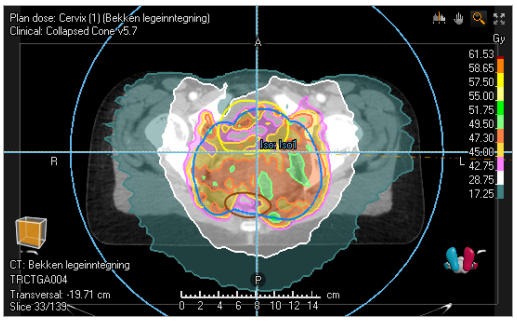

(e) Plan 5, slice 33.

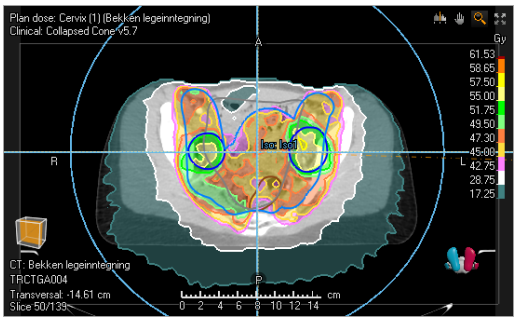

(f) Plan 5, slice 50.

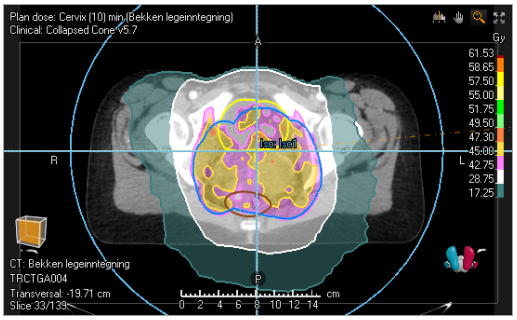

(g) Plan 10 min, slice 33.

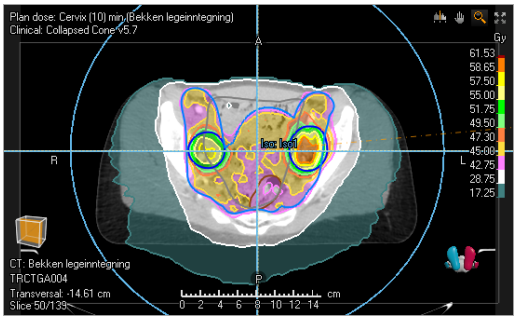

(h) Plan 10 min, slice 50.

Figure 13: Images of treatment plans made for patient 3 with FW 2.51 cm. Two slices for each row, 33 and 50: reference plan (a, b), the best HT plan (8) (c, d), worst HT plan (1) (e, f) and HT plan with minimum delivery time (10) (g, h). Isotropic distribution of lower dose levels to the body volume and horn formation in all HT plans. The best and time pressed HT plans lack dose coverage of 95 % reference isodose (pink) to part of PTV_45 (blue) that overlaps with bladder (yellow), while the best HT plan has placed hot spots within the bladder (c). High conformity, comparable to reference plan, for PTV_45 and boost volumes (PTVn_57.5) in best HT plan (d).

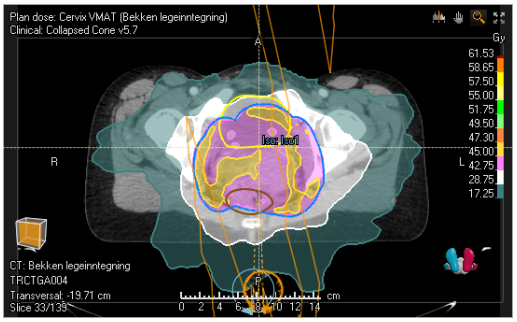

(a) Reference plan, slice 33.

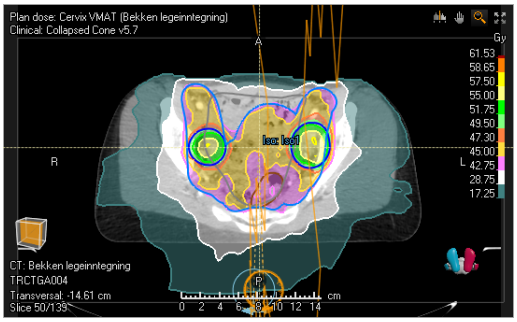

(b) Reference plan, slice 50.

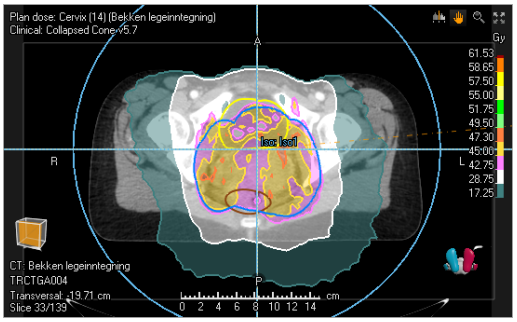

(c) Plan 14, slice 33.

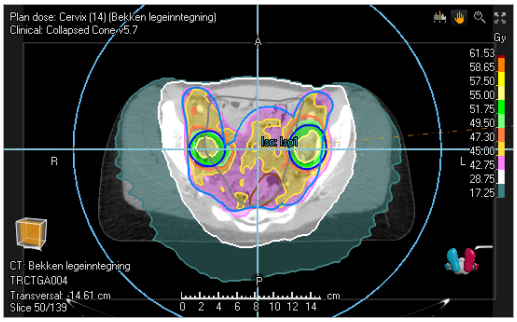

(d) Plan 14, slice 50.

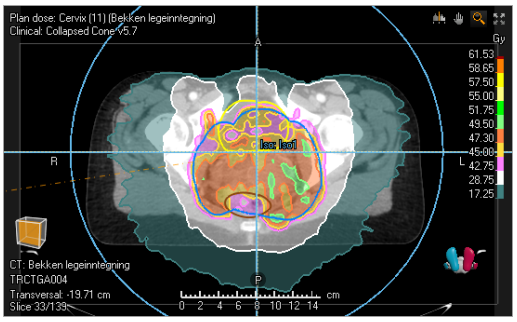

(e) Plan 11, slice 33.

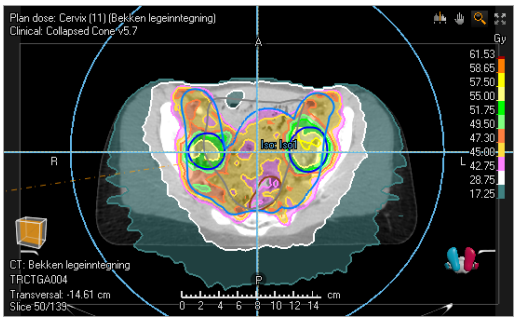

(f) Plan 11, slice 50.

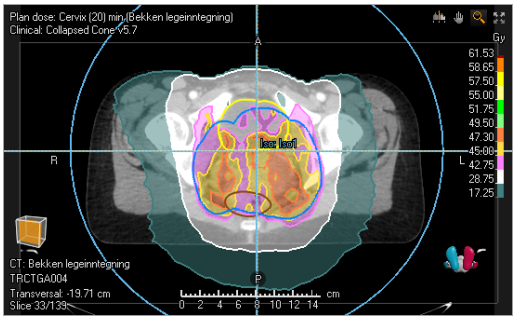

(g) Plan 20 min, slice 49.

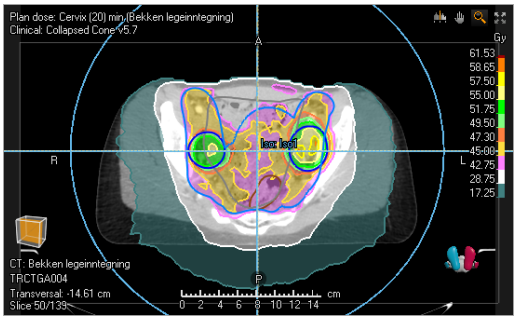

(h) Plan 20 min, slice 50.

Figure 14: Images of treatment plans made for patient 3 with FW 5.05 cm. Two slices for each row, 33 and 50: reference plan (a, b), the best HT plan (14) (c, d), worst HT plan (11) (e, f) and HT plan with minimum delivery time (20) (g, h). Isotropic distribution of lower dose levels to the body volume and horn formation in all HT plans. The best and time pressed HT plans lack dose coverage of 95 % reference isodose (pink) to part of PTV_45 (blue) that overlaps with bladder (yellow), while the worst HT plan places high dose levels with in the bladder volume. Lower conformity, compared to reference plan for boost volumes (PTVn_45 and PTVn_57.5) in best HT plan (d).

Patient 4

Table 8 shows that mean dose to xOAR are lower for FW 2.51 cm than for FW 5.05 cm. Max doses to xBladder-PTVn and xBody-PTVn are 56.73 Gy (both volumes) for Plan 4 and 51.07 Gy and 57.73 Gy for Plan 14, respectively. Figure 15 and 16 shows dose distribution for FW 2.51 cm and 5.05 cm, respectively. Formation of horns are observed for lower dose levels in all HT plans.

Selected best and worst HT plans for patient 4 were determined to be Plan 4 and Plan 1 for FW 2.51 cm, respectively, and Plan 14 and Plan 11 for FW 5.05 cm, respectively.

Table 8: Mean cumulative dose [Gy] and max dose [Gy] in selected OARs and plan delivery times for patient 4. The xOARs are color coded from lowest (green) to highest (red) dose. For the xOAR-PTVns the colors represents whether the dose constraint set to avoid hot spots in the volume is fulfilled or not, orange if it exceeds the constraint, red if it is greater than 50 Gy. Selected best plan is marked with ** and worst plan with **.

Patient 4	**Mean cumulative dose, Dmean [Gy]**				**Max dose, D0.03 [Gy]**				**Delivery time**
Plan name	xRectum	xBowelBag	xBladder	xBody	xRectum-PTVn	xBowelBag-PTVn	xBladder-PTVn	xBody-PTVn	
Reference plan	39,65	24,90	35,63	11,10	46,11	47,11	47,06	47,65	2 min 5 s
Plan 1**	40,67	26,68	35,39	12,96	50,17	53,37	54,94	57,61	9 min 23 s
Plan 2	40,75	26,85	35,72	12,59	49,54	55,81	58,49	58,49	6 min 59 s
Plan 3	41,06	27,14	37,02	12,28	48,92	52,18	52,54	52,54	5 min 32 s
Plan 4**	41,57	27,39	36,47	12,22	49,94	51,85	56,73	56,73	4 min 39 s
Plan 5	40,34	26,72	35,40	12,93	49,89	52,57	53,14	55,30	13 min 58 s
Plan 6	40,58	26,65	37,84	12,47	48,07	56,34	60,14	60,14	10 min 26 s
Plan 7	40,99	26,83	37,50	12,23	48,46	55,61	56,78	57,06	8 min 22 s
Plan 8	40,82	26,88	37,91	12,08	48,39	59,93	60,68	60,68	6 min 57 s
Plan 10 min	41,60	29,28	34,57	12,60	48,85	49,88	51,12	51,53	3 min 17 s
Plan 11**	39,73	27,37	36,25	13,28	49,37	50,42	51,50	54,79	5 min 14 s
Plan 12	40,46	27,86	36,45	13,27	48,90	50,58	50,65	53,40	3 min 57 s
Plan 13	40,83	28,24	36,14	13,27	48,65	51,23	50,67	53,97	3 min 17 s
Plan 14**	40,68	28,65	35,09	13,31	49,04	50,09	51,07	53,87	2 min 38 s
Plan 15	39,87	27,23	37,83	13,19	49,21	51,06	55,60	55,60	7 min 54 s
Plan 16	39,92	27,54	37,71	13,16	48,06	52,33	52,98	53,02	5 min 55 s
Plan 17	40,56	27,78	37,93	13,08	48,87	52,01	52,70	52,70	4 min 47 s
Plan 18	40,95	28,23	36,85	13,06	49,20	52,56	53,57	53,66	3 min 58 s
Plan 20 min	42,64	31,11	34,21	14,10	52,02	50,42	54,43	57,97	1 min 54 s

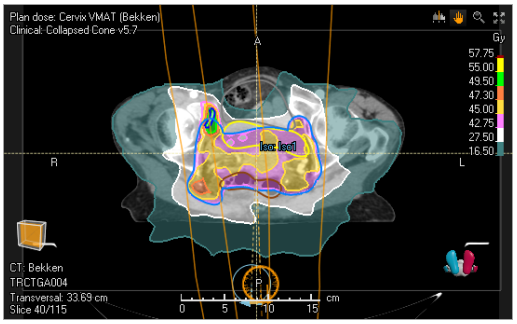

(a) Reference plan, slice 40.

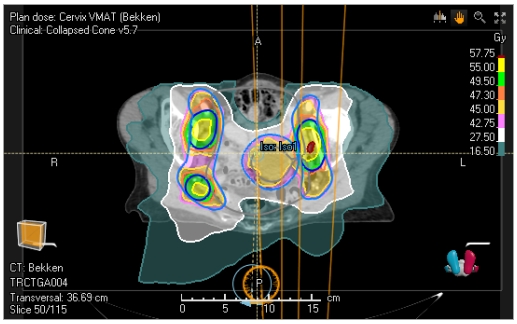

(b) Reference plan, slice 50.

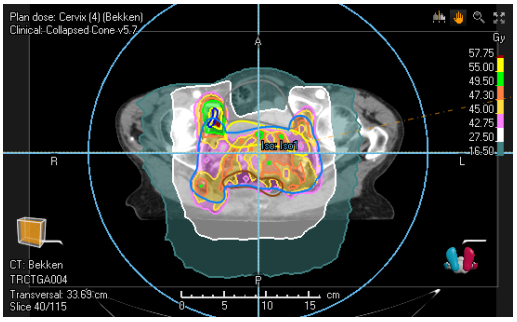

(c) Plan 4, slice 40.

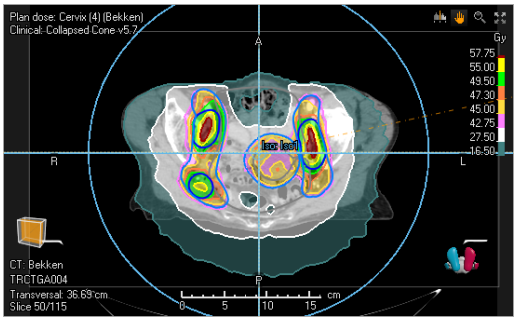

(d) Plan 4, slice 50.

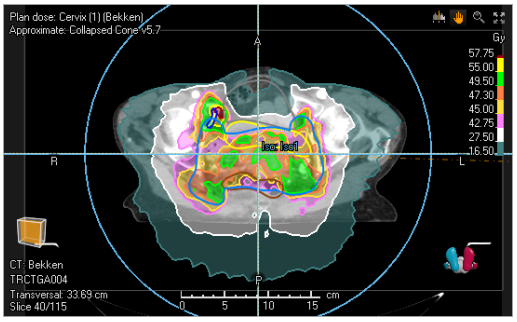

(e) Plan 1, slice 33.

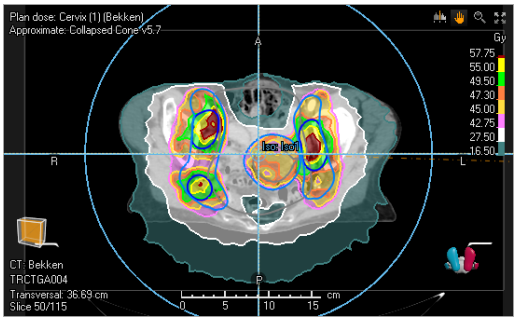

(f) Plan 1, slice 50.

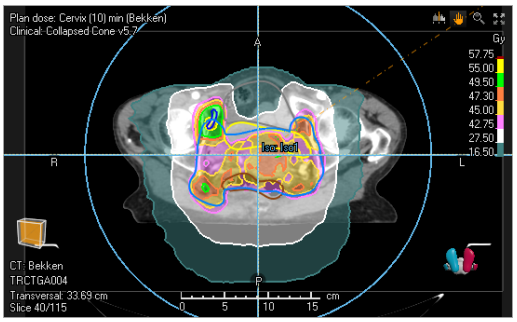

(g) Plan 10 min, slice 40.

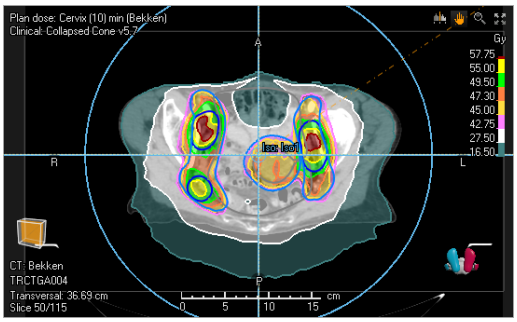

(h) Plan 10 min, slice 50.

Figure 15: Images of treatment plans made for patient 4 with FW 2.51 cm. Two slices for each row, 40 and 50: reference plan (a, b), the best HT plan (4) (c, d), worst HT plan (1) (e, f) and HT plan with minimum delivery time (10) (g, h). Isotropic distribution of lower dose levels to the body volume, especially by formation of horns in all HT plans, also present in reference plans. Lower conformity in all HT plans for PTV_45 and boost volumes (PTVn_57.5) compared to reference plans. High dose levels (47.3 Gy) are placed inside part of bladder (yellow) that intersect with PTV_45 (blue) best and worst HT plans, as well as hot spots in time pressed plans (c, e).

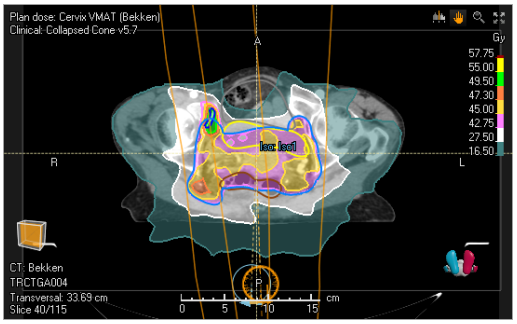

(a) Reference plan, slice 40.

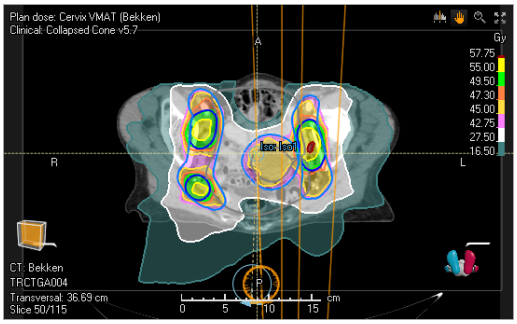

(b) Reference plan, slice 50.

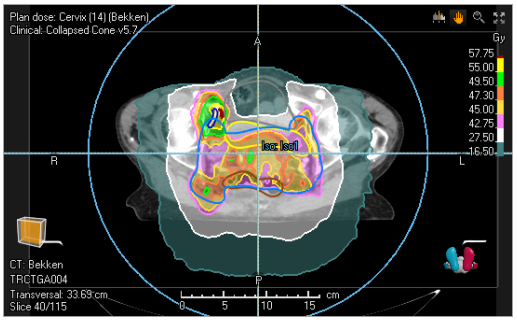

(c) Plan 14, slice 40.

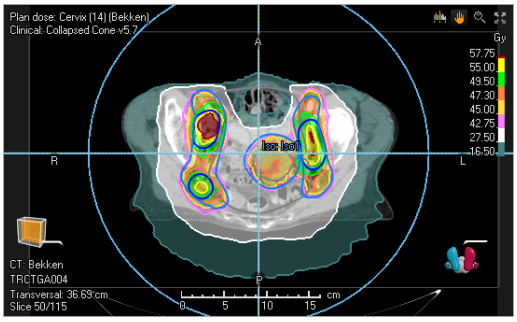

(d) Plan 14, slice 50.

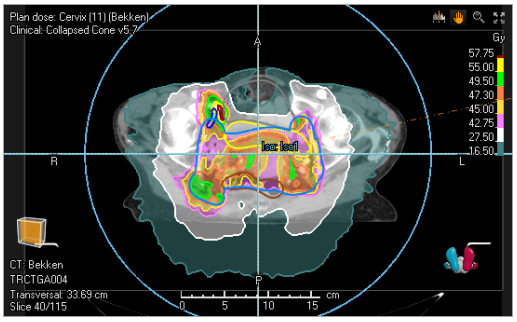

(e) Plan 11, slice 40.

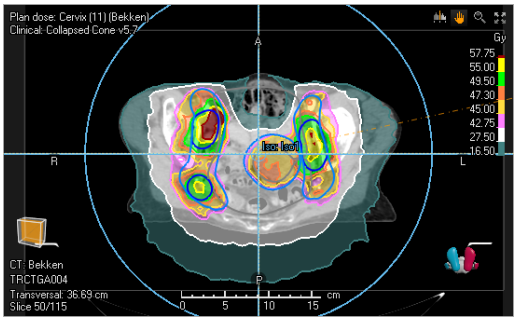

(f) Plan 11, slice 50.

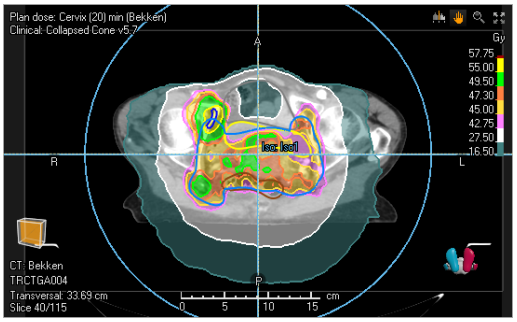

(g) Plan 20 min, slice 49.

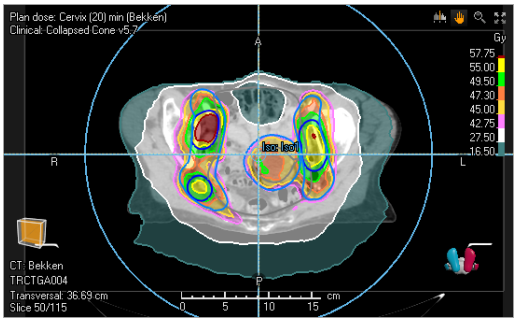

(h) Plan 20 min, slice 50.

Figure 16: Images of treatment plans made for patient 4 with FW 5.05 cm. Two slices for each row, 40 and 50: reference plan (a, b), the best HT plan (14) (c, d), worst HT plan (11) (e, f) and HT plan with minimum delivery time (20) (g, h). Isotropic distribution of lower dose levels to the body volume, especially by formation of horns in all HT plans, which is also present in reference plans. Lower conformity in all HT plans for PTV_45 and boost volumes (PTVn_57.5) compared to reference plans. High dose levels (47.3 Gy) and hot spots (49.50 Gy) (g) are placed inside part of bladder (yellow) that intersect with PTV_45 (blue) best and worst HT plans.

Patient 5

Table 9 shows that mean dose to xOAR are lower for FW 2.51 cm than for FW 5.05 cm. Figure 17 and 18 shows dose distribution for FW 2.51 cm and 5.05 cm, respectively. Isotropic distribution of lower dose levels to the body volume, as well as formation of horns in all HT plans.

Selected best and worst HT plans for patient 5 were determined to be Plan 4 and Plan 1 for FW 2.51 cm, respectively, and Plan 14 and Plan 11 for FW 5.05 cm, respectively.

Table 9: Mean cumulative dose [Gy] and max dose [Gy] in selected OARs and plan delivery times for patient 5. The xOARs are color coded from lowest (green) to highest (red) dose. For the xOAR-PTVns the colors represents whether the dose constraint set to avoid hot spots in the volume is fulfilled or not, orange if it exceeds the constraint, red if it is greater than 50 Gy. Selected best plan is marked with ** and worst plan with **.

Patient 5	**Mean cumulative dose, Dmean [Gy]**				**Max dose, D0.03 [Gy]**				**Delivery time**
Plan name	xRectum	xBowelBag	xBladder	xBody	xRectum-PTVn	xBowelBag-PTVn	xBladder-PTVn	xBody-PTVn	
Reference plan	29,04	17,46	25,71	9,78	46,99	47,06	47,05	47,60	2 min 6 s
Plan 1**	26,16	20,72	23,39	11,39	48,92	55,43	51,00	57,40	17 min 3 s
Plan 2	27,73	19,84	24,1	10,85	48,4	47,1	57,85	57,85	12 min 48 s
Plan 3	28,89	19,69	24,41	10,66	47,86	47,12	50,53	50,53	10 min 14 s
Plan 4**	29,09	19,44	23,83	10,48	47,32	47,07	50,66	50,66	8 min 32 s
Plan 5	26,33	20,53	23,08	11,34	48,66	54,39	54,31	56,77	25 min 36 s
Plan 6	27,95	19,91	24,4	10,87	48,21	47,23	57,22	57,22	19 min 12 s
Plan 7	28,69	19,7	25,11	10,66	47,88	47,58	56,57	56,57	15 min 21 s
Plan 8	28,96	19,27	25,04	10,47	48,71	47,05	54,95	54,95	12 min 47 s
Plan 10 min	30,74	19,31	26,37	10,38	47,33	47,7	49,43	49,86	5 min 57 s
Plan 11**	30,16	19,97	22,35	11,26	48,39	51,97	49,26	53,65	9 min 13 s
Plan 12	31,31	20	24,11	11,17	47,63	47,5	55,33	55,33	6 min 55 s
Plan 13	31,6	20,14	24,34	11,16	47,49	47,63	49,21	50,57	5 min 32 s
Plan 14**	31,66	20,01	24,78	11,01	47,69	47,66	50,87	50,87	4 min 37 s
Plan 15	30,33	19,85	23,56	11,22	47,8	50,77	53,26	53,26	13 min 48 s
Plan 16	31,34	19,87	23,74	11,14	47,64	47,51	53,37	53,37	10 min 22 s
Plan 17	31,64	20,05	24,88	11,14	47,48	48,92	56,86	56,86	8 min 18 s
Plan 18	31,5	19,83	25,02	10,94	47,04	48,58	54,57	54,57	6 min 55 s
Plan 20 min	32,33	20,26	28,01	10,99	47,98	47,84	48,88	51,50	3 min 13 s

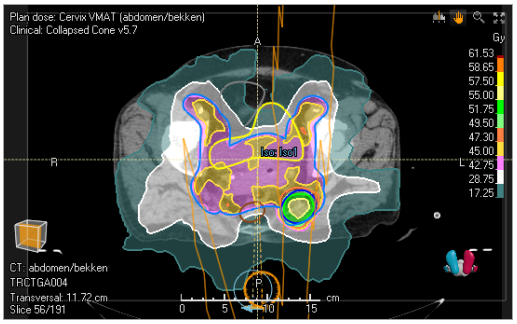

(a) Reference plan, slice 56.

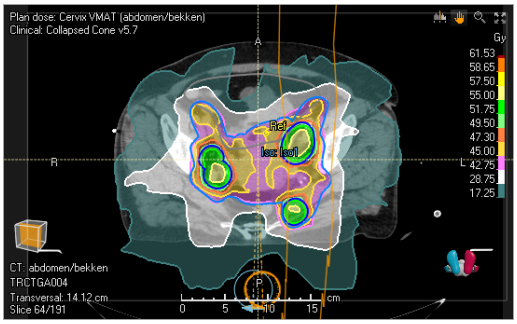

(b) Reference plan, slice 64.

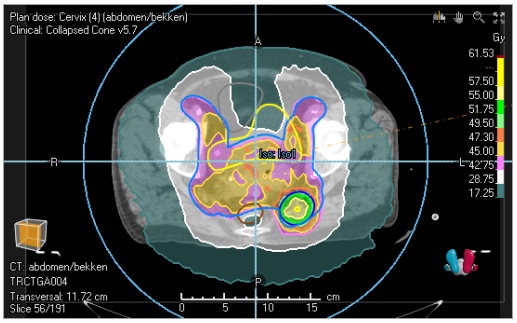

(c) Plan 4, slice 56.

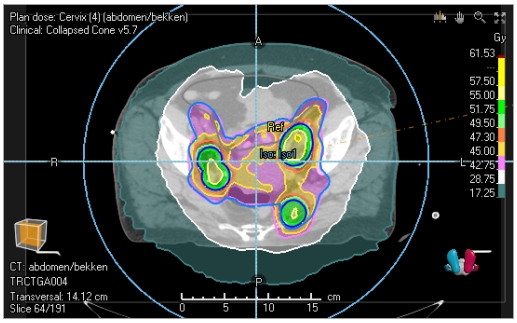

(d) Plan 4, slice 64.

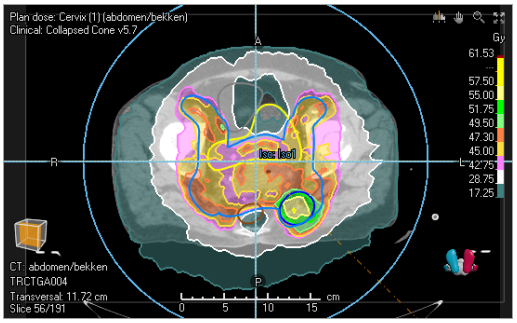

(e) Plan 1, slice 56.

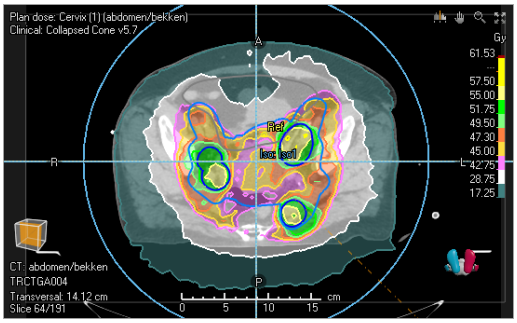

(f) Plan 1, slice 64.

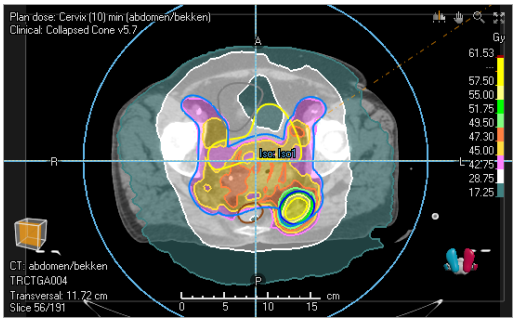

(g) Plan 10 min, slice 56.

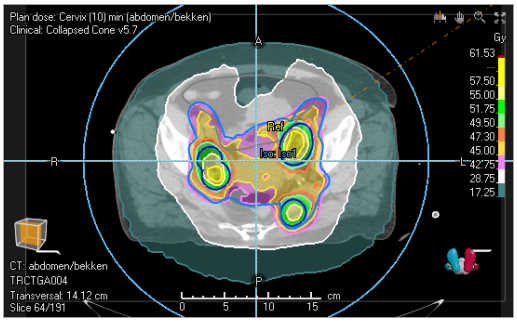

(h) Plan 10 min, slice 64.

Figure 17: Images of treatment plans made for patient 5 with FW 2.51 cm. Two slices for each row, 56 and 64: reference plan (a, b), the best HT plan (4) (c, d), worst HT plan (1) (e, f) and HT plan with minimum delivery time (10) (g, h). Isotropic distribution of lower dose levels to the bowel and the body volume, as well as formation of horns in all HT plans. Comparable conformity for PTV_45 and boost volumes (PTVn_55 and PTVn_57.5) in best HT plans. In all HT plans, high dose levels (47.3 Gy) are placed inside part of bladder (yellow) that intersect with PTV_45.

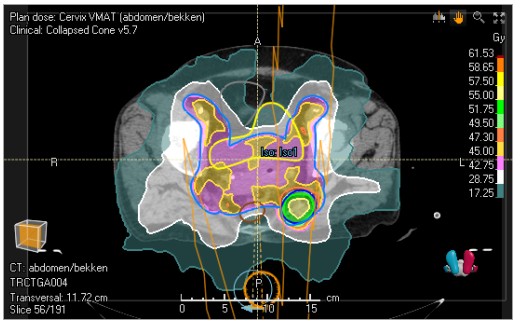

(a) Reference plan, slice 56.

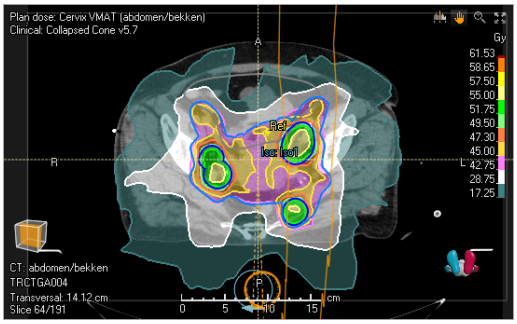

(b) Reference plan, slice 64.

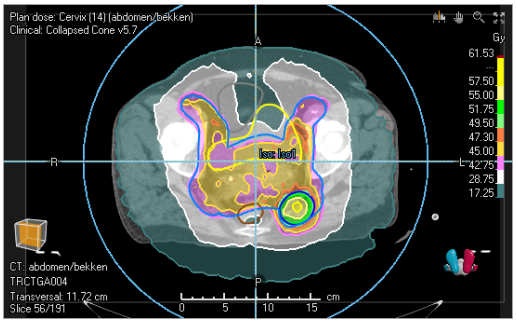

(c) Plan 14, slice 56.

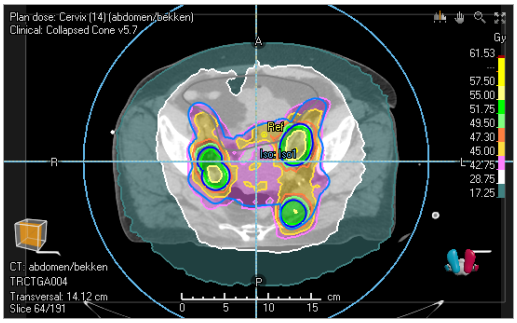

(d) Plan 14, slice 64.

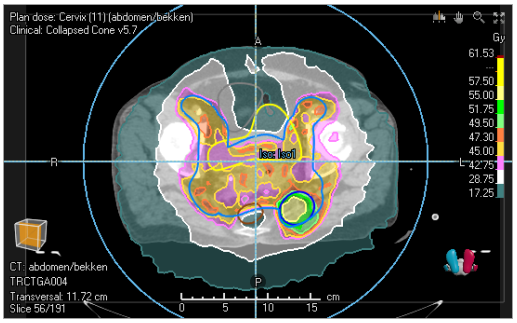

(e) Plan 11, slice 56.

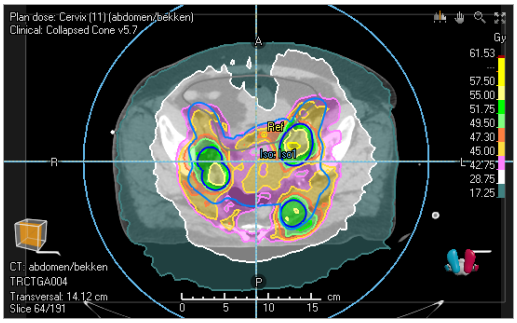

(f) Plan 11, slice 64.

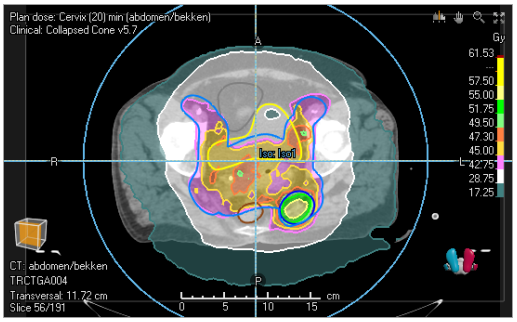

(g) Plan 20 min, slice 56.

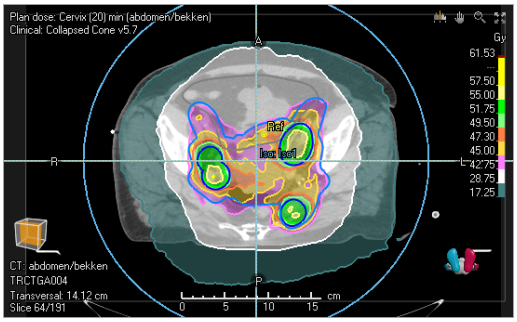

(h) Plan 20 min, slice 64.

Figure 18: Images of treatment plans made for patient 5 with FW 5.05 cm. Two slices for each row, 56 and 64: reference plan (a, b), the best HT plan (14) (c, d), worst HT plan (11) (e, f) and HT plan with minimum delivery time (20) (g, h). Isotropic distribution of lower dose levels to the bowel and the body volume, as well as formation of horns in all HT plans. Lower conformity for PTV_45 and boost volumes (PTVn_55 and PTVn_57.5) in all HT plans in terms of aligning to contour of PTV (blue) as well as breaks within the dose distribution of the reference isodose of 42.75 Gy. In all HT plans, high dose levels (47.3 Gy) are placed inside part of bladder (yellow) that intersect with PTV_45.

Patient 6

Table 10 shows that mean dose to xOAR are lower for FW 2.51 cm than for FW 5.05 cm. For xBladder, mean dose values are lower for almost all HT plans than for the reference plan. Very high max doses xOAR-PTVn, even for the selected best HT plans max dose to xBody-PTVn are 62.73 Gy and 60.70 Gy for Plan 4 and Plan 18, respectively. Figure 19 and 20 shows dose distribution for FW 2.51 cm and 5.05 cm, respectively. Isotropic distribution of lower dose levels to the body volume, as well as formation of horns in all HT plans, whereas reference plan distribute dose to the sides.

Selected best and worst HT plans for patient 6 were determined to be Plan 4 and Plan 1 for FW 2.51 cm, respectively, and Plan 18 and Plan 15 for FW 5.05 cm, respectively.

Table 10: Mean cumulative dose [Gy] and max dose [Gy] in selected OARs and plan delivery times for patient 6. The xOARs are color coded from lowest (green) to highest (red) dose. For the xOAR-PTVns the colors represents whether the dose constraint set to avoid hot spots in the volume is fulfilled or not, orange if it exceeds the constraint, red if it is greater than 50 Gy. Selected best plan is marked with ** and worst plan with **.

Patient 6	**Mean cumulative dose, Dmean [Gy]**				**Max dose, D0.03 [Gy]**				**Delivery time**
Plan name	xRectum	xBowelBag	xBladder	xBody	xRectum-PTVn	xBowelBag-PTVn	xBladder-PTVn	xBody-PTVn	
Reference plan	30,80	19,81	29,14	13,04	47,00	47,08	47,03	47,92	2 min 6 s
Plan 1**	31,68	21,31	23,87	13,37	48,71	48,81	59,51	60,29	14 min 52 s
Plan 2	32,27	21,30	25,67	13,22	48,93	48,94	58,33	60,26	11 min 16 s
Plan 3	32,99	21,29	26,78	13,20	47,44	48,16	51,54	60,59	8 min 59 s
Plan 4**	33,46	21,30	27,28	13,15	47,39	47,51	49,54	62,73	7 min 30 s
Plan 5	31,90	21,37	25,37	13,47	48,95	48,97	69,14	69,14	22 min 18 s
Plan 6	32,55	21,24	25,64	13,20	48,44	48,48	62,71	62,71	16 min 49 s
Plan 7	32,72	21,18	26,31	13,14	47,66	48,90	58,30	60,00	13 min 28 s
Plan 8	32,72	21,00	27,07	13,11	48,00	48,25	56,49	59,84	11 min 14 s
Plan 10 min	35,76	21,88	29,60	13,22	49,91	49,39	48,31	61,43	5 miin 14 s
Plan 11	33,92	21,36	24,44	13,60	47,49	49,40	50,45	60,49	8 min 1 s
Plan 12	34,39	21,73	25,73	13,81	47,56	48,48	52,40	60,89	6 min 4 s
Plan 13	34,60	21,73	26,96	13,84	47,46	48,31	57,80	60,60	7 min 21 s
Plan 14	35,18	22,22	28,29	13,78	47,63	47,72	48,73	62,27	4 min 4 s
Plan 15**	34,06	21,33	25,17	13,62	47,99	49,23	55,10	60,20	12 min 0 s
Plan 16	34,23	21,54	26,00	13,70	47,98	48,78	50,80	60,41	9 min 6 s
Plan 17	34,60	21,73	26,96	13,84	47,46	48,31	57,80	60,60	7 min 21 s
Plan 18**	34,38	21,69	27,33	13,70	47,13	48,63	52,47	60,70	6 min 6 s
Plan 20 min	37,36	22,98	29,58	14,15	47,38	48,26	48,43	61,40	2 min 53 s

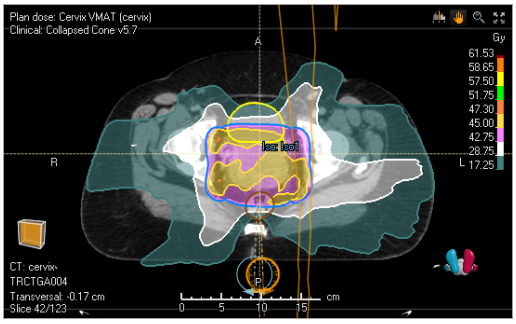

(a) Reference plan, slice 42.

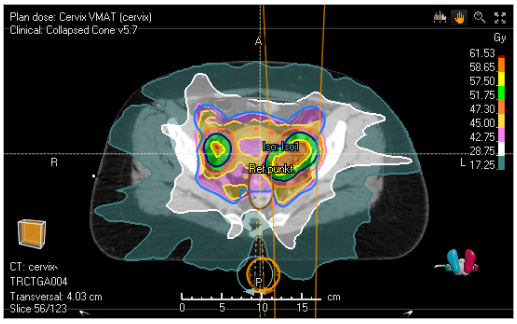

(b) Reference plan, slice 56.

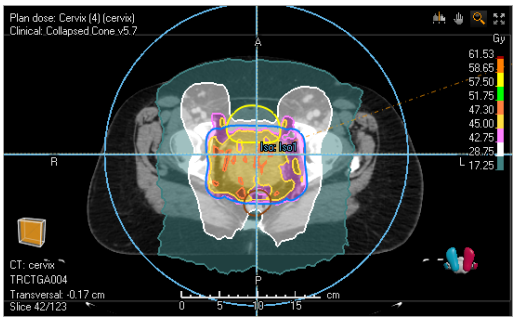

(c) Plan 4, slice 42.

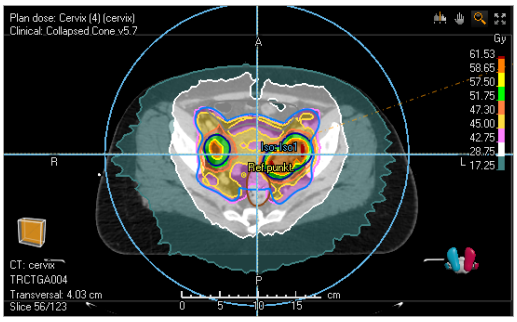

(d) Plan 4, slice 56.

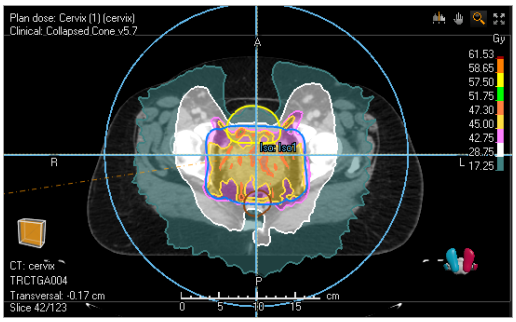

(e) Plan 1, slice 42.

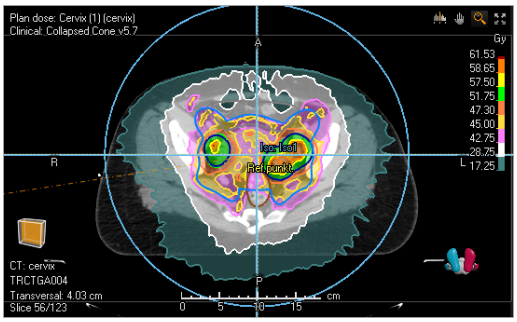

(f) Plan 1, slice 56.

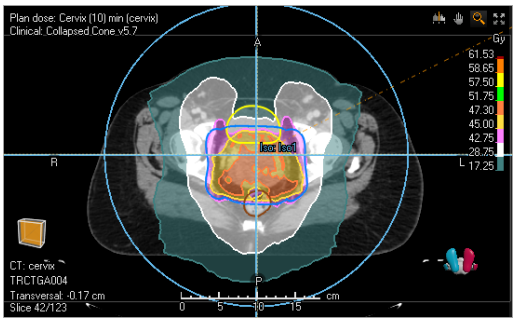

(g) Plan 10 min, slice 42.

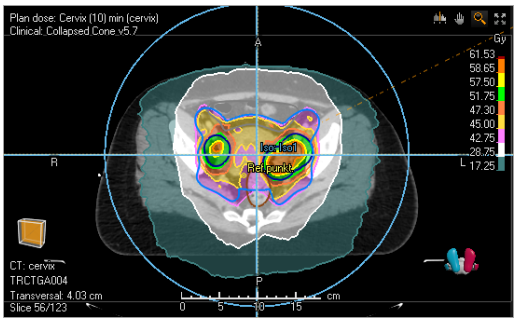

(h) Plan 10 min, slice 56.

Figure 19: Images of treatment plans made for patient 6 with FW 2.51 cm. Two slices for each row, 42 and 56: reference plan (a, b), the best HT plan (4) (c, d), worst HT plan (1) (e, f) and HT plan with minimum delivery time (10) (g, h). Isotropic distribution of lower dose levels to the body volume, as well as formation of horns in all HT plans. All HT plans lack dose coverage of 95 % reference isodose (pink) to part of PTV_45 (blue) that overlaps with bladder (yellow). High conformity, comparable to reference plan, for PTV_45 and boost volumes (PTVn_57.5) in best HT plan (d) and time pressed plan (h). In all HT plans, high dose levels are placed inside part of bladder (yellow) that intersect with PTV_45.

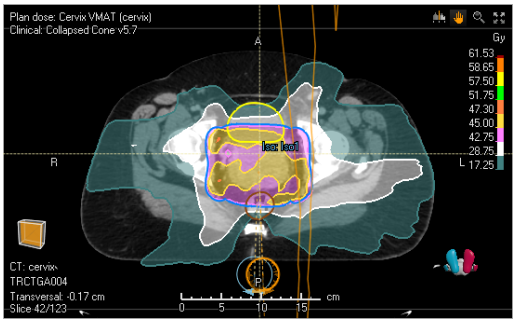

(a) Reference plan, slice 42.

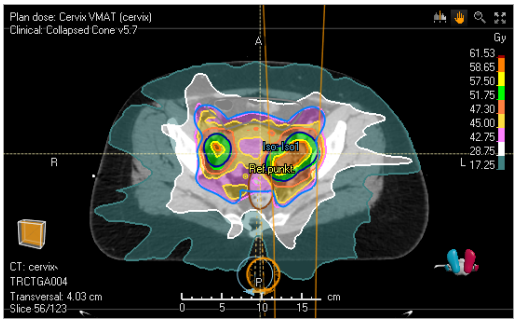

(b) Reference plan, slice 56.

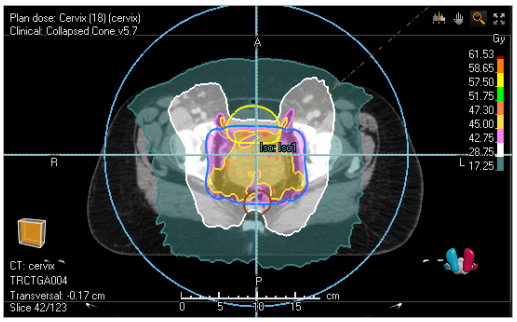

(c) Plan 18, slice 42.

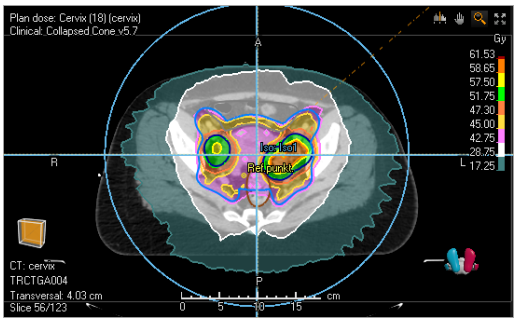

(d) Plan 18, slice 56.

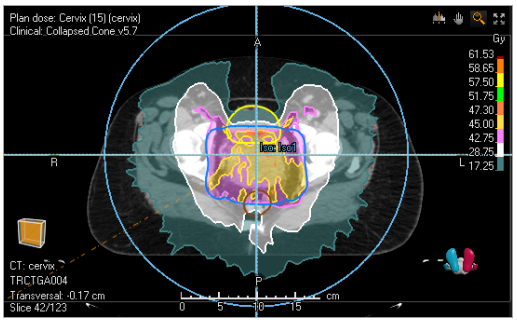

(e) Plan 15, slice 42.

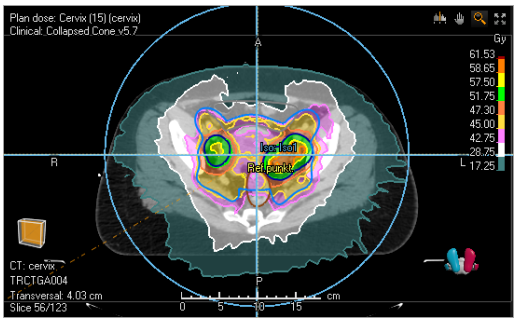

(f) Plan 15, slice 56.

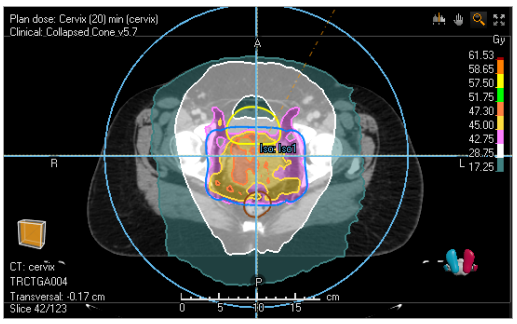

(g) Plan 20 min, slice 42.

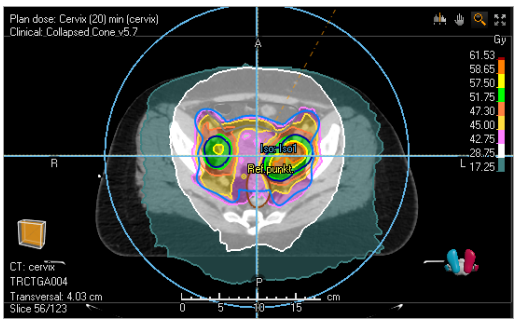

(h) Plan 20 min, slice 56.

Figure 20: Images of treatment plans made for patient 6 with FW 5.05 cm. Two slices for each row, 42 and 56: reference plan (a, b), the best HT plan (18) (c, d), worst HT plan (15) (e, f) and HT plan with minimum delivery time (20) (g, h). Isotropic distribution of lower dose levels to the body volume, as well as formation of horns in all HT plans. All HT plans lack dose coverage of 95 % reference isodose (pink) to part of PTV_45 (blue) that overlaps with bladder (yellow). High conformity, comparable to reference plan, for PTV_45 and boost volumes (PTVn_57.5) in best HT plan (d) and time pressed plan (h). In all HT plan high dose levels are placed inside bladder (yellow).

Patient 7

Table 11 shows that mean dose to xOAR are similar for the two FWs. Mean dose to xBowelBag is noticeably low. Max doses to xBowelBag-PTVns is slightly higher for reference plan than selected best HT plans. Figure 21 and 22 shows dose distribution for FW 2.51 cm and 5.05 cm, respectively. Significant distribution of lower dose levels to the body volume in HT plans, compared to reference plans.

Selected best and worst HT plans for patient 7 were determined to be Plan 4 and Plan 5 for FW 2.51 cm, respectively, and Plan 14 and Plan 11 for FW 5.05 cm, respectively.

Table 11: Mean cumulative dose [Gy] and max dose [Gy] in selected OARs and plan delivery times for patient 7. The xOARs are color coded from lowest (green) to highest (red) dose. For the xOAR-PTVns the colors represents whether the dose constraint set to avoid hot spots in the volume is fulfilled or not, orange if it exceeds the constraint, red if it is greater than 50 Gy. Selected best plan is marked with ** and worst plan with **.

Patient 7	**Mean cumulative dose, Dmean [Gy]**				**Max dose, D0.03 [Gy]**				**Delivery time**
Plan name	xRectum	xBowelBag	xBladder	xBody	xRectum-PTVn	xBowelBag-PTVn	xBladder-PTVn	xBody-PTVn	
Reference plan	32,25	6,72	36,61	6,97	46,99	47,98	47,08	47,98	2 min 8 s
Plan 1	26,75	9,43	33,50	8,14	49,05	58,30	51,59	59,10	12 min 37 s
Plan 2	29,32	9,24	33,67	7,91	52,28	49,32	57,26	57,26	9 min 31 s
Plan 3	30,39	8,95	32,40	7,77	47,70	47,65	51,64	52,06	7 min 36 s
Plan 4**	31,07	8,65	31,65	7,68	48,27	47,23	49,56	50,89	6 min 0 s
Plan 5**	26,75	9,51	34,53	8,22	49,22	57,72	52,46	59,41	18 min 55 s
Plan 6	29,02	9,28	35,27	7,96	47,94	50,05	57,08	57,09	14 min 16 s
Plan 7	30,33	8,95	34,78	7,78	51,82	47,70	56,42	56,42	11 min 24 s
Plan 8	30,78	8,62	34,35	7,66	47,99	47,26	58,97	58,97	9 min 11 s
Plan 10 min	33,17	8,22	30,58	7,60	48,62	48,32	49,42	51,11	4 min 25 s
Plan 11**	29,43	9,40	33,92	8,37	48,82	47,82	55,71	58,23	7 min 2 s
Plan 12	31,23	9,24	33,80	8,28	47,64	47,90	54,87	54,87	5 min 17 s
Plan 13	32,27	9,13	33,38	8,29	48,08	47,44	51,49	51,62	4 min 14 s
Plan 14**	32,68	8,94	32,18	8,14	47,51	47,28	51,46	52,45	3 min 31 s
Plan 15	29,45	9,32	36,09	8,36	48,78	50,15	61,05	61,94	10 min 32 s
Plan 16	31,37	9,20	35,35	8,29	48,33	47,53	57,40	57,50	7 min 55 s
Plan 17	32,10	9,04	35,79	8,24	49,47	47,36	55,54	55,55	6 min 20 s
Plan 18	32,39	8,86	35,12	8,09	47,46	47,83	52,14	52,15	5 min 17 s
Plan 20 min	34,22	8,74	32,07	8,19	48,80	48,72	50,08	51,06	2 min 28 s

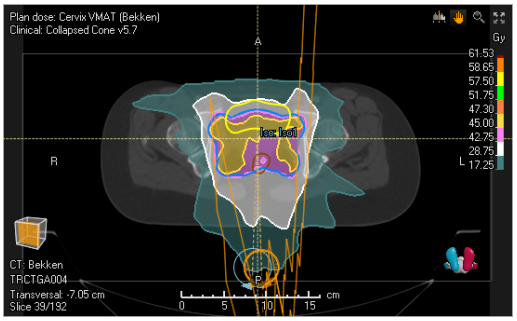

(a) Reference plan, slice 39.

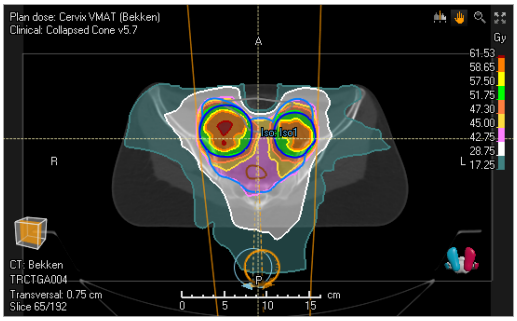

(b) Reference plan, slice 65.

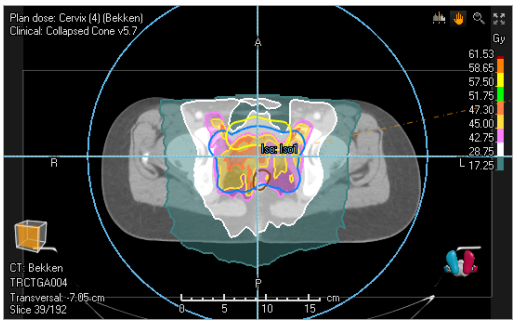

(c) Plan 4, slice 39.

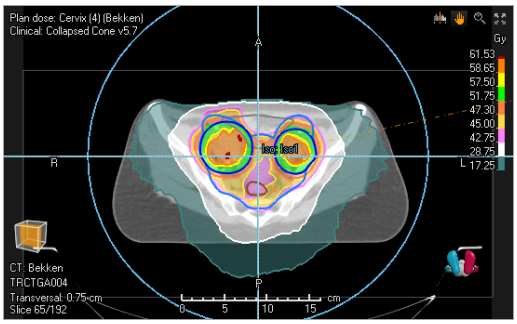

(d) Plan 4, slice 65.

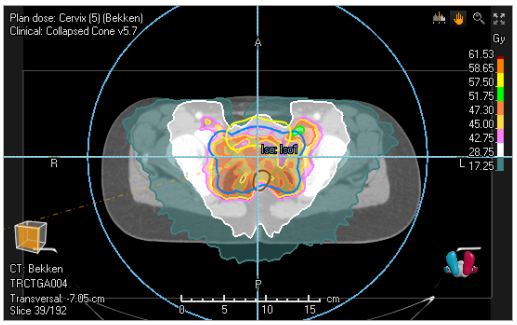

(e) Plan 5, slice 39.

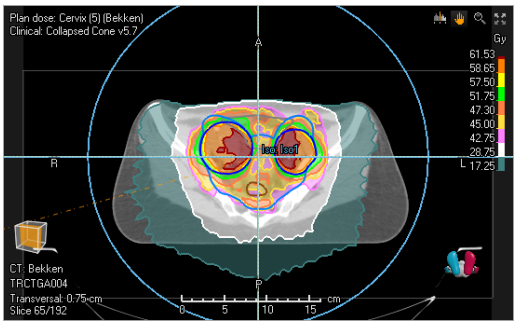

(f) Plan 5, slice 65.

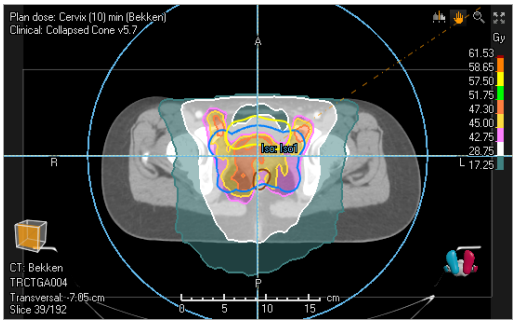

(g) Plan 10 min, slice 39.

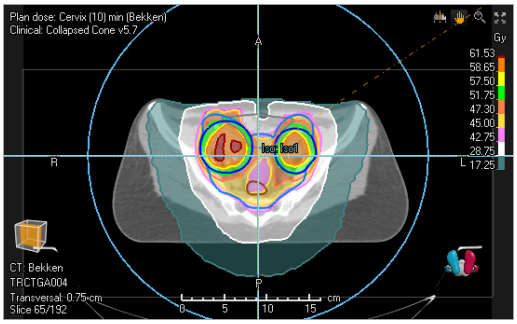

(h) Plan 10 min, slice 65.

Figure 21: Images of treatment plans made for patient 7 with FW 2.51 cm. Two slices for each row, 39 and 65: reference plan (a, b), the best HT plan (4) (c, d), worst HT plan (5) (e, f) and HT plan with minimum delivery time (10) (g, h). Significant distribution of lower dose levels to the body volume in HT plans. All HT plans lack dose coverage of 95 % reference isodose (pink) to part of PTV_45 (blue) that overlaps with bladder (yellow). High conformity, comparable to reference plan for boost volumes (PTVn_57.5) in best HT plan (d). Hot spot outside of PTV_45 (blue) and close to bladder (yellow) in worst HT plan (e). High max doses within boost volumes for all HT plans, as well as reference plan.

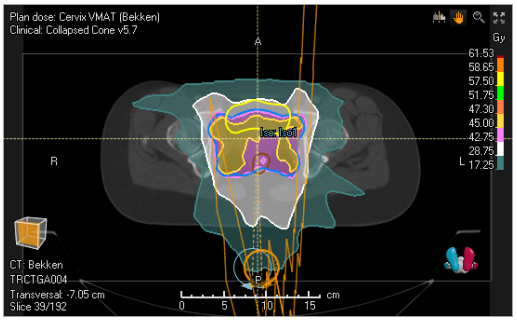

(a) Reference plan, slice 39.

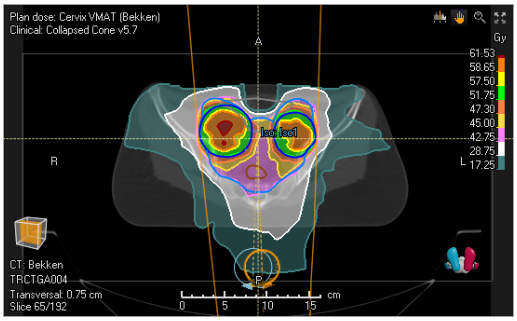

(b) Reference plan, slice 65.

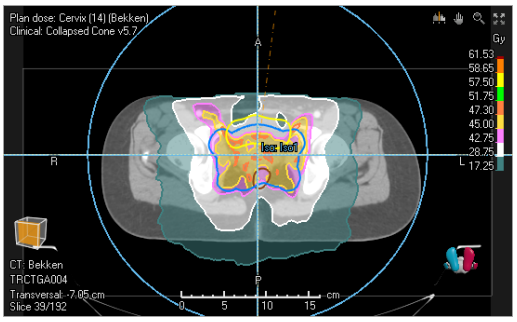

(c) Plan 14, slice 39.

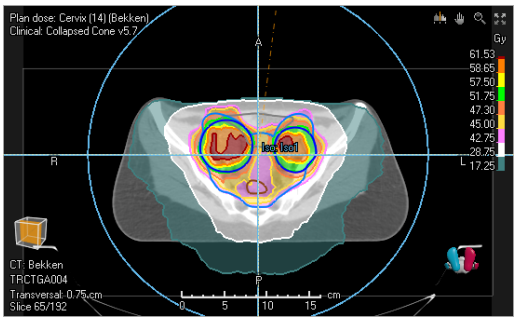

(d) Plan 14, slice 65.

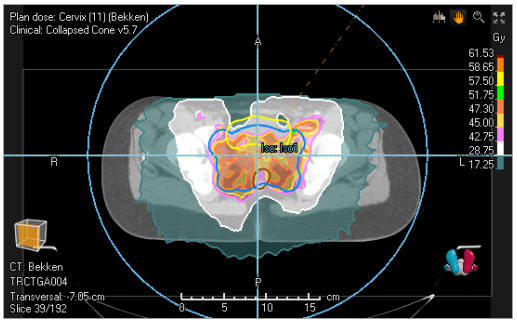

(e) Plan 11, slice 39.

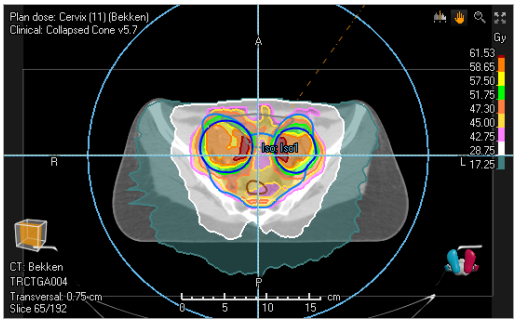

(f) Plan 11, slice 65.

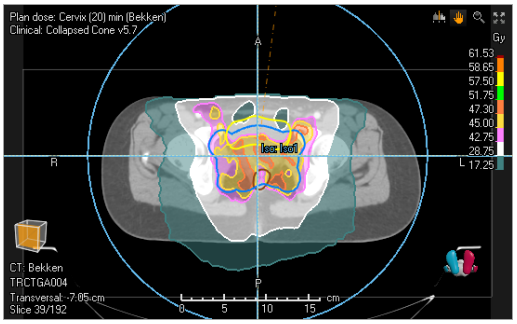

(g) Plan 20 min, slice 39.

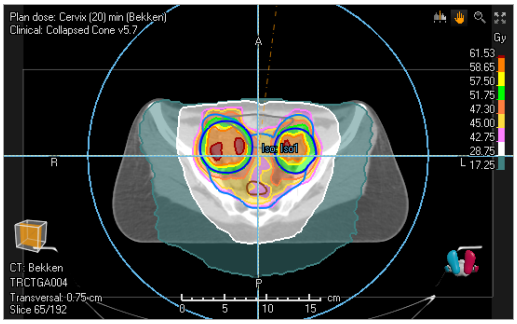

(h) Plan 20 min, slice 65.

Figure 22: Images of treatment plans made for patient 7 with FW 5.05 cm. Two slices for each row, 39 and 65: reference plan (a, b), the best HT plan (14) (c, d), worst HT plan (11) (e, f) and HT plan with minimum delivery time (20) (g, h). Significant distribution of lower dose levels to the body volume in HT plans. All HT plans lack dose coverage of 95 % reference isodose (pink) to part of PTV_45 (blue) that overlaps with bladder (yellow). Comparable conformity to reference plan for boost volumes (PTVn_57.5) in best HT plan (d). In worst HT plan (e, f) and time pressed plan (g, h), generally higher dose levels (45 Gy and 47.30 Gy). High max doses within boost volumes for all HT plans, as well as reference plan.

Patient 8

Table 12 shows that mean dose to xOAR are lower for FW 2.51 cm than for FW 5.05 cm. Max doses to xOAR-PTVns in selected best plans are higher, but comparable to the reference plans. Figure 23 and 24 shows dose distribution for FW 2.51 cm and 5.05 cm, respectively. Isotropic distribution of lower dose levels to the body volume in all HT plans, whereas reference plan distribute dose to the sides. Lack of dose coverage is observed of 95 % reference isodose to part of PTV_45 that overlaps with bladder is observed for all HT plans.

Selected best and worst HT plans for patient 8 were determined to be Plan 7 and Plan 1 for FW 2.51 cm, respectively, and Plan 14 and Plan 11 for FW 5.05 cm, respectively.

Table 12: Mean cumulative dose [Gy] and max dose [Gy] in selected OARs and plan delivery times for patient 8. The xOARs are color coded from lowest (green) to highest (red) dose. For the xOAR-PTVns the colors represents whether the dose constraint set to avoid hot spots in the volume is fulfilled or not, orange if it exceeds the constraint, red if it is greater than 50 Gy. Selected best plan is marked with ** and worst plan with **.

Patient 8	**Mean cumulative dose, Dmean [Gy]**				**Max dose, D0.03 [Gy]**				**Delivery time**
Plan name	xRectum	xBowelBag	xBladder	xBody	xRectum-PTVn	xBowelBag-PTVn	xBladder-PTVn	xBody-PTVn	
Reference plan	37,18	21,61	35,07	10,53	47,05	47,11	47,02	47,56	2 min 4 s
Plan 1**	37,46	22,82	39,26	11,4	48,98	51,41	53,69	55,78	15 min 57 s
Plan 2	37,82	22,69	38,53	11	47,18	47,47	48,93	49,94	11 min 57 s
Plan 3	37,94	22,74	38,67	10,92	47,31	47,68	50,09	50,09	9 min 35 s
Plan 4	38,04	22,79	38,75	10,82	47,37	47,78	50,07	50,07	7 min 59 s
Plan 5	36,98	22,66	39,62	11,36	48,07	51,53	54,33	55,76	23 min 53 s
Plan 6	37,74	22,61	39,26	10,99	47,83	48,03	52,05	52,05	17 min 55 s
Plan 7**	37,67	22,49	38,85	10,87	47,15	47,84	48,16	49,29	14 min 21 s
Plan 8	37,48	22,34	39,08	10,75	47,12	48,62	51,18	51,18	11 min 58 s
Plan 10 min	39,82	23,37	35,48	11,05	47,85	48,13	49,09	50,41	5 min 34 s
Plan 11**	38,43	22,88	37,79	11,57	47,94	48,79	50,67	53,82	8 min 41 s
Plan 12	38,86	23,13	37,89	11,53	47,63	48,77	49,35	51,42	6 min 31 s
Plan 13	38,54	23,41	38,44	11,52	48,11	47,67	49,13	51,24	5 min 13 s
Plan 14	39,13	23,7	38,62	11,41	47,38	47,99	49,05	50,40	4 min 21 s
Plan 15	38,38	22,77	38,75	11,61	47,97	47,71	50,90	53,08	12 min 58 s
Plan 16	38,7	23,01	38,54	11,51	47,44	47,92	51,41	51,73	9 min 45 s
Plan 17**	38,36	23,22	39,15	11,43	47,25	48,13	50,36	50,46	7 min 46 s
Plan 18	38,54	23,16	40,43	11,27	47,41	47,34	50,67	50,67	6 min 31 s
Plan 20 min	41,66	24,75	36,89	12,13	49,37	49,09	51,09	53,64	3 min 2 s

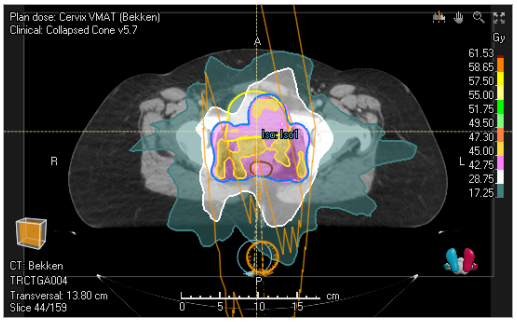

(a) Reference plan, slice 44.

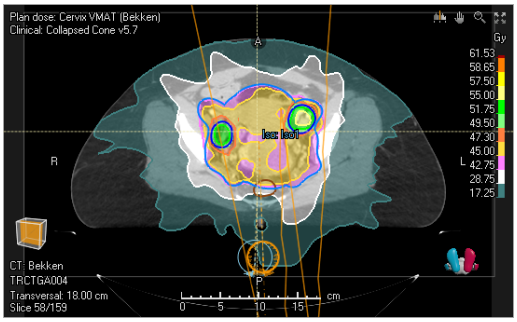

(b) Reference plan, slice 58.

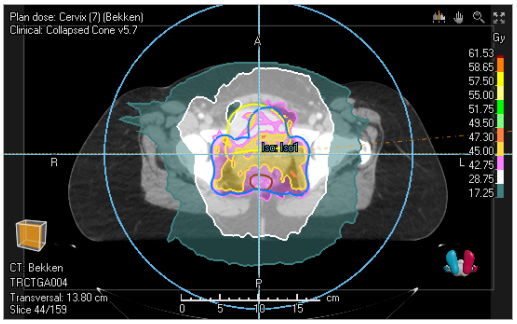

(c) Plan 7, slice 44.

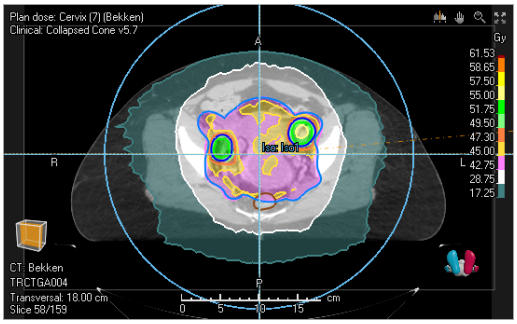

(d) Plan 7, slice 58.

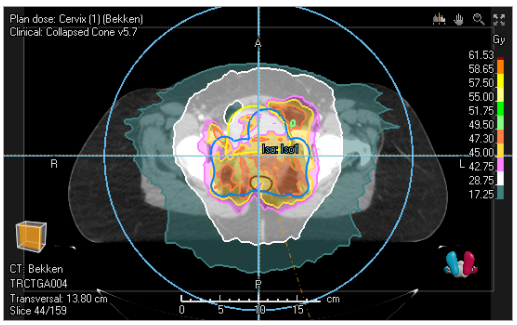

(e) Plan 1, slice 44.

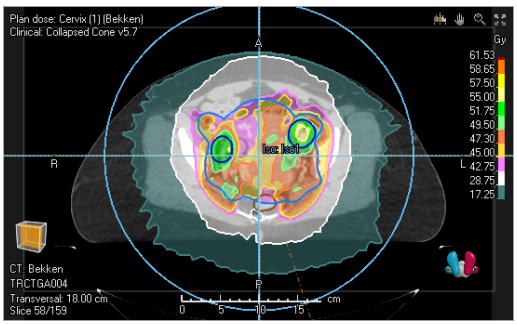

(f) Plan 1, slice 58.

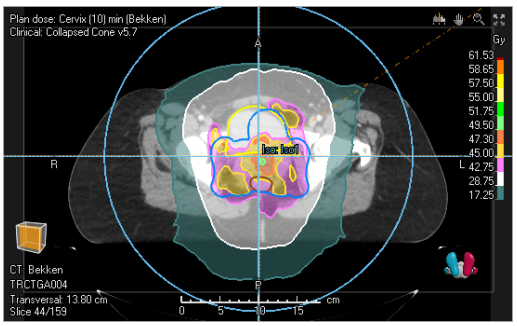

(g) Plan 10 min, slice 44.

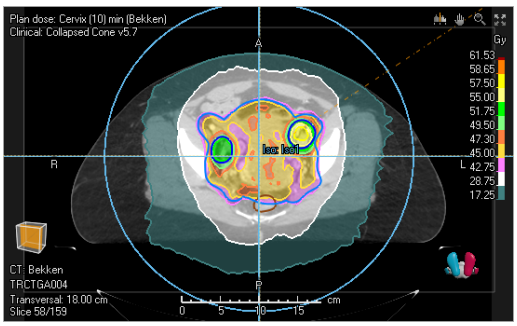

(h) Plan 10 min, slice 58.

Figure 23: Images of treatment plans made for patient 8 with FW 2.51 cm. Two slices for each row, 44 and 58: reference plan (a, b), the best HT plan (7) (c, d), worst HT plan (1) (e, f) and HT plan with minimum delivery time (10) (g, h). Isotropic distribution of lower dose levels to the body volume in HT plans. All HT plans lack dose coverage of 95 % reference isodose (pink) to part of PTV_45 (blue) that overlaps with bladder (yellow). High conformity for PTV_45 and boost volumes (PTVn_57.5) in best HT plan (d) and time pressed plan (h). In worst HT plan (e, f) and time pressed plan (g, h), generally higher dose levels (45 Gy and 47.30 Gy), and hot spots placed close to bladder (yellow).

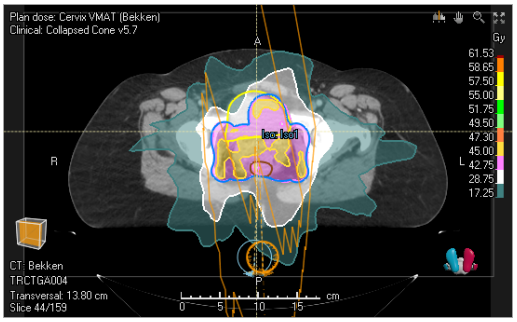

(a) Reference plan, slice 44.

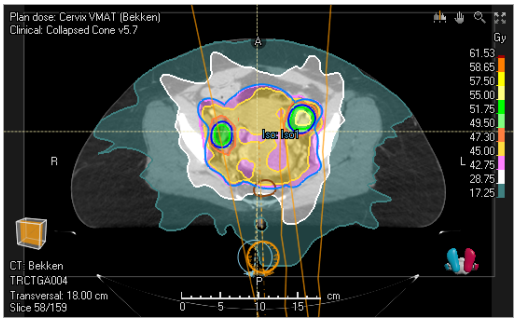

(b) Reference plan, slice 58.

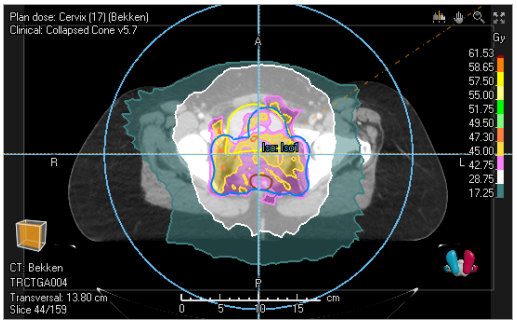

(c) Plan 14, slice 44.

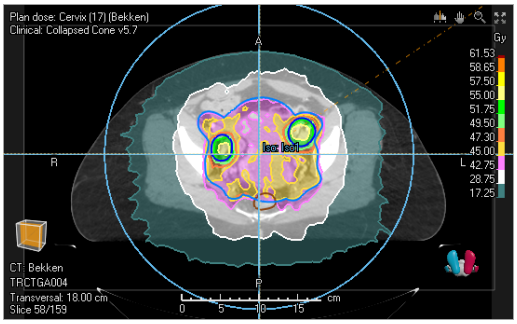

(d) Plan 14, slice 58.

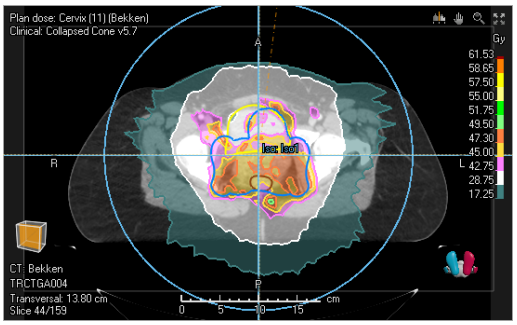

(e) Plan 11, slice 44.

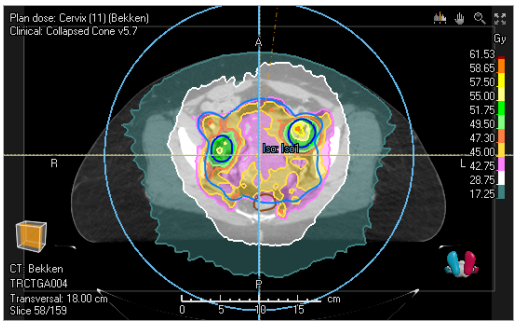

(f) Plan 11, slice 58.

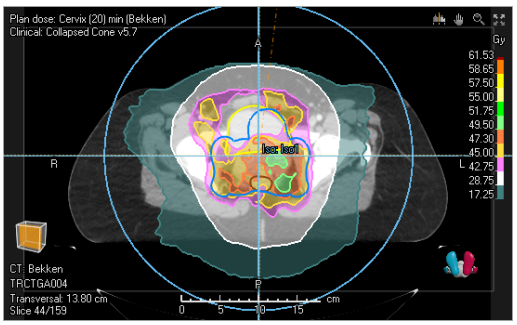

(g) Plan 20 min, slice 44.

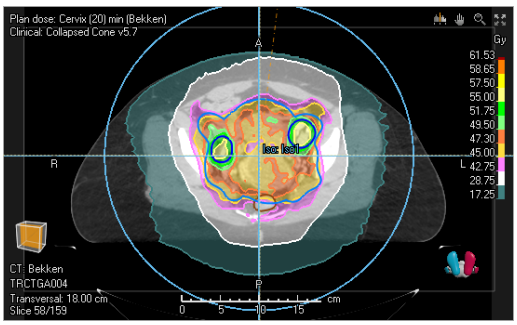

(h) Plan 20 min, slice 58.

Figure 24: Images of treatment plans made for patient 8 with FW 5.05 cm. Two slices for each row, 39 and 65: reference plan (a, b), the best HT plan (14) (c, d), worst HT plan (11) (e, f) and HT plan with minimum delivery time (20) (g, h). Isotropic distribution of lower dose levels to the body volume in HT plans. All HT plans lack dose coverage of 95 % reference isodose (pink) to part of PTV_45 (blue) that overlaps with bladder (yellow). The 90 % reference isodose (green) to PTVn_57.5 (dark blue) is spread beyond the contour in the HT plans (d, e, f). In worst and time pressed HT plans (e, g), horns are formed of dose distribution of lower dose levels and the 42.75 Gy isodose (pink) and hot spots are placed close to rectum (brown).

Patient 9

Table 13 shows that mean dose to xOAR are lower for FW 2.51 cm. For xBladder, mean dose values are lower for almost all HT plans than for the reference plan. Figure 25 and 26 shows dose distribution for FW 2.51 cm and 5.05 cm, respectively. Isotropic dose distribution and horns are formed of lower dose levels for all HT plans. In worst HT plans with FW 2.51 cm, hot spots are placed close to bladder and bowel.

Selected best and worst HT plans for patient 9 were determined to be Plan 4 and Plan 1 for FW 2.51 cm, respectively, and Plan 18 and Plan 11 for FW 5.05 cm, respectively.

Table 13: Mean cumulative dose [Gy] and max dose [Gy] in selected OARs and plan delivery times for patient 9. The xOARs are color coded from lowest (green) to highest (red) dose. For the xOAR-PTVns the colors represents whether the dose constraint set to avoid hot spots in the volume is fulfilled or not, orange if it exceeds the constraint, red if it is greater than 50 Gy. Selected best plan is marked with ** and worst plan with **.

Patient 9	**Mean cumulative dose, Dmean [Gy]**				**Max dose, D0.03 [Gy]**				**Delivery time**
Plan name	xRectum	xBowelBag	xBladder	xBody	xRectum-PTVn	xBowelBag-PTVn	xBladder-PTVn	xBody-PTVn	
Reference plan	31,44	23,47	28,43	13,19	47,09	47,11	46,88	47,86	2 min 6 s
Plan 1	30,83	25,26	24,28	13,92	50,94	51,16	53,40	59,35	12 min 44 s
Plan 2	31,15	25,39	25,25	13,77	51,77	48,89	51,62	53,01	9 min 35 s
Plan 3	31,46	25,09	26,32	13,51	50,82	50,11	54,76	54,76	7 min 38 s
Plan 4**	31,48	24,88	27,05	13,45	47,99	47,69	54,50	54,50	6 min 23 s
Plan 5**	30,72	25,11	24,78	14,02	50,33	50,64	53,18	60,29	19 min 5 s
Plan 6	30,67	25,28	26,15	13,65	48,39	47,97	60,01	60,01	14 min 23 s
Plan 7	30,73	24,95	27,56	13,49	49,68	49,31	61,33	61,33	11 min 34 s
Plan 8	30,94	24,70	27,92	13,37	48,27	50,04	59,24	59,24	6 min 11 s
Plan 10 min	32,31	25,44	28,55	13,49	47,90	48,80	48,86	50,52	4 min 28 s
Plan 11**	33,34	25,68	26,21	14,24	50,06	50,51	56,57	56,57	6 min 59 s
Plan 12	33,64	25,79	26,31	14,31	49,91	50,39	53,96	53,97	5 min 17 s
Plan 13	33,64	26,09	27,36	14,28	49,39	48,44	51,67	51,85	4 min 15 s
Plan 14	33,34	26,07	27,49	14,19	49,15	48,87	51,67	52,89	3 min 33 s
Plan 15	33,38	25,65	26,50	14,19	49,32	50,09	53,76	54,94	10 min 26 s
Plan 16	33,64	25,58	26,74	14,16	50,94	49,56	55,63	55,92	7 min 5 s
Plan 17	33,30	25,65	27,42	14,17	50,39	49,18	52,15	52,63	6 min 19 s
Plan 18**	33,36	25,50	28,08	14,05	49,53	49,57	53,52	53,52	5 min 20 s
Plan 20 min	34,68	27,11	28,45	14,55	50,11	49,94	50,58	51,85	2 min 29

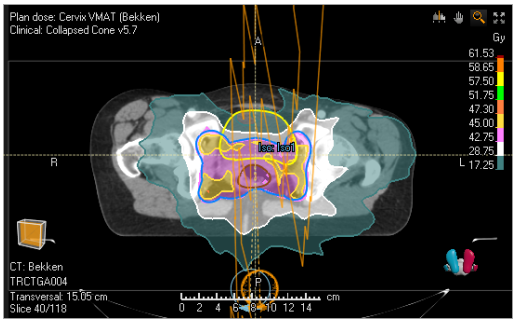

(a) Reference plan, slice 40.

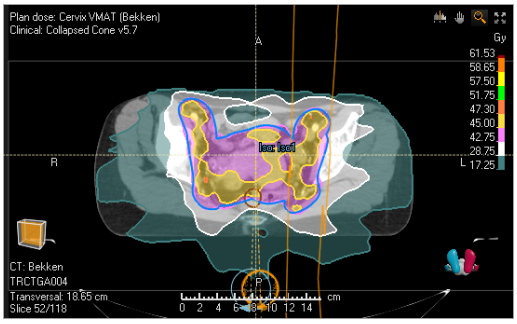

(b) Reference plan, slice 52.

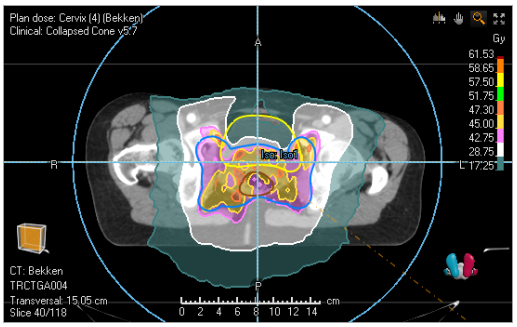

(c) Plan 4, slice 40.

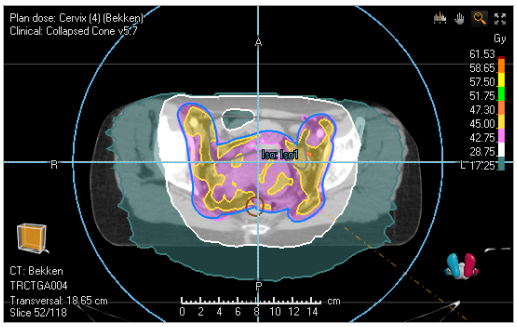

(d) Plan 4, slice 52.

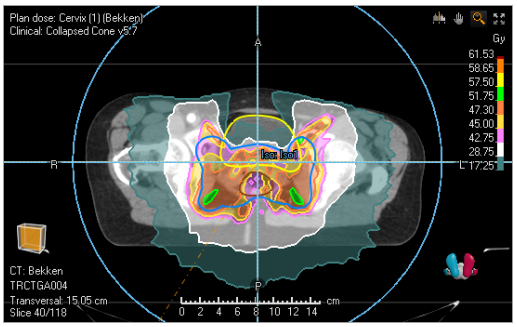

(e) Plan 1, slice 40.

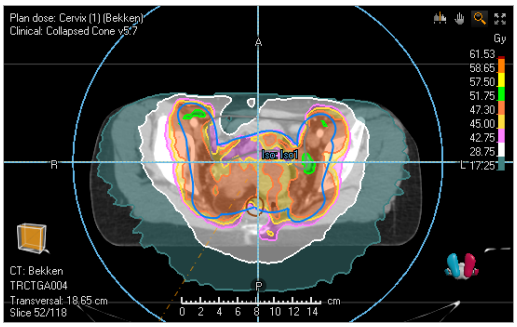

(f) Plan 1, slice 52.

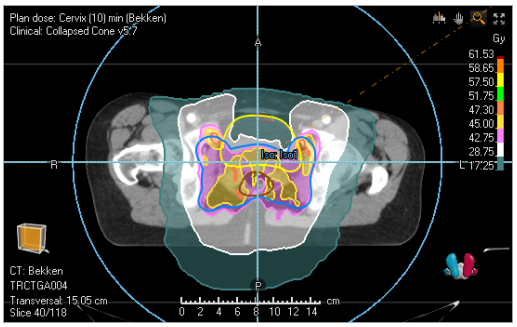

(g) Plan 10 min, slice 40.

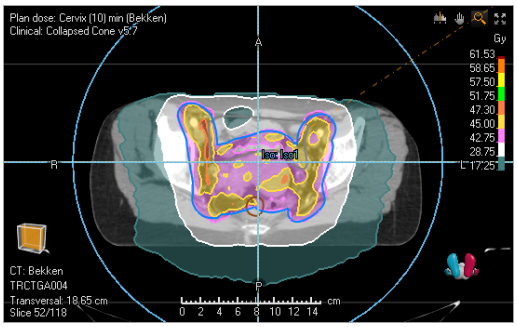

(h) Plan 10 min, slice 52.

Figure 25: Images of treatment plans made for patient 9. Two slices in each row, 40 and 52: reference plan (a, b), the best HT plan (4) (c, d), worst HT plan (1) (e, f) and HT plan with minimum delivery time (10) (g, h). The HT plans are made with FW 2.51 cm. Acceptable conformity of the 95 % reference isodose (pink) to PTV_45 (blue), however higher conformity in selected best HT plans (c, d) than the other HT plans. Higher dose levels (45 Gy and 47.30 Gy) in worst HT plan (e, f) and time pressed plan (g, h). Horns are formed of dose distribution of lower dose levels. In worst HT plans, hot spots are placed close to bladder (yellow) (e) and bowel (grey) (f).

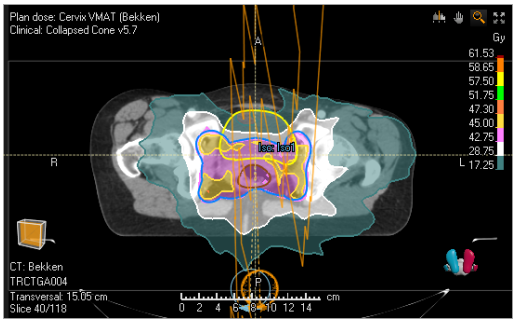

(a) Reference plan, slice 40.

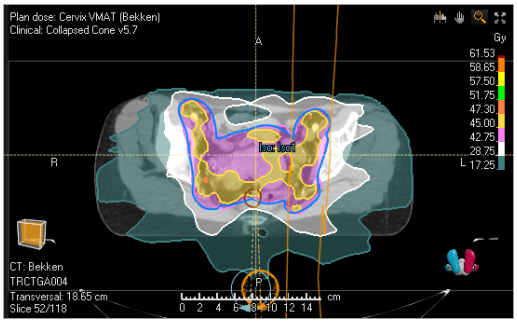

(b) Reference plan, slice 52.

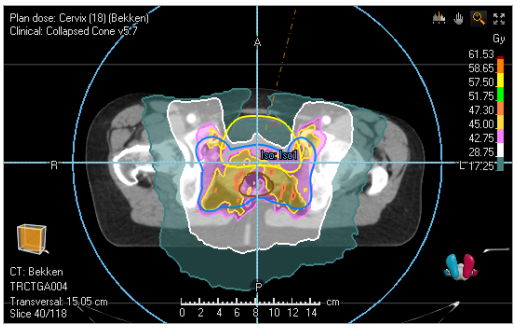

(c) Plan 18, slice 40.

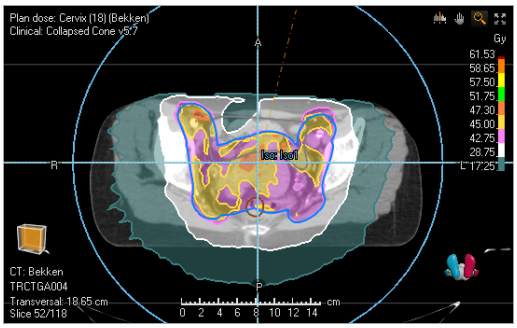

(d) Plan 18, slice 52.

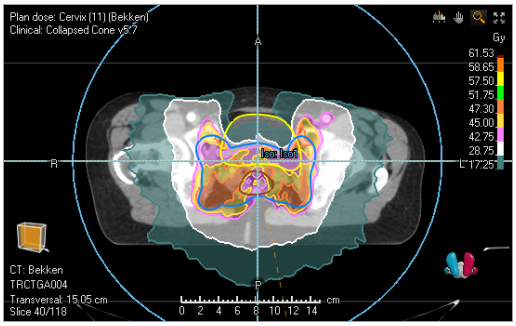

(e) Plan 11, slice 40.

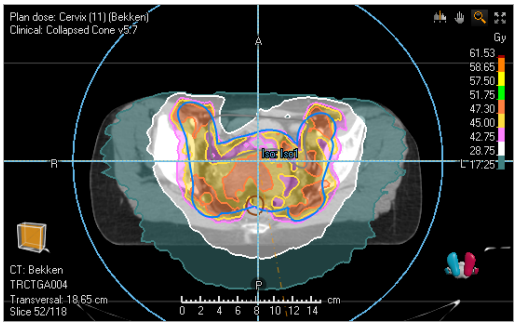

(f) Plan 11, slice 52.

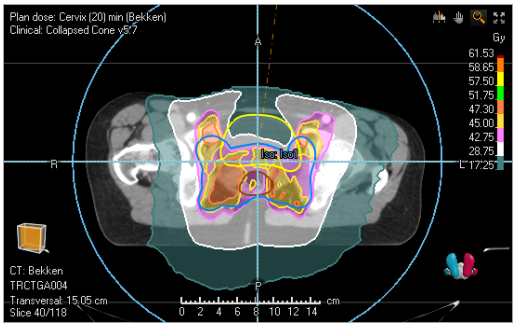

(g) Plan 20 min, slice 40.

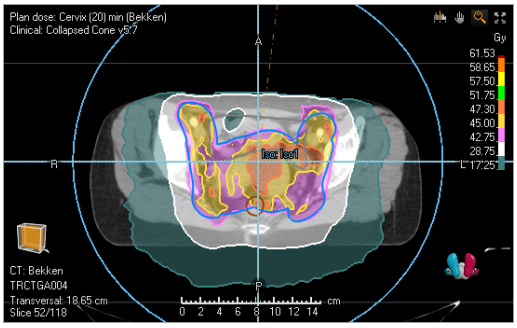

(h) Plan 20 min, slice 52.

Figure 26: Images of treatment plans made for patient 9. Two slices for each row, 40 and 52: reference plan (a, b), the best HT plan (18) (c, d), worst HT plan (11) (e, f) and HT plan with minimum delivery time (20) (g, h). The HT plans are made with FW 5.05 cm. Acceptable conformity of the 95 % reference isodose (pink) to PTV_45 (blue), however higher conformity in selected best HT plans (c, d) than the other HT plans. Higher dose levels (45 Gy and 47.30 Gy) in worst HT plan (e, f) and time pressed plan (g, h). Horns are formed of dose distribution of lower dose levels.

Patient 10

Table 14 shows that mean dose to xOARs is consistently higher in HT plans with FW 5.05 cm than HT plans with smaller FW and reference plans. Mean dose and max dose is lower in the reference plans than for HT plans. Figure 27 and 28 shows dose distribution for FW 2.51 cm and 5.05 cm, respectively, as well as lack of dose coverage in HT plans to part of PTV_45 that overlaps with bladder.

Selected best and worst HT plans for patient 10 were determined to be Plan 8 and Plan 5 for FW 2.51 cm, respectively, and Plan 17 and Plan 11 for FW 5.05 cm, respectively.

Table 14: Mean cumulative dose [Gy] and max dose [Gy] in selected OARs and plan delivery times for patient 10. The xOARs are color coded from lowest (green) to highest (red) dose. For the xOAR-PTVns the colors represents whether the dose constraint set to avoid hot spots in the volume is fulfilled or not, orange if it exceeds the constraint, red if it is greater than 50 Gy. Selected best plan is marked with ** and worst plan with **.

Patient 10	**Mean cumulative dose, Dmean [Gy]**				**Max dose, D0.03 [Gy]**				**Delivery time**
Plan name	xRectum	xBowelBag	xBladder	xBody	xRectum-PTVn	xBowelBag-PTVn	xBladder-PTVn	xBody-PTVn	
Reference plan	28,95	23,02	37,35	12,71	46,90	47,18	46,74	47,84	2 min 4 s
Plan 1	32,37	25,50	37,60	13,98	48,17	50,08	51,92	54,33	12 min 0 s
Plan 2	32,31	24,65	39,21	14,31	51,14	54,78	55,43	59,20	9 min 5 s
Plan 3	31,73	25,19	38,63	13,68	47,75	48,20	50,96	52,50	7 min 18 s
Plan 4	31,85	24,98	38,25	13,62	47,61	48,00	51,28	52,44	6 min 6 s
Plan 5**	32,46	24,63	38,97	14,16	49,35	53,24	53,01	57,11	17 min 59 s
Plan 6	32,08	25,15	37,25	13,86	47,47	48,95	54,64	57,46	13 min 39 s
Plan 7	31,55	24,98	37,23	13,51	47,36	50,17	53,21	54,59	10 min 52 s
Plan 8**	31,34	24,87	38,13	13,47	47,24	48,39	52,15	53,69	9 min 8 s
Plan 10 min	32,56	25,07	36,72	13,82	47,87	49,15	50,24	51,45	4 min 15 s
Plan 11**	32,70	26,54	40,85	14,61	48,51	52,27	52,35	56,87	6 min 39 s
Plan 12	33,34	26,52	40,14	14,41	48,04	50,44	50,04	54,49	5 min 0 s
Plan 13	33,48	26,29	40,57	14,41	47,83	49,24	49,85	51,50	4 min 1 s
Plan 14	33,22	26,28	39,92	14,38	47,67	48,98	49,89	51,30	3 min 24 s
Plan 15	33,23	26,56	42,17	14,55	47,96	51,44	51,34	57,02	9 min 56 s
Plan 16	32,88	26,25	41,27	14,33	47,66	49,11	52,56	54,92	7 min 27 s
Plan 17**	32,99	26,01	41,41	14,28	47,98	48,65	50,40	51,58	6 min 2 s
Plan 18	32,69	25,79	41,53	14,07	47,14	48,65	49,55	51,74	5 min 1 s
Plan 20 min	35,20	26,95	38,43	14,89	47,92	49,13	49,23	50,79	2 min 22 s

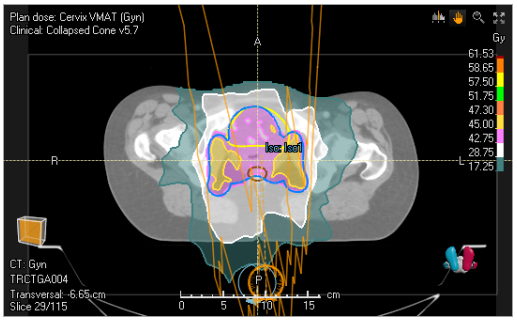

(a) Reference plan, slice 29.

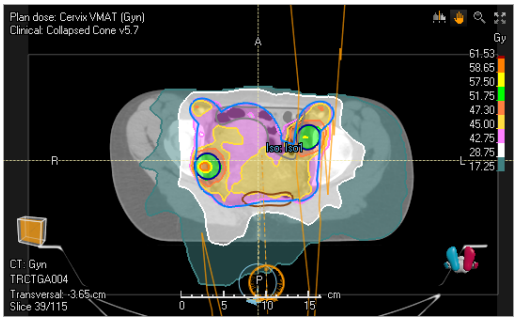

(b) Reference plan, slice 39.

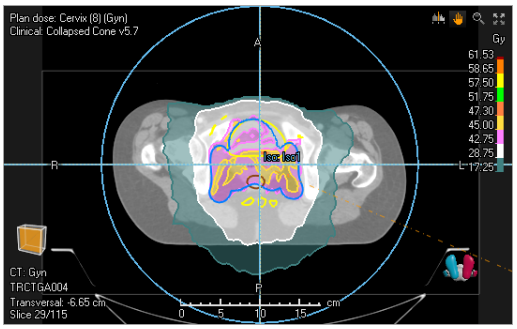

(c) Plan 8, slice 20.

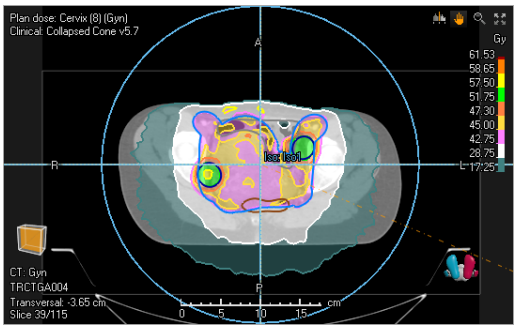

(d) Plan 8, slice 39.

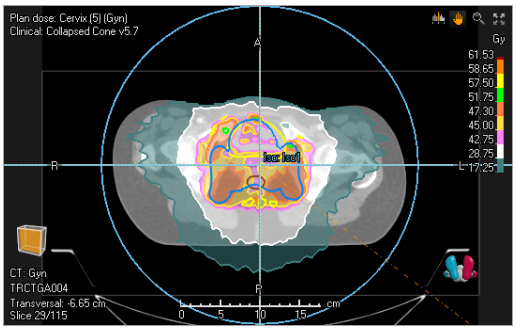

(e) Plan 5, slice 29.

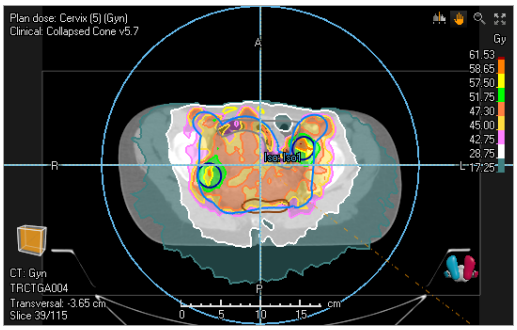

(f) Plan 5, slice 39.

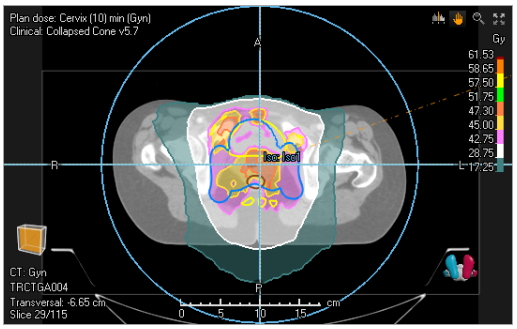

(g) Plan 10 min, slice 29.

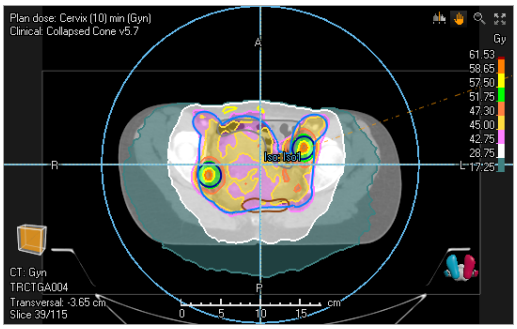

(h) Plan 10 min, slice 39.

Figure 27: Images of treatment plans made for patient 10. Two slices in each row, 40 and 52: reference plan (a, b), the best HT plan (8) (c, d), worst HT plan (5) (e, f) and HT plan with minimum delivery time (10) (g, h). The HT plans are made with FW 2.51 cm. All HT plans lack dose coverage of 95 % reference isodose (pink) to part of PTV_45 (blue) that overlaps with bladder (yellow). High conformity, comparable to reference plan, for PTV_45 and boost volumes (PTVn_57.5) in best HT plan (d) and time pressed plan (h).

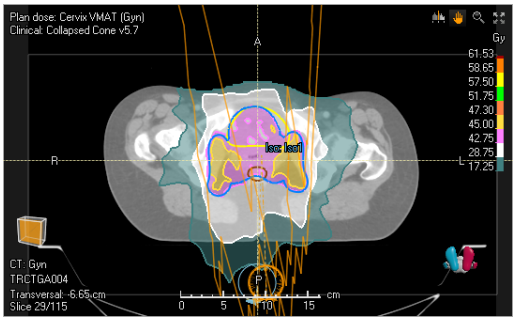

(a) Reference plan, slice 29.

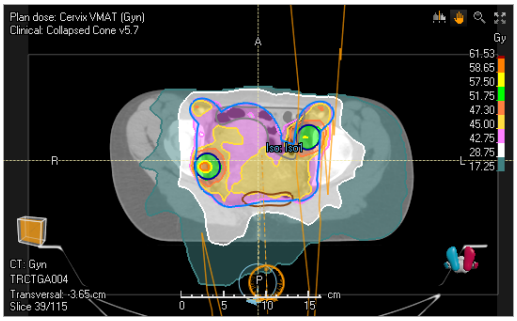

(b) Reference plan, slice 39.

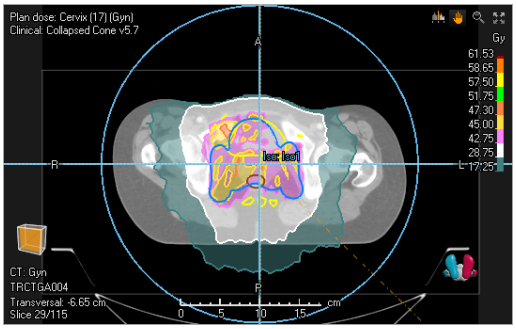

(c) Plan 17, slice 29.

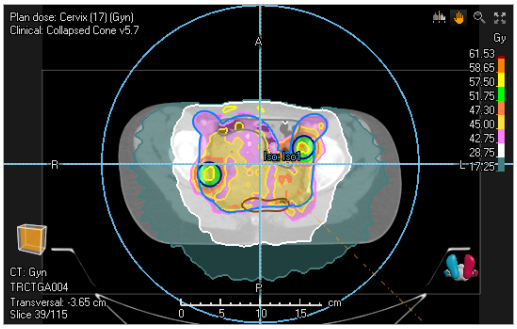

(d) Plan 17, slice 39.

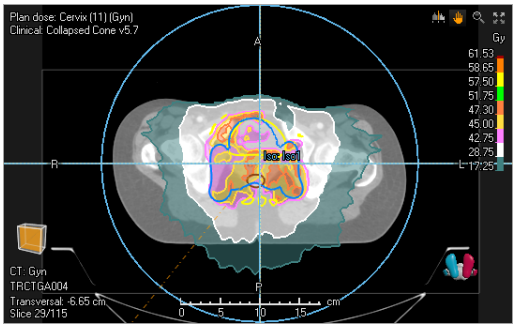

(e) Plan 11, slice 29.

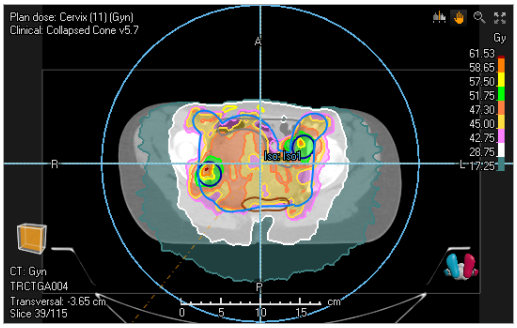

(f) Plan 11, slice 39.

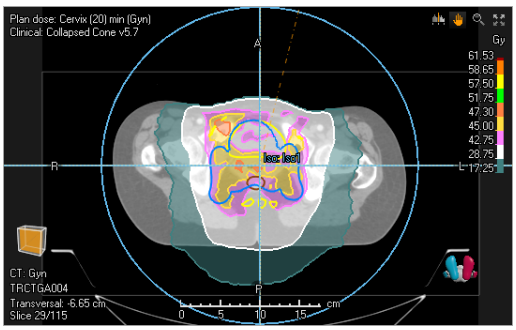

(g) Plan 20 min, slice 29.

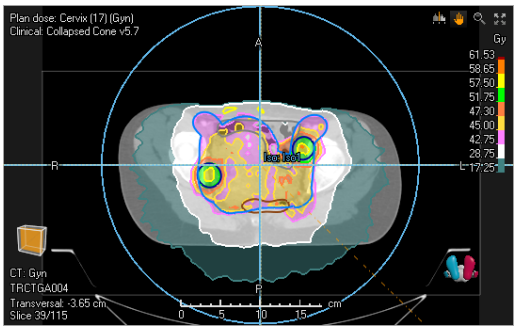

(h) Plan 20 min, slice 39.

Figure 28: Images of treatment plans made for patient 10 . Two slices for each row, 40 and 52: reference plan (a, b), the best HT plan (17) (c, d), worst HT plan (11) (e, f) and HT plan with minimum delivery time (20) (g, h). The HT plans are made with FW 5.05 cm. All HT plans lack dose coverage of 95 % reference isodose (pink) to part of PTV_45 (blue) that overlaps with bladder (yellow). High conformity, comparable to reference plan, for PTV_45 and boost volumes (PTVn_57.5) in best HT plan (d) and time pressed plan (h).

Mean cumulative dose in xOARs

The p-values from Wilcoxon signed-rank test for the mean cumulative dose in xRectum, xBowelBag, xBladder and xBody from HT plans compared to reference plans are presented in Table 15. Statistically significant results determined for p-value < 0.05 and are marked in bold.

Table 15: Wilcoxon signed-rank test performed on mean cumulative dose in xOARs in selected best HT plans and reference plan. The p-value was evaluated at a significance limit $p < 0.05$ (in bold).

Volume	**FW [cm]**	**p-value**
xRectum	2.51	0.83
	5.05	$<$ **0.05**
xBowelBag	2.51	$<$ **0.05**
	5.05	$<$ **0.05**
xBladder	2.51	1.0
	5.05	0.77
xBody	2.51	$<$ **0.05**
	5.05	$<$ **0.05**

4.1.2 Other Visual Observations

Hot Spots

Dose distribution in transversal plane for patient 3 is presented in Figure 29b, visualizing placement of hot spots in the volume where bladder and PTV intersect in best HT plans with FWs 2.51 cm. The green and orange spot visualize the 110 % and 105 % (47.3 Gy and 51.75 Gy) of the reference isodose of 45 Gy.

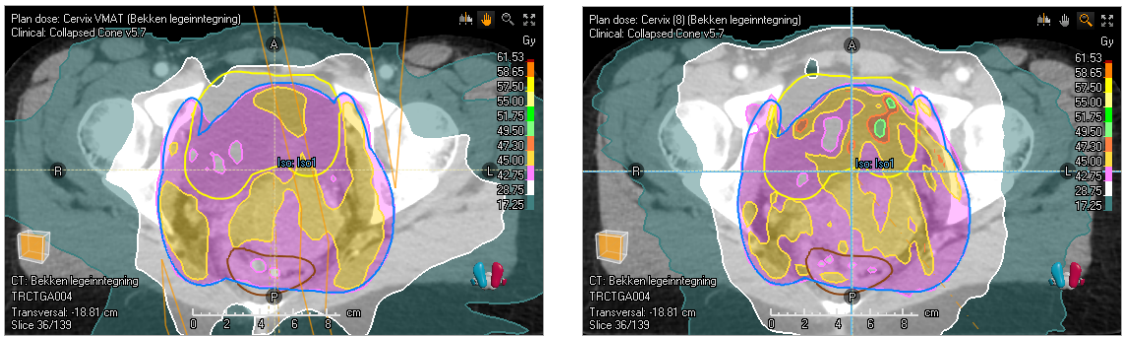

(a) Reference plan (b) Plan 8

Figure 29: Visualization of target coverage of 95 % reference isodose (pink) to PTV_45 (blue) for the reference plan (a) and best HT plan with FW 2.51 cm (Plan 8) (b) for patient 3. In the HT plan, lack of dose coverage and placement of hot spot (51.75 Gy (green)) within the bladder (yellow).

Sagittal View and Thread Effect

Images in the sagittal plane (at 0.17 cm) of Plan 15, Plan 16 and Plan 17 for patient 1 are presented in Figure 30, showing the dose distribution along the longitudinal axis visualizing the thread effect, seen as "ripples" and is most apparent for Plan 17 (c). The appearance of the tread effect varies with the parameter combination of the beam settings, the occurrence increases with increasing PF (30a-30c), but has an decrease in the effect when increasing pitch, shown in Figure 30d, all plans have FW 5.05 cm .

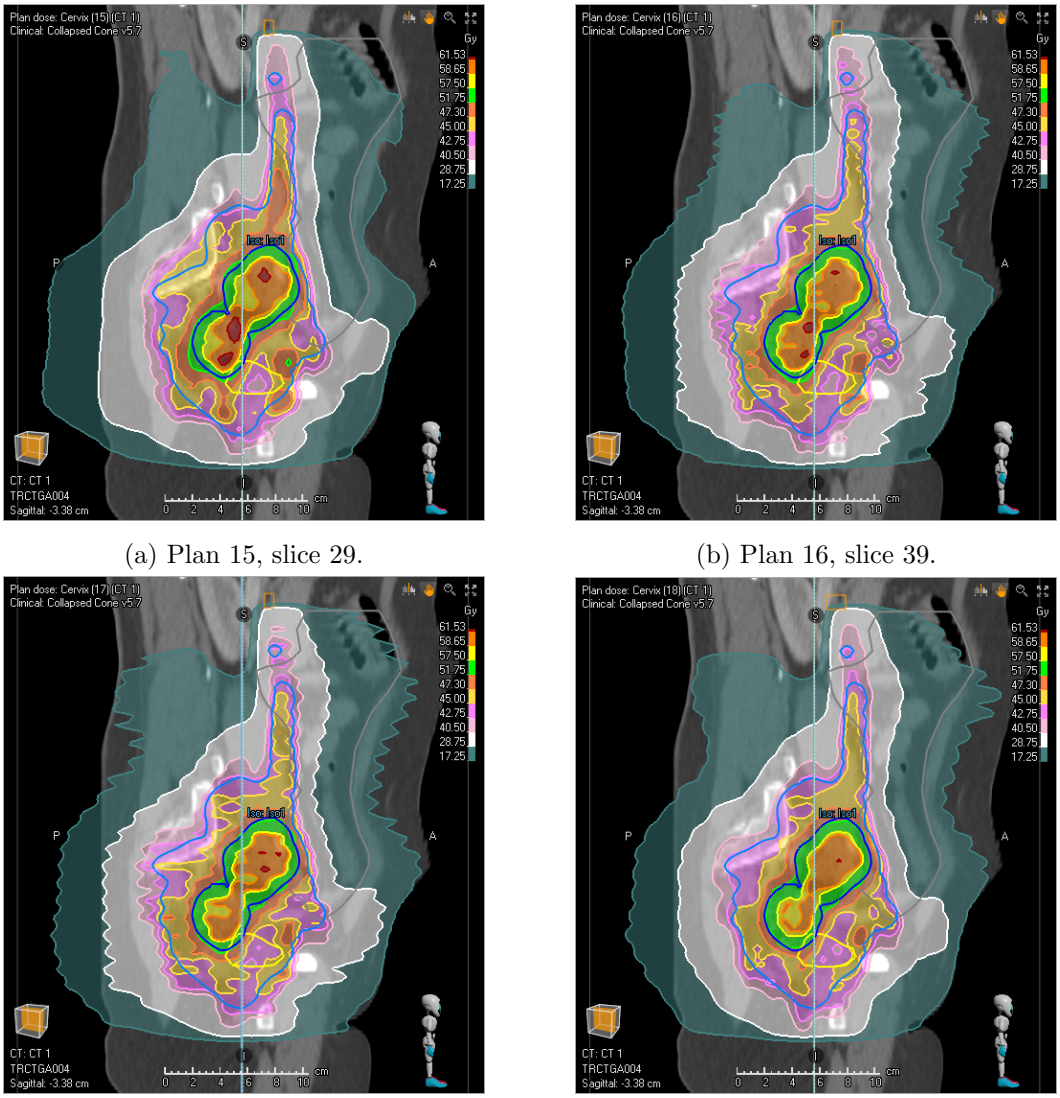

(a) Plan 15, slice 29.

(b) Plan 16, slice 39.

(c) Plan 17, slice 29.

(d) Plan 18, slice 39.

Figure 30: Images in the sagittal plane (at 0.17 cm) of Plan 15, Plan 16 and Plan 17 for patient 1 showing dose distribution along the longitudinal axis visualizing the thread effect, seen as "ripples" and is most apparent for Plan 17 (c).

4.2 Selected Best HT Plans

From visual evaluation and analysis of the dose statistics the best and worst HT plans for both FWs for each patient was selected, presented in Table 16 below with the corresponding parameter settings. Mainly, the best HT plans are used for further comparison to the reference plan made for the same patient.

Table 16: Overview of the selected best HT plans with the corresponding tomo-specific parameter combinations of PF, DTf and FW.

Patient	**Plan name**	**Parameters**		
		FW	**PF**	**DTf**
1	Plan 4	2.51	0.30	1.0
	Plan 18	5.05	0.30	1.5
2	Plan 8	2.51	0.30	1.5
	Plan 18	5.05	0.30	1.5
3	Plan 8	2.51	0.30	1.5
	Plan 14	5.05	0.30	1.0
4	Plan 4	2.51	0.30	1.0
	Plan 14	5.05	0.30	1.0
5	Plan 4	2.51	0.30	1.0
	Plan 14	5.05	0.30	1.0
6	Plan 4	2.51	0.30	1.0
	Plan 18	5.05	0.30	1.5
7	Plan 4	2.51	0.30	1.0
	Plan 14	5.05	0.30	1.0
8	Plan 7	2.51	0.25	1.5
	Plan 17	5.05	0.25	1.5
9	Plan 4	2.51	0.30	1.0
	Plan 18	5.05	0.30	1.5
10	Plan 8	2.51	0.30	1.5
	Plan 17	5.05	0.25	1.5

4.2.1 Dose-Volume Histograms

In Figure 31, 32, 33 and 34 shows the (mean cumulative) DVH curves for xRectum, xBowelBag, xBladder and xBody, respectively, for the reference plan and best HT plans with FW 2.51 cm (a) and 5.05 cm (b). The collected dose data from all patients for the reference plans, the best HT plans with FW 2.51 cm and the best HT with FW 5.05 cm are plotted as green, orange and blue, respectively. The solid lines represent the mean values, and the dotted lines represents the minimum and maximum dose values. The shaded areas are the calculated first standard deviation. In both figures, the DVH curves for xRectum and xBowelBag show similar or higher received dose for the HT than for the reference plans at any volume percentage. While for xBladder and xBody the trend is not as consistent showing similar, higher or lower received dose for the HT plans than for automatic reference plans at any volume percentage. For xRectum and xBody the difference between reference plans and HT is bigger for the selected best plans with 5.05 cm than for FW 2.51 cm. This result is observed for both the mean DVH curves, and in the calculated standard deviation.

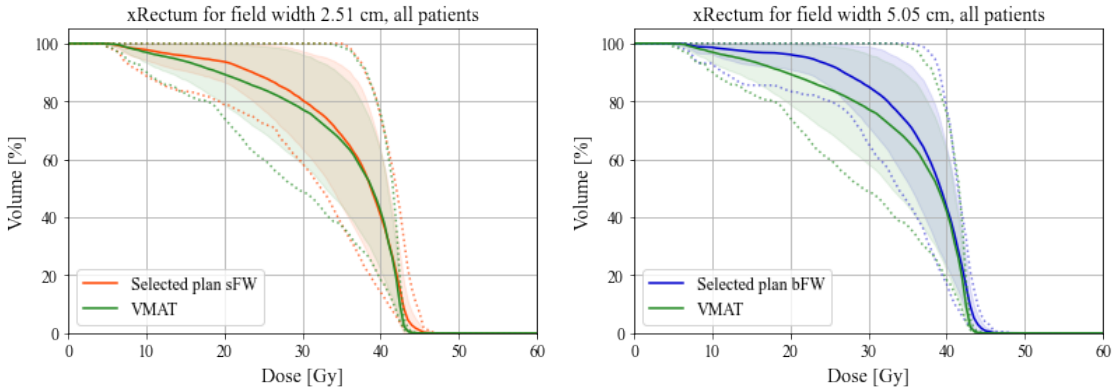

(a) xRectum 2.51 cm

(b) xRectum 5.05 cm

Figure 31: Mean cumulative DVHs for xRectum for all patients. Data from the reference plans (green) and the best HT with FW 2.51 cm (orange) (a) and 5.05 cm (blue) (b), respectively. The solid lines represent the mean values, and the dotted lines represents the minimum and maximum dose values. The shaded areas are the calculated first standard deviation.

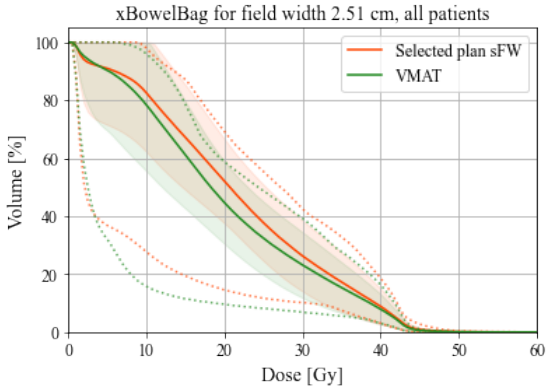

(a) xBowelBag 2.51 cm

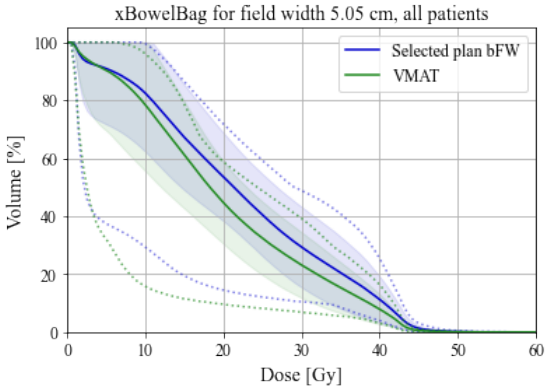

(b) xBowelBag 5.05 cm

Figure 32: Mean cumulative DVHs for xBowelBag for all patients. Data from the plans made from automatic VMAT planning (green) and the best HT plans with FW 2.51 cm (orange) (a) and 5.05 cm (blue) (b), respectively. The solid lines represent the mean values, and the dotted lines represents the minimum and maximum dose values. The shaded areas are the calculated first standard deviation.

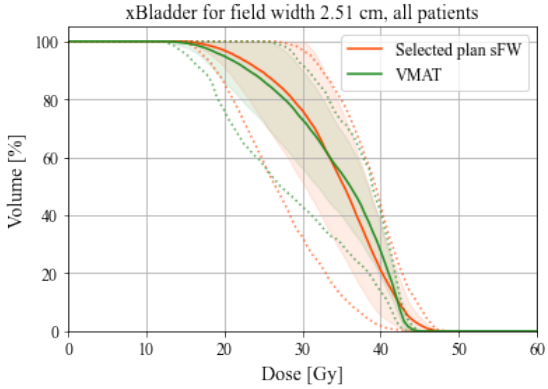

(a) xBladder 2.51 cm

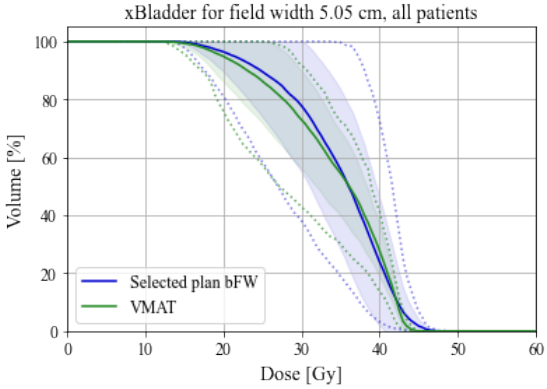

(b) xBladder 5.05 cm

Figure 33: Mean cumulative DVHs for xBladder for all patients. Data from the reference plans (green) and the best HT plans with FW 2.51 cm (orange) (a) and 5.05 cm (blue) (b), respectively. The solid lines represent the mean values, and the dotted lines represents the minimum and maximum dose values. The shaded areas are the calculated first standard deviation.

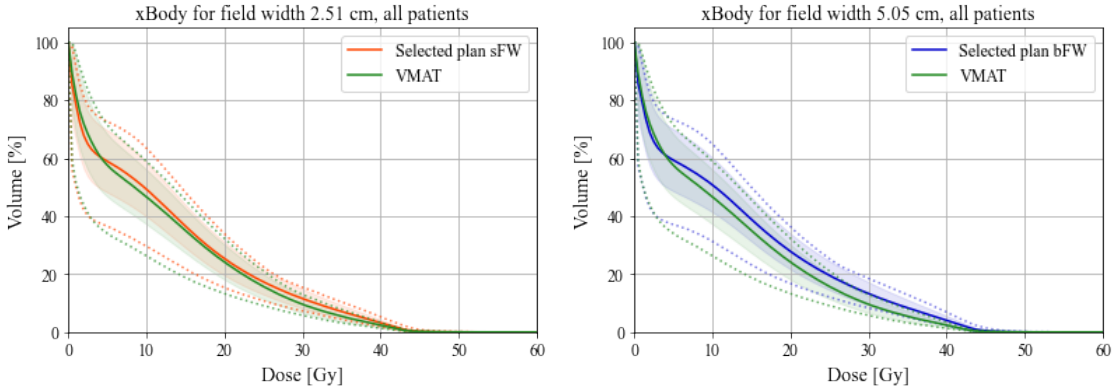

(a) xBody 2.51 cm

(b) xBody 5.05 cm

Figure 34: Mean cumulative DVHs for the xBody for all patients. Data from the reference plans (green) and the best HT plans with FW 2.51 cm (orange) (a) and 5.05 cm (blue) (b), respectively. The solid lines represent the mean values, and the dotted lines represents the minimum and maximum dose values. The shaded areas are the calculated first standard deviation.

4.2.2 Conformity Index

The CIs defined by the CN in Equation (1) were calculated for reference plans and HT plans for the boost volumes PTVn_55 and PTVn_57.5 are shown in Table 17 as the mean values and range. Box plots of the obtained CNs are shown in Figure 35. The worst HT plans are included for comparison. The reference plans have higher CNs for the boost volumes than the HT plans for all patients. However, the CNs for the best HT plans with FW 2.51 cm were very similar to that of the reference plan, whereas the worst HT plans have consistently significant lower values for CNs. Associated p-values of the mean are given in Table 17, with statistical significance marked in bold. Figure 36 and 37 show the conformity of a boost volume (SIB volume) for patient 2 for reference plans and HT plans with FW 5.05 cm and 5.05 cm, respectively. Whereas the 51.75 Gy reference isodose is visualised around the PTVn_57.5.

Table 17: CNs calculated from Equation (1) for the reference plans and selected best and worst HT plans for all patients, presented as the mean, data range and p-value for each plan type. Statistical significance is marked in bold.

Plan type	**FW**	**Descritive statistics (CI)**		**p-value**
		Mean ± SD	**Min - max**	
VMAT	-	0.74 ± 0.06	0.44 - 0.92	
Best HT plan	2.51	0.72 ± 0.06	0.44 - 0.91	**0.03**
	5.05	0.68 ± 0.06	0.40 - 0.88	< 0.05
Worst HT plan	2.51	0.39 ± 0.07	0.16 - 0.86	< 0.05
	5.05	0.53 ± 0.06	0.29 - 0.84	< 0.05

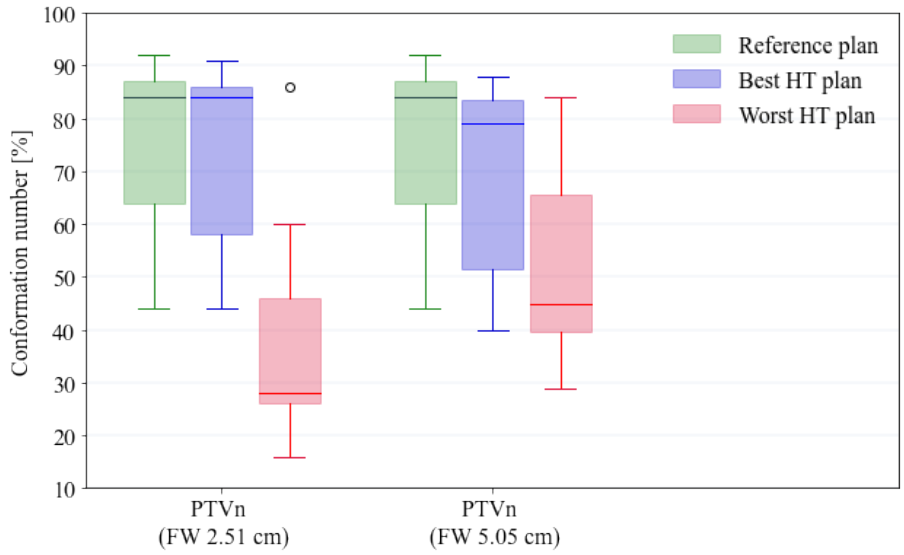

Figure 35: Box plot of the conformation number of PTVn for all patients. Reference plan, selected best and worst HT plans are plotted in green, blue and red, respectively, for both FWs (referring to the HT plans). The median value is marked with a darker line.

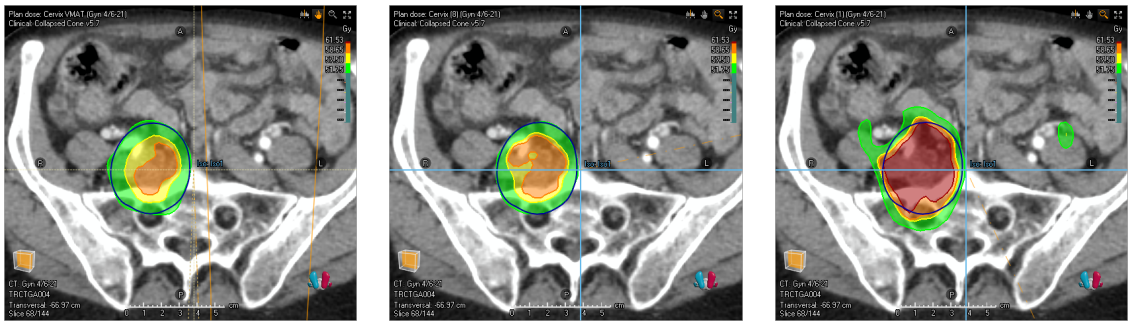

(a) Reference plan (b) Plan 8 (c) Plan 1

Figure 36: Image of the conformity of PTVn_57.5 in dark blue for patient 2 for a positive LN with prescribed SIB to 57.5 Gy. Visualised in green is the 51.75 Gy isodose, ie.e the 90 %-isodose of 57.5, which ideally is perfectly conformed to the PTVn_57.5. Yellow and orange represent dose levels of 57.5 Gy and 58.65 Gy, respectively. All three images are from the same transversal image slice. From left: The reference plan (a) with CN = 0.86, best HT plan (Plan 8) (b) with CN = 0.86 and worst HT plan (Plan 1) (c) with CN = 0.27. HT plans have FW 2.51 cm.

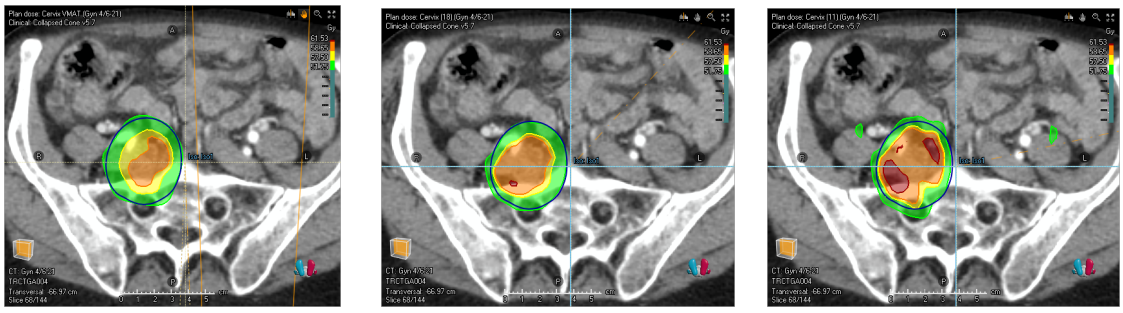

(a) Reference plan (b) Plan 18 (c) Plan 1

Figure 37: Image of the conformity of PTVn_57.5 in dark blue for patient 2 for a positive LN with prescribed SIB to 57.5 Gy. Visualised in green is the 51.75 Gy isodose, ie.e the 90 %-isodose of 57.5, which ideally is perfectly conformed to the PTVn_57.5. Yellow and orange represent dose levels of 57.5 Gy and 58.65 Gy, respectively. All three images are from the same transversal image slice. From left: The reference plan (a) with CN = 0.86, best HT plan (Plan 18) (b) with CN = 0.81 and worst HT plan (Plan 11) (c) with CN = 0.55. HT plans have FW 5.05 cm.

4.2.3 Homogeneity Index

The DHIs calculated by Equation (2) for reference plans and HT plans volume xPTV_45! are presented in Table 18 as the mean values and range. Box plots of the obtained DHIs are presented in Figure 38. The worst HT plans are included for comparison. The reference plans have constantly higher DHIs for the xPTV_45!-volume than HT plans for all patients, while generally small differences observed, as the best and worst plans are quite similar. Associated p-values of the mean are given in Table 18, with statistical significance marked

in bold. Images of the dose distribution within volume xPTV_45! is presented in Figure 39 for patient 2 showing the prevalence of more and higher dose levels for HT plans than reference plan.

Table 18: DHIs calculated from Equation (2) for the reference plans and selected best and worst HT plans for all patients, presented as the mean, data range and p-value for each plan type.

Plan type	**FW**	**Descritive statistics (DHI)**		**p-value**
		Mean ± SD	**Min - max**	
VMAT	-	0.99 ± 0	0.99 - 0.99	
Best HT plan	2.51	0.95 ± 0.008	0.92 - 0.98	$<$ **0.05**
	5.05	0.96 ± 0.004	0.94 - 0.98	$<$ **0.05**
Worst HT plan	2.51	0.95 ± 0.009	0.88 - 0.99	$<$ **0.05**
	5.05	0.94 ± 0.008	0.88 - 0.97	$<$ **0.05**

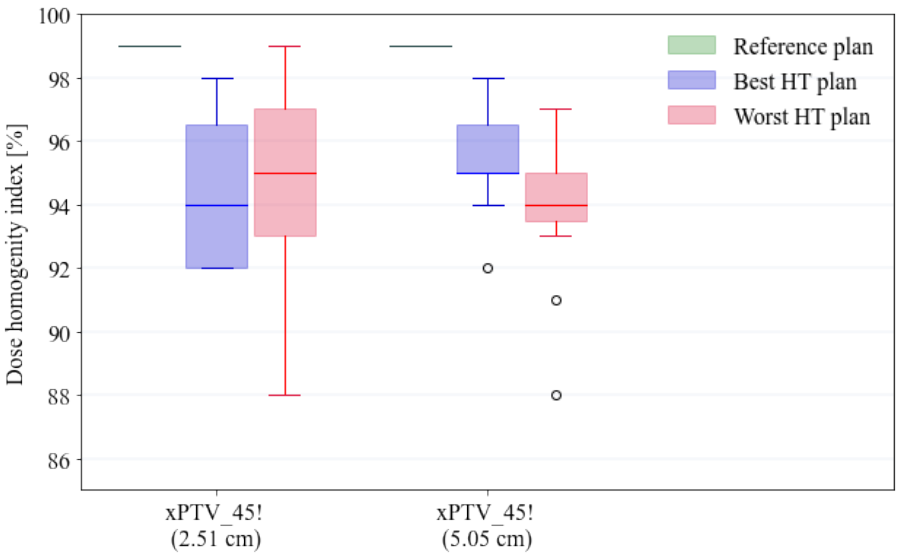

Figure 38: Box plot of the dose homogeneity index of xPTV_45! for all patients. Reference plan, selected best and worst HT plans are plotted in green, blue and red, respectively, for both FWs (referring to the HT plans). The median value is marked with a line.

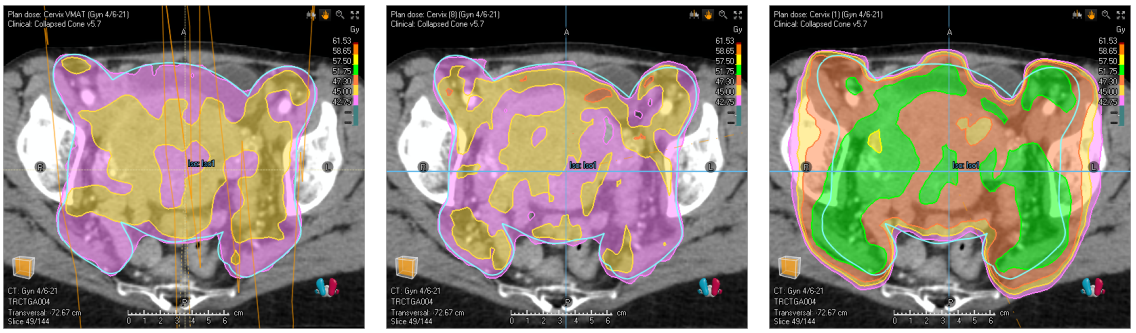

(a) Reference plan (b) Plan 8 (c) Plan 1

Figure 39: Image of the dose distribution in volume xPTV_45! in light blue for patient 2, i.e. PTV_45 excluding PTVn with a 10 mm margin. The prescribed primary dose to PTV_45 is 45 Gy. The reference isodose of 42.75 Gy is visualised in pink. Yellow, orange and green represent dose levels of 45 Gy and 47.3 Gy, 51.75 Gy, respectively.

4.2.4 Treatment Delivery Time

Total treatment delivery time is included in the dose statistics in Figure 5-14. The reference plan have the shortest delivery time for all patients. For HT plans, treatment delivery time was inversely proportional to PF and FW, while proportional to DTf.

5 Discussion

This study aimed to apply an automatic planning script for treatment planning with HT for LACC patients. In the clinic, the automatic planning script is implemented for EBRT with VMAT for cervical cancer, and similar scripts for automatic planning are also evaluated in the clinic for breast and prostate cancer. The planning script is designed to generate plans with sufficient dose to target volumes according to the dose constraints for cervical cancer from the Norwegian Directory of Health [16], while limiting dose to the nearby OARs. The outcome of using the automatic planning script is very good and give precise plans for the VMAT modality. Therefore, the automatic planning for cervical cancer with VMAT is considered the "golden standard" in the clinic. The automatic planning script is used for treatment of cervical cancer with VMAT modality on the Elekta linacs in the clinic, and is yet to be clinically tested on other modalities and machines with different MLCs or constant dose rate. The motivation for this project was to investigate the potential of HT as an alternative treatment technique for LACC patients by use of the current automatic planning script. The physical and technical features of HT that allows for radiation delivery to large volumes by irradiating the target volume slice by slice are assumed to be beneficial for LACC patients. The desire to ensure good quality plans for HT, as well as assuring an unbiased planning comparison was the incentive for applying the same script for the planning of this modality. For HT to be of interest for implementation in the clinic, the plan quality of the HT plans would have to be of same quality as for the VMAT technique. The physical and technical difference between linac and HT machine must be kept in mind while comparing plan quality.

Considering the ability of the automatic planning script to generate high-quality plans for VMAT, it was anticipated to achieve good quality HT plans when the script was adapted for HT. The plan quality of the treatment plans, both reference plans and HT were assessed through visual evaluation and evaluation of the dose statistics, including DVHs, CNs and performing statistical analysis. Many factors were considered for evaluation of the dose distribution in the HT plans, as the conformity and homogeneity to primary target volumes and boost volumes, spread of both high and low dose levels to OARs, sparing of OARs, and effect of varying the beam optimization parameters. Increasing FW from 2.51 cm to 5.05 cm reduced the total treatment delivery time with $40-50\%$ and some times improved the homogeneity of the primary target volume. However, these plans generally resulted in poorer plan quality, as dose were distributed across the contours of the target volumes, less conformity. By tightening the value of the PF from 0.15 to 0.30 improved target volume conformity and sparing of OARs. The main findings of the evaluations are that the automatic planning script does not generate plans with the same good quality for HT as it does for VMAT. This is most apparent when visually examining the treatment plans, but is also reflected in the statistics.

5.1 Plan Evaluation

5.1.1 Visual evaluation

In Figures 9-28, images of plans for all patients are presented to give an impression of the dose distribution and quality of the plans. The images are shown for the transversal plane to best visualize the dose distribution in the target volumes and the vicinity to the nearby risk organs and the plans' ability to account for these volumes. Several key considerations were assessed during the visual evaluation focusing on the distribution of different dose levels and its proximity to ascertain adequate dose coverage, while sparing OARs.

Among the most noticeable differences between reference plans and HT plans is the abnormal distribution of dose in the body volume (as a whole) observed for all HT plans. Whereas the reference spare dose distribution in the anterior and posterior directions, effectively distributing low dose levels to the sides in the transversal plane, HT plans spread a considerably large amount of lower dose levels across large areas of the body volume. This phenomenon is commonly observed as an isotropic shape of the dose distribution, and is attributed to the physical and technical characteristics of the HT machine. Due to the helical pattern followed by the radiation source as it moves around the target volume at a constant speed, the radiation is uniformly delivered in all directions, resulting in a even distribution of low dose levels to a large part of the body volume. Consequently, the organs located anterior and posterior in the transversal plane, such as bowel, bladder and rectum is expected to receive higher doses than in the respective reference plan. The characteristic dose distribution is visually evident in the images of patient 6 in Figure 19 and 20. These images vividly reveal that in the attempt to spare OARs, horns are formed, as discontinuity in the isotropic dose distribution. Similarly, images of the plans for patient 5 also visualize this in Figure 21 and 22.

The conformity of the dose distribution to the target volumes was assessed. For the primary dose conformity, the objective is to ensure that the 95 % of 45 Gy, 42.75 Gy, followed the contour of PTVp and PTVe. For the boost volumes the objective was to ensure that the 90 % isodose lines of the prescription doses of 55 Gy and 57.5 Gy, i.e. 49.5 Gy and 51.75 Gy respectively, encompassed the PTVn, while also assessing any potential dose spillage beyond the boundaries of PTVn. As expected, the reference VMAT plans consistently have good conformation for all target volumes independent of the patient. On the contrary, the HT plans vary in conformity depending on patient and parameter combination. For some patients, the selected best HT plans has comparable conformity to the reference plans. This is observed for boost volumes in patient 3, 7, 8 and 10, and is more prevalent for FW 2.51 cm. However, some of the selected best plans do not have as good boost dose conformity, e.g. patient 4 as shown in Figure 15-16. Other plans have generally worse conformity than the reference plans as high dose levels are spread outside of the contour of the PTVns. Additionally, all HT plans has consistently less conformity of the PTV_45 volume in the sense of both spreading dose beyond the contour lines and breaks in the dose distribution. The latter is commonly seen in the overlap between OARs

and PTV and is assumed to be a result of the HT plans attempting to spare the OAR. For instance, for patient 10, breaks in the dose distribution are observed in areas where PTV and bladder overlap, depicted in Figure 27 and 28.

Further, VMAT plans deliver homogeneous dose distribution to the target volumes, while many of the HT plans are have higher prevalence of hot spots. Hot spots mostly appear within the target volume, additionally it is observed within parts of PTV that overlap with OARs. This is seen for patient 3 and 4 in Figure 13-14 and Figure 15-16, respectively. Placement of high dose levels within OARs is considered critical, reduces overall plan quality and can result in unacceptable plans, due to the associated risks of acute and late toxicity. Higher max doses are observed in HT plans than corresponding reference plans. Very high doses are observed within boost volumes, for instance boost volumes in patient 6: Figure 19 and 20 and patient 7, Figure 21 and 22.

The quality of HT plans with minimum delivery time are generally determined to be between the best and worst HT plans. In the images of plans for all patients, the plan quality of time pressed plans some times are almost as good as selected best plans. Whereas for other patients, the time pressed plans has many abnormal dose distributions, horns and hot spots. The fast gantry speed, thus skipping fast past volumes is thought to be the reason for such observations. This is especially evident in time pressed plans (g-h) in patient 3, shown in Figure 13 and 14.

For all patients, differences between HT plans made with different parameter settings are observed. The conformity to both primary target volumes and boost volumes, the area of the spread of lower dose distribution, as well as prevalence of hot spots. In general, HT plans with FW 2.51 cm appear of better overall plan quality. The variations of the parameter also arises the prevalence of other HT related effects, such as the thread effect. However, these assumptions should not be made solely on visual evaluation, but similar perception are reflected in the dose statistics and is discusses later.

Visual evaluation has been an informative tool for the assessment of plan quality of HT planning and to reveal the significant differences to VMAT planning. These observations were made to determine which HT plans had clinically unacceptable dose distributions and which plans were considered the best and most favorable for both field widths for each patient. However, this is comprehensive work and there was a great challenge in evaluating plans of generally bad quality, especially for the patients where none of the generated plans could be considered to have any acceptable dose distribution. Additionally, it is difficult to assess and ascertain the importance or severity of the abnormal observations, such as hot spots or unusual horn-like dose distribution.

5.1.2 Dose Statistics

Target volumes

The dose coverage to primary target volumes and boost volumes are comparable and sufficiently met for all plans for both VMAT and HT. The primary PTV receiving at least 95 % (42.75 Gy) of the prescribed isodose to 98 % of the volume, with a maximum deviation of 0.37 %. For the boost volumes with prescribed doses 57.5 Gy or 51.75 Gy, received successfully 90 % (51.75 Gy or 49.5 Gy) of the dose to 98 % of the volume, with a maximum deviation of 0.37 %. From this, there are no indications of dose coverage being an issue in any of the plans created for either VMAT or HT.

As expected from the visual evaluation, the CNs for the HT plans are lower than for the reference plans, implying generally better conformity in the reference plans. However, the selected best plans have done a significantly better job of maintaining an acceptable conformity for the boost volumes, as seen for the 51.75 Gy reference isodose for patient 2 in Figure 36. Box plots of the CNs, in Figure 35, clearly show that for conformity in plans with FW 2.51 cm are comparable to that of the reference plans. The p-values implies that the values for both the best and worst HT plans differs from the reference plans with statistical significance. However, Figure 36 shows that with FW 2.51 cm the best plan (b) has significantly better conformity than the worst plan (c). It is also observed that in the best HT plans, Figure 36b and 37b, the boost dose conformity is better for FW 2.51 cm. Improved conformity is pursued to help deliver minimum dose to OARs and maximum dose to the PTVs. According to requirements of modern radiotherapy, 95 % isodose should cover the PTV, so CIs are frequently used for evaluating quality of conformation of treatment plans [68]. Guerrero et. al emphasize the importance of a high degree of conformity in treatment plans not only because it provides less dose to OARs, but also allows for escalation of the dose without increasing toxicity in normal tissue [69]. For gynecological patients who are unable to receive BT as part of their radiotherapy this could be useful. In a study from 2010, Hsieh et al. explored stereotactic body radiation therapy (SBRT) delivered with HT as a feasible alternative to BT in treatment of LACC [70]. HT administered SBRT is acknowledged as an effective modality for treating lung cancer and metastatic liver tumors [71]. Through improved CBCT, HT has the ability to accurately identify the exact shape and location of the tumor. Thus, thanks to improved imaging and conformity of target volumes documented HT-guided SBRT appeared to be an effective, and safe, alternative to BT for treatment of LACC in patients compared to that of a conventional treatment modality. However, the effectiveness of many of those therapeutic modalities was not proven in controlled trials [70].

The DHI was calculated as measurement of the ratio between the dose reached by 95 % dose to a specific volume and the dose to 5 % of the same volume. This is seen as a measurement of the homogeneity of the volume as a value of 1 would imply the same dose to the whole volume. DHI was calculated for volume was xPTV_45!, which is the target volume PTV_45 excluding boost volumes PTVn_55 or PTVn_57.5 with a margin of 10 mm.

Even though DHI gives information about the homogeneity in a selected volume, it is not related to a specific reference isodose. Looking at the distribution of the cumulative dose to the volume, thus a higher DHI implies lesser of the higher dose levels. All plans have relatively high DHI values. The resulting DHIs indicate that the homogeneity with in the xPTV_45! is similar, or lower, for all plans, even though differences between the VMAT plans and HT plans determined statistically significant with a p-value less than 0.05. This is explained by DHIs for the reference plans are equal, therefore any deviation from this value (0.99) is assumed significant. However, DHI should not be viewed as a tool that could replace the qualitative analysis of a plan slice by slice for detecting any unreasonably high or low doses. From the visual evaluation the homogeneity was not as evident due to the occurrences of breaks and hot spots within the volume. Also the HT plans that are considered bad have high homogeneity and seem to maintain homogeneity at the cost of conformity, this is visualized in Figure 39. Figure 39c shows that even though there is less conformity and visually higher dose levels, the homogeneity is conserved.

OARs

Due to the many nearby OARs, treatment planning for LACC patients is a complicated process. It is important to keep dose to the risk organs: For OARs with more serial than parallel arrangements of subvolumes, such as the rectum, bladder, and bowel, low D_{max} is essential for keeping the organ function and avoid complications. There is a compromise between achieving adequate dose coverage to target volumes as well as minimizing dose distribution to these organs, determined by a set of dose constraints. As dose coverage to targets are prioritized to maximize effect of treatment, dose distribution to risk organs is inevitable.

In VMAT planning, a tendency of spreading dose to the sides is observed and is considered to be a result of attempting to spare the nearby OARs, especially bowel and bladder. This is observed for many of the patients in (a-b) in Figure 9-28. On the contrary, the HT plans spread dose isotropically throughout the body volume, as visualized in all the HT plans for patient 8 in Figure 23 and 24. This difference in dose distribution is thought to be due to the physical limitations of the HT machine, and constant speed of gantry and couch and constant dose rate. resulting in spread in low dose levels to the bowel and body volume, this is reflected in the dose statistics as well.

Since the coverage to target volumes was adequate for all plans, the distribution of dose to the OARs is important to consider for determining plan quality. Therefore, the dose statistics extracted from RayStation concerning the planned dose to the nearby OARs were used to make final decision of selecting best and worst HT plans. In addition, the statistics were used for the comparison between the selected HT plans and the VMAT reference plans. The dose to OARs was analyzed by looking at the mean cumulative dose and maximum dose to the selected volumes of interest. Evaluation of dose distribution to the whole OAR volumes is not included in the thesis as it is not emphasised during the assessment of the plan quality. It was observed that the reference plan, did not fulfill the clinical goals for some of the OARs (whole volume), although they are considered the

best possible treatment plans in the clinic. In addition, it is challenging to compare these volumes when they are positioned within or partially within target volumes. Consequently, it was chosen to look at two different partial volumes of rectum, bowel, bladder and body, as it was expected to find the greatest differences in dose distributions here. The two partial volumes were defined as the part of the OAR that does *not* overlap with PTVn, with a 15 mm margin, named xOAR-PTVn, and the volume that exclude *all* of PTV, named xOAR. Tables 5-14 shows the statistics for all patients. $D_{0.03}$, in terms of max dose to 0.03 cm^3 volume, is presented for xOAR-PTVn and D_{mean} is presented for xOARs.

The xOAR-PTVns are used in optimisation process to avoid hotspots in OARs even though they intersect with PTVp. For these volumes the maximum doses are evaluated and it is observed that the reference plans almost always have better sparing of OAR (but not always), keeping the maximum dose under the set limits for the different organs. The HT plans generally struggle to achieve the same sparing of high doses to the xOAR-PTVn, this is persistent for all the selected OARs. For example, dose values of 60.56 Gy and 65.85 Gy is seen in xBody-PTVn for patient 1 and 2, respectively. However, selected best plan for the same patients is 52.81 Gy and 56.22 Gy for FW 2.51 cm and 49.15 Gy and 50.1 Gy FW 5.05 cm. Additionally, it was taken into account whether the max dose limits exceeds an upper limit of 50 Gy, clinicians would find it difficult to accept plans that place higher max doses within risk organs. The highest values are observed for bladder, body and sometimes bowel. Max dose values for rectum is generally within the set constraint, 47.3 Gy, or lower than 50 Gy. Although a plan of best quality was determined for both FWs for each patient, it is not implied clinical acceptance. Best plans selected for patient 4 and 6, even the selected best plans have high dose levels at max of 56.73 Gy and 62.73 Gy, respectively, which is not accepted for clinical use. However, for some patients, e.g. patient 8, the best HT plan has comparable overall plan quality to the reference plan.

The mean cumulative dose to xOAR is a measurement of the dose that is distributed exceeding the contours of the target volumes. In the case of comparing HT plans to reference plans, it was thought more interesting to look at the spreading of the dose to these volumes. From visual evaluation it is observed that there is a significant spread of dose to the bowel, as well as to the general body volume. This spread is most apparent generally for lower dose levels. This is observed in DVH curves for the same volumes, Figure 31-34.

DVHs curves were made from the dose statistics of the xOARs to show the percentage of the volume receiving specific doses. It is observed that HT plans generally have higher volume percentage than the reference plan for all doses. For xRectum, in Figure 31, the reference curve is generally lower than the curve for the HT plan. However, the curves are quite similar in the higher dose range. The HT plan shows that for higher dose levels the volume percentage receiving these doses are slightly higher. For FW 5.05 cm, the minimum doses for HT plan is higher. The curves presenting the dose distribution in xBladder are crossing several times, as seen in Figure 33. Therefore it is not consistent in what plan has the highest volume percentages of a specific dose. For xBowel and xBody the volume

percentages are consistently higher in HT plans than in reference plan for all dose levels.

Statistical analysis were performed to determine whether the obtained differences in the dose values between the HT plans and the reference plans were due to chance or real, and therefore statistically significant. A paired Student t-test was considered due to its ability to compare paired data. However this test assume normal distribution of data being tested, hence a *Shapiro-Wilk* test for normality was performed. This test revealed that not all data had normal distribution and a non-parametric test would be more suitable. Therefore, a Wilcoxon signed-rank test was performed to determine whether there was statistical significance of the obtained doses in xOARs in HT plans compared to the reference plans. By obtaining the mean cumulative dose to the xOARs for the reference plan and the selected best HT plans for each patient, paired observations are ensured. The test ascertain statistical significance for rectum, bowel and body with p-values < 0.05. Which implies that there is significant differences in the dose spread to this part of the OARs between the HT plans and the reference plans. For bladder the p-value is greater than 0.05 and no statistical significant differences are found between the two different plan types. This is consistent with what is observed in DVH for this organ, Figure 33.

In box plot showing the CNs for selected HT plans compared to reference plans, the median value for best plan with FW 2.51 cm, as well as the interval, are very similar. Associated p-value was determined to 0.03, therefore statistical significant. Although the medians of the two data sets are the same, the test takes into account the magnitude and direction of the differences between the paired observations, in this particular case all ranks are consistently negative due to CNs for HT plans being equal or lower than the reference plans'. Therefore, the box plots give a better indication of the actual differences and distribution of the CNs. Statistical significance is also determined for all HT plans for the DHI values. This is more apparent from box plots in Figure 38. All DHIs for reference plan were 0.99, significance, but all obtained DHIs for HT plans are within a 11 % difference interval from the reference plan.

However, from observing the dose statistics in the plans for each patient the differences are generally small and it remains uncertain whether these dose differences are clinically relevant or if they are acceptable. The average differences are found to be between 0.53-1.53 Gy for FW 2.51 cm, and 1.19-2.19 Gy for FW 5.05 cm, depending on the OAR. The effect of these variations in dose is unknown, hence the significance of these differences should be considered from a clinical point of view, not only statistically. However, the biggest differences are found in the volume for bowel bag which is consistent with the observations of spread of lower dose levels to the volume.

In some of the HT plans an effect known as the threading effect is visible. This effect is indicated by ripples in the longitudinal dose profile and seem to be parameter dependent. The effect of varying the pitch factor is shown in the sagittal plane in Figure 30. The threading effect is said to occur due to beam divergence in the fan beam geometry used in HT which result in issues with helical junctioning causing small dose delivery patterns,

such as ripples [72]. Reducing this effect is beneficial for improving dose conformity in the target volumes. Different values for reducing threading has been proposed [72, 73]. Double threading has also been suggested as solution to reduce occurrence and effect of such ripples. The technique involves repeating the dose delivery process, but starting the gantry rotation at 180 degrees off-phase from the initial delivery to level out the ripple waves [72].

5.1.3 Parameter Combinations

The combination of the tomo-specific parameters evidently influence the plan quality. From visual evaluation of the plans, the selected HT plans that achieve best plan quality are Plan 4, 7 and 8 with field width 2.51 cm, and Plan 14, 17 and 18 for HT plans with FW 5.05 cm. Common for these are a pitch of 0.25 or 0.30 regardless of which delivery time factor is used. Moreover, Plan 1-2, 5-6, 11-12 and 15-16 overall resulted in poorer plan quality. Common to these plans is a PF of 0.15 - 0.20 regardless of which delivery time factor. The PF is observed to influence the prevalence of the thread effect discussed above.

It was selected best and worst HT plans for both field widths. Due to large target volumes common for LACC patients, it might be expected to prefer a larger FW in terms of achieving reasonable delivery times. However, studies have shown to be using both FWs [74, 75]. Wu et al. studied the use of both fixed and dynamic jaw observing that improved target coverage and sparing of most OARs was achieved by using the dynamic jaw. Further, they conclude that the dynamic jaw 2.5 cm mode should be used for treatment of cervical carcinoma with HT. Considering the risk of long treatment times, the dynamic jaw 5.0 cm mode could be an option [75]. In this study it was not focused on which of the two FWs resulted in better plans. However, it is observed that thread effect discussed above is more prevalent for bigger FWs. In addition, the CN is higher for smaller FW. The DVHs reveal slightly bigger differences between HT plans and reference plans for the mean cumulative dose to xOARs for HT plans with FW 5.05 cm than for HT plans with 2.51 cm, with the difference increasing from 42 % to 68 %. It was further observed that for larger FWs, the dose gradient got worse in the cranial–caudal direction, even though the beam-on-time is reduced. Many studies have analyzed the relationship between these parameters and their influence on the quality of treatment plans and beam-on time. Whereas some have made it possible to predict the treatment time for a given MF, FW and it can be used in clinical practice [76]. An unreleased feature for optimization for HT offers a solution to this, by allowing for dynamically changing the jaws in the longitudinal direction, thus FW. Jaw optimization is not available in TPS yet, and has to has to be validated by clinics to evaluate whether this is indeed a way of improving plan quality. However, this feature could be of interest for these kinds of diagnosis.

Further, other publication have included tuning of the modulation factor (MF) in evaluation of plan quality for treatment with HT. Modulation factor (MF) is common set by the

vendor-recommended settings, but is documented to have an impact on HT plan quality as it can be used to restrict the delivery time. Optimal values of MF have been review for various cancer types and is documented to influence the plan quality and treatment time [76, 77, 78]. That for small pitch factors (< 0.20) MF does not affect the delivery time, while for the contrary is true for larger pitches (> 0.25) as lowering MF will both decrease treatment time and plan quality until maximum gantry speed is reached [78]. As improvement of MF can be associated increasing the delivery time it confirms that the clinics need to determine their preferred combination of parameters for generation of optimal plan quality, as well as adjusting them for different cancer types [77].

Treatment delivery time was not considered during selection of the best HT plans for evaluation of plan quality in terms of dose distribution. However, delivery time should be a subject of consideration if implementation in the clinic is considered. Even if the overall plan quality is good, longer delivery times could potentially increase the probability of geometric uncertainties e.g. due to patient movement and variations of PTV, as well as OAR (such as air in rectum or bladder fill), hence inaccurate delivery. Additionally, for longer treatment sessions the clinic would not be able to treat as many patients per day with HT than with a linac. The delivery times displayed together with the dose statistics in Figure 5-14 implies evidently that HT demands a considerably longer total treatment delivery time than treatment with a linac. This is primarily due to the set-up of the HT machine, its limitations, and the beam and parameter settings. In particular, the combination of FW, PF and DTf was investigated. It was expected that utilizing parameter combinations allowing for long delivery times would result in optimised treatment deliveries as the machine had more time to distribute the radiation doses. On the contrary, HT plans with the longest delivery times are considered among the worst plans. Increasing FW from 2.51 cm to 5.05 cm reducing the total treatment delivery time with $40 - 50\%$ and improved the homogeneity of the primary target volume. Tightening the value of the PF from 0.15 to 0.30 improved target volume conformity as well as OAR doses as well as decreasing the treatment delivery time. In addition, as expected, the treatment delivery time increased when increasing treatment delivery factor from 1 to 1.5. Minimum treatment delivery time was achieved by manually setting the time, the associated parameter combination was a PF of 0.43 and a DTf of 1.5 for both field widths. Considering the plan quality, the HT plans with shortest delivery time are neither considered best nor worst. Overall, the selected best plans have shorter delivery times than most of the other plans, but have significantly longer delivery times compared to other techniques, such as VMAT. Therefore, whether treatment delivery times is proportional to the quality remains uncertain. The delivery time is estimated by the software of the TPS and in the clinic it has been observed to deviate with 30-50 sec from real beam-on-time on the linac, however for many of the HT plans corresponding deviations is not significant.

5.2 Automatic Planning for HT

When relying on manual treatment planning, maintaining (complete) neutrality and achieving optimal plans can be challenging. This issue is particularly evident in dose planning studies that involve comparing proton and photon techniques, as photon plans often fall short of their maximum potential. In such cases, utilizing a script becomes a vital tool. By ensuring that all plans are subjected to identical prerequisites, including the same number of iterations, the script helps level the playing field. This standardized approach allows for fair and objective comparisons between different treatment techniques. It minimizes the influence of human bias and ensures that each plan is evaluated based on its intrinsic quality rather than variations in manual planning methodologies. Thus, implementing a script as part of the dose planning process promotes consistency and eliminates potential inconsistencies arising from individual planner preferences or limitations. With this approach, the focus shifts toward optimizing treatment plans to their fullest potential, leading to more reliable and informative outcomes in comparative studies.

The automatic plans were created using an in-house developed Python script within the scripting environment of RayStation. All plans made in this master project are generated by running this planning script to maintain a comparative basis and hopefully achieve optimized HT plans. VMAT plans are used as reference plans since they are considered the best achievable treatment plans in the clinic.

The automatic planning script has facilitated and optimised treatment planning for cervical cancer patients using VMAT modality in the clinic at RT department at St. Olavs Hospital. The automatic planning script is developed for different cancer types, and in theory, it takes into account different treatment delivery systems. However, the automatic script has never been tested for other treatment modalities or treatment machines than VMAT and Elekta linac used in the clinic, not until now. As it turns out, this is not an optimal planning approach for HT, while it remains uncertain if it would be suitable for other modalities, e.g. IMRT. The automatic script is not suitable for planning for HT for a number of reasons discussed previously in the discussion. Whereas, the main observations are isotropic spread of lower dose levels to OARs and body volume, hot spots in bladder, occurrence of lower of conform dose coverage to target volumes and boost volumes, as well as longer treatment delivery time. This could be due to the structure of and constraints in the planning script, the need to consider tomo-specific parameters and the difference in physical constraints during delivery. The results indicate that the automatic planning script might be more specifically optimised for VMAT planning it is than initially thought.

The structure of the optimisation process for VMAT planning is presented in Figure 3. The plan optimization strategy consisted of two phases: initially minimizing the dose to relevant OARs and secondly securing target coverage. To lower the OAR doses as much as possible for each individual patient the doses to individual OARs are evaluated and optimization objective doses are adjusted down by 70 % accordingly after each round of optimization. Considering HT, a potential challenge in the optimization process is this

intricate compromise minimizing OAR doses and meeting target volume requirements. Utilizing optimization objective doses that are progressively adjusted down after each iteration of the optimization process. It remains uncertain whether this iterative approach of systematically reducing OAR doses while concurrently striving to maintain target coverage within predefined requirements set too hard constraints on the OARs. It is a relatively demanding constraint. For HT it seems to lead to the appearance of breaks in dose coverage in parts of PTV that overlap with OARs, as well as abnormal spreading of low dose levels in the body volume in the HT plans. Setting a looser constrain, e.g. by adjusting down only by 90 % for each iteration, could be a possible solution to this challenge.

The objective functions presented in Figure B.1 are used in optimization process to decide the allowed dose distributions, in terms of restrictions based on different weightings. Among these objective functions it was observed that it is not explicitly set a constraint that avoids placement of higher dose levels in the part of OARs that overlap with the PTV rather focusing on the mean dose to the volumes. This is seen for the bladder. Rather than setting a D_max constraint, there is determined a maximum value for doses at the D_{50} in DVH. Consequently, no restrictions are set to specifically avoid maximum doses in this volume, allowing high dose levels to the volume, while keeping the mean dose below a certain value.

The partial OAR volumes excluding PTVn (xOAR-PTVn) are used by the script as hot spots isodose volumes to maintain an acceptable maximum dose. As it appears from the dose statistics for Dmax in these volumes, this is not always achieved in the HT plans. This was also observed in the visual evaluation and is visualized in the transversal slices of patient 3 and 4, shown in Figure 13 and 15. Most apparent in the volume of the bladder. The script further assures target coverage by increasing the weight of the objectives of the minimum dose by a suitable factor, based on how far the current dose distribution is from reaching the clinical goal set for the target volume coverage.

VMAT and HT are two distinct treatment techniques with different planning requirements. VMAT utilizes rotating arcs, while HT employs dynamic delivery through a ring gantry. The planning script designed for VMAT may not effectively address the tomo-specific parameters, such as pitch factor, field width and modulation factor, as well as the constraints associated with HT planning. Thus, modifications for optimizing parameter combinations should be included. By looking at parameter combination for the selected best plans for all patients, this project might give an idea of which parameters that can provide basis for creating good treatment plans. Failure to account for these tomo-specific parameters in the automatic planning process can result in plans that do not adequately optimize dose distribution, target coverage, and sparing of OARs, as seen in selected worst plans.

In HT planning, balancing the dose requirements for the target volume and OARs can be challenging due to the complex interplay between these structures. Achieving high conformity to the target while simultaneously minimizing dose to OARs often necessitates

an iterative planning process. The automatic planning script may not provide sufficient flexibility or iterations to address this interplay effectively. In relation to the technical and physical limitations of the HT machine, such as constant gantry speed and constant dose rate, seem to be hindering the efficiency and effectiveness of the planning process.

A few reviews of automation of HT planning have been published using different approaches than the one explored in this project. In 2021, Castriconi et al. evaluated knowledge-based (KB) automatic planning for HT for clinical implementation for of high-risk prostate cancer, including pelvic node irradiation. By using the RapidPlan tool incorporated in the TPS called Eclipse they successfully generated automatic plans of similar or better quality compared to corresponding manual plans [79]. Other studies have used KB and RapidPlan for planning for left-sided whole breast using HT [80]. This methodology was reported to improve planning in terms of time-sparing, elimination of interplanner variability, and reduce risk of suboptimal planning [79]. Others have used deep learning methods for prediction of 3D voxel-by-voxel dose distributions of HT using previously treated HT plans as training data, to predict a 3D dose distribution [81]. In the pursuit of improving RT planning design, by ensuring plan quality and consistency, comparisons of clinical techniques, and guidance of automatic treatment planning.

Automatic planning algorithms, including those used for VMAT, often rely on predefined optimization objectives and constraints. However, these objectives and constraints may not be applicable or optimal for HT planning considering the planning of HT often involves complex cases with varying anatomical and dosimetric considerations. To overcome these limitations, it would be necessary to develop planning algorithms specifically tailored for HT. These algorithms should consider the unique parameters, constraints, as well as working out a suitable compromise between target volumes and OARs. It should be possible to design more effective and efficient automatic planning approaches for HT. A further development of this project is to identify the inappropriate factors in the optimisation structure of the automatic VMAT script and adjust the script accordingly. Alternatively, an automatic planning script could be built specifically for HT from scratch. Additionally, this could be adapted for treatment of other diagnosis than LACC. Nevertheless, the automatic planning script is not suitable for generating clinical LACC plans for treatment with HT, without making further adjustments of the optimization structure.

5.3 Future work

This (sub)section includes a summary of future work already proposed during the discussion, in addition to some new proposals.

The results (visual evaluation and dose statistics) clearly indicate that the automatic script is not an optimal approach for generating treatment plans for HT, which implies that the optimization structure of the script need to be adjusted for adaption for HT. Proposed approaches are to change weighting in optimization process or loosen the dose constraints to the OARs, i.e. from 0.7 to 0.9. Adjusting the function weight of the max DVH optimisation functions based on the function value to reduce OAR doses could be changed in the first phase of optimization process. Other suggestions are to change number of iteration and loops, or building a new automatic planning script from scratch. Modification of the script, as well as considerations for other cancer types, structure is necessary if a HT system were to be implemented as an alternative treatment option at St. Olavs Hospital. Additionally, it would have to be adapted for all cancer types. Moreover, other types of TPS could be considered due to good documentation, such as planning in Eclipse Varian Medical Systems) [79, 80].

Also evident is that optimal parameter combination should be determined, especially FW and PF, consequently having great impact on the plan quality in terms of dose distribution and its conformity. In addition, the effect of varying the MF could be taken into account. As well as consideration of the acceptable treatment delivery time for HT. In this project, two different FWs were used. However, an unreleased feature for HT planning in RayStation, called jaw optimization, enables for variations of the FW during treatment and could be of interest for HT plan quality optimization. However, this feature has to be validated by clinics to evaluate whether this is beneficial for plan quality of treatment plans.

Additionally, fallback (FB) planning is another planning technique available for HT in RayStation. RaySearch RayStation FB planning module can generate an equivalent backup RT plans facilitating treatment on other linacs. Studies have showm that FB plans can be clinically comparable to the overall treatment plan when utilized as a backup option, with practical and efficient work flow for patient treatment in the event of machine down. In terms of optimizing the quality and flexibility of FB planning for cross-platform technologies, there is a possibility to explore this feature for HT [82, 83].

6 Conclusion

A script used for automatic treatment planning in RayStation at St. Olavs Hospital was applied for planning for external irradiation with HT for LACC to evaluate HT as an alternative treatment delivery technique for this patient group. A comparative base was kept for unbiased planning with HT and VMAT by utilizing the automatic planning script for both modalities. By combining visual and quantitative evaluation of the treatment plans it was observed that HT plans had a lower boost dose conformity, appearance of hot spots in OARs, overlapping with target volumes and extensive spread of lower dose levels outside of target volumes. Although the dose statistics revealed that dose coverage to target volumes were sufficient for both treatment modalities, the reference plans showed significantly better target coverage in terms of conformity and homogeneity of the dose distribution of the primary PTV (PTV_45). Breaks observed in dose distribution in areas of target volumes overlapping with OARs were found to arise from the physical limitations of the HT system and strict constraints set by the structure of the automatic planning script. The plan quality of HT plans were found to be directly related to the tomo-specific parameter combinations, observing improved boost dose conformity for FW 2.51 cm than for FW 5.05 cm, and more sparing of OARs by increasing the PF from 0.15 to 0.30, as well as decreasing total delivery time. The automatic planning script aimed to deliver enough dose to target volumes according to the dose-volume constraints, while maintaining as low dose as possible to OARs. The plan quality assessments revealed that this aim is not completely accomplished for creation treatment plans for HT, as observed for VMAT. This implies that a different optimisation structure that accounts for the tomo-specific parameters and technical features is required for adapting automatic planning for HT. Consequently, it was concluded that the automatic planning script is not suitable for generating clinical LACC plans for treatment with HT, without making further adjustments.

References

[1] P. Mayles, A. Nahum and J. Rosenwald. *Handbook of Radiotherapy Physics: Theory and Practice*. Taylor & Francis Group, 2007.

[2] S. Chiavassa et al. 'Complexity metrics for IMRT and VMAT plans: a review of current literature and applications'. In: *The British Journal of Radiology* 92 (2019).

[3] M. Teoh et al. 'Volumetric modulated arc therapy: a review of current literature and clinical use in practice'. en. In: *Br. J. Radiol.* 84.1007 (Nov. 2011), pp. 967–996.

[4] Y. Fu et al. 'Artificial intelligence in radiation therapy'. en. In: *IEEE Trans. Radiat. Plasma Med. Sci.* 6.2 (Feb. 2022), pp. 158–181.

[5] T. R. Mackie. 'History of tomotherapy'. en. In: *Phys. Med. Biol.* 51.13 (July 2006), R427–53.

[6] S. U. Pigorsch et al. 'Report on planning comparison of VMAT, IMRT and helical tomotherapy for the ESCALOX-trial pre-study'. In: *Radiation Oncology* 15 (2020), pp. 1–10.

[7] A. A. Loginova et al. 'Optimized conformal total body irradiation methods with helical TomoTherapy and elekta VMAT: Implementation, imaging, planning and dose delivery for pediatric patients'. In: *Frontiers in Oncology* 12 (2022).

[8] O. Lauche et al. 'Helical tomotherapy and volumetric modulated arc therapy: new therapeutic arms in the breast cancer radiotherapy'. In: *World Journal of Radiology* 8.8 (2016), p. 735.

[9] M. Serra et al. 'Dosimetric comparison among cyberknife, helical tomotherapy and VMAT for hypofractionated treatment in localized prostate cancer'. In: *Medicine* 99.50 (2020).

[10] D. Nguyen et al. 'Advances in automated treatment planning'. en. In: *Semin. Radiat. Oncol.* 32.4 (Oct. 2022), pp. 343–350.

[11] I. Gleeson et al. 'Implementation of automated personalised breast radiotherapy planning techniques with scripting in Raystation'. en. In: *Br. J. Radiol.* 96.1144 (Mar. 2023).

[12] D. J. Rhee et al. 'Automated radiation treatment planning for cervical cancer'. en. In: *Semin. Radiat. Oncol.* 30.4 (Oct. 2020), pp. 340–347.

[13] Z. Yuan et al. 'Accelerate treatment planning process using deep learning generated fluence maps for cervical cancer radiation therapy'. en. In: *Med. Phys.* 49.4 (Apr. 2022), pp. 2631–2641.

[14] I. S. Hoem. *Automatic VMAT planning in RayStation for locally advanced cervical cancer.* 2022.

[15] K. Tanderup et al. 'Effect of tumor dose, volume and overall treatment time on local control after radiochemotherapy including MRI guided brachytherapy of locally advanced cervical cancer'. en. In: *Radiother. Oncol.* 120.3 (Sept. 2016), pp. 441–446.

[16] T. N. D. of Health. *Nasjonalt handlingsprogram med retningslinjer for gynekologisk kreft.* URL: https://www.helsedirektoratet.no/%20retningslinjer/gynekologisk-kreft-handlingsprogram (visited on 12/05/2023).

[17] S. Panda et al. 'Treatment planning comparison of volumetric modulated arc therapy employing a dual-layer stacked multi-leaf collimator and helical tomotherapy for cervix uteri'. In: *Radiation Oncology* 15.1 (2020), pp. 1–12.

[18] D. B. Richardson. 'Occupational health risks in nuclear power'. In: *Encyclopedia of Energy*. Elsevier, 2004, pp. 489–496.

[19] A. Patel. 'Benign vs malignant tumors'. en. In: *JAMA Oncol.* 6.9 (Sept. 2020), p. 1488.

[20] E. B. Podgorsak. *Radiation Oncology Physics: A Handbook for teachers and Students*. International Atomic Energy Agency, 2005.

[21] P. L. Olive. 'The role of DNA single- and double-strand breaks in cell killing by ionizing radiation'. en. In: *Radiat. Res.* 150.5 Suppl (Nov. 1998), S42–51.

[22] R. B. Painter. 'DNA damage and repair in eukaryotic cells'. en. In: *Genetics* 78.1 (Sept. 1974), pp. 139–148.

[23] S. J. McMahon. 'The linear quadratic model: usage, interpretation and challenges'. en. In: *Phys. Med. Biol.* 64.1 (Dec. 2018), 01TR01.

[24] E. Daguenet et al. 'To exploit the 5 'R' of radiobiology and unleash the 3 'E' of immunoediting: 'RE'-inventing the radiotherapy-immunotherapy combination'. en. In: *Ther. Adv. Med. Oncol.* 12 (May 2020).

[25] Oncology Medical Physics LLC. *Serial and Parallel Organs — Oncology Medical Physics.* 2018. URL: https://oncologymedicalphysics.com/serial-and-parallel-organs/ (visited on 20/05/2022).

[26] A. Niemierko and M. Goitein. 'Calculation of normal tissue complication probability and dose-volume histogram reduction schemes for tissues with a critical element architecture'. en. In: *Radiother. Oncol.* 20.3 (Mar. 1991), pp. 166–176.

[27] D. S. Chang et al. 'Normal Tissue Radiation Responses'. In: *Basic Radiotherapy Physics and Biology*. Cham: Springer International Publishing, 2014, pp. 265–275.

[28] N. C. Institute. *Radiation Therapy to Treat Cancer*. URL: https://www.cancer.gov/about-cancer/treatment/types/radiation-therapy (visited on 12/12/2022).

[29] R. Mohan. 'A review of proton therapy - current status and future directions'. en. In: *Precis. Radiat. Oncol.* 6.2 (June 2022), pp. 164–176.

[30] RadiologyInfo. *Intensity-Modulated Radiation Therapy*. URL: https://www.radiologyinfo.org/en/info/imrt (visited on 13/12/2022).

[31] Q.-P. Zhou, Y.-H. Zhao and L. Gao. 'Positron emission tomography and magnetic resonance imaging combined with computed tomography in tumor volume delineation: A case report'. en. In: *World J. Clin. Cases* 10.1 (Jan. 2022), pp. 249–253.

[32] S. B. Saeed. 'Dynamic log files analysis for different dose rate IMRT using DVH and gamma index'. PhD thesis. PhD thesis, Aga Khan University, 2015.

[33] Statens strålevern. *Volum og doser i ekstern stråleterapi.* Statens Strålevern, 2012. URL: https://dsa.no/publikasjoner/_/attachment/inline/bee8860b-36d1-42e7-8d64-f5ad4fcef2e8:8ebb86decddc2818ec31e4999d26cdf7aec14ac2/StralevernRapport_09-2012.pdf.

[34] S. J. Gardner, J. Kim and I. J. Chetty. 'Modern Radiation Therapy Planning and Delivery'. In: (2019).

[35] R. K. Funk, A. L. Stockham and N. N. I. Laack. 'Basics of Radiation Therapy'. In: *Clinical Cardio-Oncology.* Elsevier, 2016, pp. 39–60.

[36] G. K. R. S. Mallick and R. Benson. *Practical Radiation Oncology.* Springer, 2020.

[37] P. Meyer et al. 'Automation in radiotherapy treatment planning: Examples of use in clinical practice and future trends for a complete automated workflow'. en. In: *Cancer Radiother.* 25.6-7 (Oct. 2021), pp. 617–622.

[38] RaySearch Labs. *High Quality VMAT Planning.* 2023. URL: https://www.raysearchlabs.com/vmat-treatment-planning-raystation/ (visited on 14/04/2023).

[39] C. Wang et al. 'Artificial intelligence in radiotherapy treatment planning: Present and future'. en. In: *Technol. Cancer Res. Treat.* 18 (Jan. 2019).

[40] Y. Yang et al. 'Automatic planning for nasopharyngeal carcinoma based on progressive optimization in RayStation treatment planning system'. en. In: *Technol. Cancer Res. Treat.* 19 (Jan. 2020).

[41] D. Zhang et al. 'Automatic treatment planning for cervical cancer radiation therapy using direct three-dimensional patient anatomy match'. en. In: *J. Appl. Clin. Med. Phys.* 23.8 (Aug. 2022).

[42] C. Jihong et al. 'Automated intensity modulated radiation therapy treatment planning for cervical cancer based on Convolution Neural Network'. en. In: *Technol. Cancer Res. Treat.* 19 (Jan. 2020).

[43] S. Trivellato et al. 'Comprehensive dosimetric and clinical evaluation of lexicographic optimization-based planning for cervical cancer'. en. In: *Front. Oncol.* 12 (Nov. 2022).

[44] K. Kisling et al. 'A risk assessment of automated treatment planning and recommendations for clinical deployment'. en. In: *Med. Phys.* 46.6 (June 2019), pp. 2567–2574.

[45] K. A. Nealon et al. 'Using failure mode and effects analysis to evaluate risk in the clinical adoption of automated contouring and treatment planning tools'. en. In: *Pract. Radiat. Oncol.* 12.4 (July 2022), pp. 344–353.

[46] R. Petragallo et al. 'Barriers and facilitators to clinical implementation of radiotherapy treatment planning automation: A survey study of medical dosimetrists'. en. In: *J. Appl. Clin. Med. Phys.* 23.5 (May 2022).

[47] S. Cilla et al. 'Personalized automation of treatment planning in head-neck cancer: A step forward for quality in radiation therapy?' en. In: *Phys. Med.* 82 (Feb. 2021), pp. 7–16.

[48] J. S. Welsh et al. 'Helical tomotherapy: an innovative technology and approach to radiation therapy'. en. In: *Technol. Cancer Res. Treat.* 1.4 (Aug. 2002), pp. 311–316.

[49] A. J. Chang et al. 'Split-field helical tomotherapy with or without chemotherapy for definitive treatment of cervical cancer'. en. In: *Int. J. Radiat. Oncol. Biol. Phys.* 82.1 (Jan. 2012), pp. 263–269.

[50] Accuray Incorporated. *Tomotherapy Products*. 2023. URL: https://www.accuray.com/tomotherapy/ (visited on 20/04/2023).

[51] RayStation Laboratories. *RAYSTATION 12A. User Manual*. English.

[52] S. H. Levitt et al., eds. *Technical basis of radiation therapy*. en. 5th ed. Radiation Oncology. Berlin, Germany: Springer, Nov. 2011.

[53] H. Li and J. Y. Chang. 'Accounting for, mitigating, and choice of margins for moving tumors'. In: *Semin. Radiat. Oncol.* 28.3 (July 2018), pp. 194–200.

[54] M. R. Young and J. B. Yu. *Prostate Cancer (Second edition)*. Academic Press, 2016.

[55] L. Feuvret et al. 'Conformity index: a review'. en. In: *Int. J. Radiat. Oncol. Biol. Phys.* 64.2 (Feb. 2006), pp. 333–342.

[56] A. van't Riet et al. 'A conformation number to quantify the degree of conformality in brachytherapy and external beam irradiation: application to the prostate'. en. In: *Int. J. Radiat. Oncol. Biol. Phys.* 37.3 (Feb. 1997), pp. 731–736.

[57] T. Kataria et al. 'Homogeneity Index: An objective tool for assessment of conformal radiation treatments'. In: *J. Med. Phys.* 37.4 (Oct. 2012), pp. 207–213.

[58] S. Harikrishnaperumal. 'SU-E-T-278: Dose Conformity Index for the Target in a Multitarget Environment'. In: *Medical Physics* 42.6 (June 2015). ISSN: 0094-2405. DOI: 10.1118/1.4924640. URL: https://www.osti.gov/biblio/22548335.

[59] D. Petrova, S. Smickovska and E. Lazarevska. 'Conformity index and homogeneity index of the postoperative whole breast radiotherapy'. en. In: *Open Access Maced. J. Med. Sci.* 5.6 (Oct. 2017), pp. 736–739.

[60] E. McCleneaghan. *The Wilcoxon Signed-Rank Test*. URL: https://www.technologynetworks.com/informatics/articles/the-wilcoxon-signed-rank-test-370384 (visited on 02/06/2023).

[61] W. Small Jr et al. 'Cervical cancer: A global health crisis'. en. In: *Cancer* 123.13 (July 2017), pp. 2404–2412.

[62] National Cancer Institute. *What is Cervical Cancer?* 2023. URL: https://www.cancer.gov/types/cervical (visited on 20/03/2023).

[63] E. Bengtsson and P. Malm. 'Screening for cervical cancer using automated analysis of PAP-smears'. en. In: *Comput. Math. Methods Med.* 2014 (Mar. 2014), p. 842037.

[64] D. Mekonnen and Y. Kebede. 'The prevalence of suicidal ideation and attempts among individuals attending an adult psychiatry out-patient clinic in Gondar, Ethiopia'. en. In: *Afr. Health Sci.* 11.1 (Mar. 2011), pp. 103–107.

[65] P. A. Cohen et al. 'Cervical cancer'. en. In: *Lancet* 393.10167 (Jan. 2019), pp. 169–182.

[66] C. Gennigens et al. 'Optimal treatment in locally advanced cervical cancer'. en. In: 21.6 (June 2021), pp. 657–671.

[67] R. Pötter et al. 'The EMBRACE II study: The outcome and prospect of two decades of evolution within the GEC-ESTRO GYN working group and the EMBRACE studies'. en. In: *Clin. Transl. Radiat. Oncol.* 9 (Feb. 2018), pp. 48–60.

[68] M. Atiq et al. 'Evaluation of dose conformity and coverage of target volume for intensity-modulated radiotherapy of pelvic cancer treatment'. en. In: *Indian J. Cancer* 54.1 (Jan. 2017), pp. 379–384.

[69] M. Guerrero et al. 'Simultaneous integrated intensity-modulated radiotherapy boost for locally advanced gynecological cancer: radiobiological and dosimetric considerations'. en. In: *Int. J. Radiat. Oncol. Biol. Phys.* 62.3 (July 2005), pp. 933–939.

[70] C.-H. Hsieh et al. 'Should helical tomotherapy replace brachytherapy for cervical cancer? Case report'. In: *BMC cancer* 10.1 (2010), pp. 1–5.

[71] J. M. Baisden et al. 'Dose as a function of liver volume and planning target volume in helical tomotherapy, intensity-modulated radiation therapy–based stereotactic body radiation therapy for hepatic metastasis'. In: *International Journal of Radiation Oncology* Biology* Physics* 66.2 (2006), pp. 620–625.

[72] M. W. Kissick et al. 'The helical tomotherapy thread effect'. en. In: *Med. Phys.* 32.5 (May 2005), pp. 1414–1423.

[73] S. G. Ju et al. 'Dosimetric comparison between VMAT plans using the fast-rotating O-ring linac with dual-layer stacked MLC and helical tomotherapy for nasopharyngeal carcinoma'. en. In: *Radiat. Oncol.* 17.1 (Sept. 2022), p. 155.

[74] S. Marnitz et al. 'Which technique for radiation is most beneficial for patients with locally advanced cervical cancer? Intensity modulated proton therapy versus intensity modulated photon treatment, helical tomotherapy and volumetric arc therapy for primary radiation - an intraindividual comparison'. en. In: *Radiat. Oncol.* 10.1 (Apr. 2015), p. 91.

[75] J. Wu et al. 'Dosimetric and delivery comparison of helical tomotherapy with dynamic jaw and fixed jaw for cervical carcinoma'. en. In: 17.7 (Dec. 2021), pp. 1626–1630.

[76] M. Skórska and T. Piotrowski. 'Optimization of treatment planning parameters used in tomotherapy for prostate cancer patients'. en. In: *Phys. Med.* 29.3 (May 2013), pp. 273–285.

[77] C. A. Muthuselvi, T. K. Bijina and A. Pichandi. 'Evaluation of optimal combination of planning parameters (field width, pitch, and modulation factor) in helical tomotherapy for bilateral breast cancer'. en. In: *J. Med. Phys.* 45.4 (Oct. 2020), pp. 234–239.

[78] G. De Kerf et al. 'Evaluation of the optimal combinations of modulation factor and pitch for Helical TomoTherapy plans made with TomoEdge using Pareto optimal fronts'. en. In: *Radiat. Oncol.* 10.1 (Sept. 2015), p. 191.

[79] R. Castriconi et al. 'Clinical implementation of knowledge-based automatic plan optimization for helical TomoTherapy'. en. In: *Pract. Radiat. Oncol.* 11.2 (Mar. 2021), e236–e244.

[80] P. G. Esposito et al. 'Knowledge-based automatic plan optimization for left-sided whole breast tomotherapy'. en. In: *Phys. Imaging Radiat. Oncol.* 23 (July 2022), pp. 54–59.

[81] Z. Liu et al. 'A deep learning method for prediction of three-dimensional dose distribution of helical tomotherapy'. en. In: *Med. Phys.* 46.5 (May 2019), pp. 1972–1983.

[82] X. Zhang et al. 'Helical tomotherapy to LINAC plan conversion utilizing RayStation Fallback planning'. In: *Journal of Applied Clinical Medical Physics* 18.1 (2017), pp. 178–185.

[83] Z. Yuan et al. 'Converting treatment plans from helical tomotherapy to L-shape Linac: clinical workflow and dosimetric evaluation'. In: *Technology in cancer research & treatment* 17 (2018), p. 1533033818785279.

Appendices

A Clinical Goals

Dose constraints are set as desired clinical goals for creating optimal treatment plans. Figure A.1, A.2 and A.3 show the clinical goals for patients with prescribed SIB of 55 Gy, 57.5 Gy, and both, respectively.

Priority	Dose	ROI/POI	Clinical goal
1	Plan dose: Cervix (14)...	CTVn1_55	At least 98.00 % volume at 55.00 Gy dose
1	Plan dose: Cervix (14)...	CTVn2_55	At least 98.00 % volume at 55.00 Gy dose
1	Plan dose: Cervix (14)...	CTVn3_55	At least 98.00 % volume at 55.00 Gy dose
2	Plan dose: Cervix (14)...	*SpinalCord*	At most 48.00 Gy dose at 0.03 cm^3 volume
3	Plan dose: Cervix (14)...	CTV_45	At least 99.50 % volume at 42.75 Gy dose
3	Plan dose: Cervix (14)...	PTV_45	At least 98.00 % volume at 42.75 Gy dose
3	Plan dose: Cervix (14)...	PTVn_55	At least 98.00 % volume at 49.50 Gy dose
4	Plan dose: Cervix (14)...	Bladder	At most 55.00 Gy dose at 0.03 cm^3 volume
4	Plan dose: Cervix (14)...	Bladder	At most 75.00 % volume at 40.00 Gy dose
4	Plan dose: Cervix (14)...	Bladder	At most 85.00 % volume at 30.00 Gy dose
4	Plan dose: Cervix (14)...	Body	At most 58.85 Gy dose at 0.03 cm^3 volume
4	Plan dose: Cervix (14)...	BowelBag	At most 55.00 Gy dose at 0.03 cm^3 volume
4	Plan dose: Cervix (14)...	FemoralHead_L	At most 50.00 Gy dose at 0.03 cm^3 volume
4	Plan dose: Cervix (14)...	FemoralHead_R	At most 50.00 Gy dose at 0.03 cm^3 volume
4	Plan dose: Cervix (14)...	Rectum	At most 55.00 Gy dose at 0.03 cm^3 volume
4	Plan dose: Cervix (14)...	Rectum	At most 85.00 % volume at 40.00 Gy dose
4	Plan dose: Cervix (14)...	Rectum	At most 95.00 % volume at 30.00 Gy dose
4	Plan dose: Cervix (14)...	xBody-PTVn	At most 48.20 Gy dose at 0.03 cm^3 volume
5	Plan dose: Cervix (14)...	BowelBag	At most 250.00 cm^3 volume at 40.00 Gy dose
5	Plan dose: Cervix (14)...	BowelBag	At most 500.00 cm^3 volume at 30.00 Gy dose
6	Plan dose: Cervix (14)...	xCTVp	At most 46.35 Gy dose at 0.03 cm^3 volume
7	Plan dose: Cervix (14)...	xBladder-PTVn	At most 47.30 Gy dose at 0.03 cm^3 volume
7	Plan dose: Cervix (14)...	xBowelBag-PTVn	At most 47.30 Gy dose at 0.03 cm^3 volume
7	Plan dose: Cervix (14)...	xRectum-PTVn	At most 47.30 Gy dose at 0.03 cm^3 volume

Table A.1: The clinical goals of treatment planning for LACC with prescribes dose 55 Gy to boost volumes.

Priority	Dose	ROI/POI	Clinical goal
1	Plan dose: Cervix (12)...	CTVn1_55	At least 98.00 % volume at 55.00 Gy dose
1	Plan dose: Cervix (12)...	CTVn1_57.5	At least 98.00 % volume at 57.50 Gy dose
1	Plan dose: Cervix (12)...	CTVn2_55	At least 98.00 % volume at 55.00 Gy dose
1	Plan dose: Cervix (12)...	CTVn2_57.5	At least 98.00 % volume at 57.50 Gy dose
2	Plan dose: Cervix (12)...	SpinalCord	At most 48.00 Gy dose at 0.03 cm³ volume
3	Plan dose: Cervix (12)...	CTV_45	At least 99.50 % volume at 42.75 Gy dose
3	Plan dose: Cervix (12)...	PTV_45	At least 98.00 % volume at 42.75 Gy dose
3	Plan dose: Cervix (12)...	PTVn_55	At least 98.00 % volume at 49.50 Gy dose
3	Plan dose: Cervix (12)...	PTVn_57.5	At least 98.00 % volume at 51.75 Gy dose
4	Plan dose: Cervix (12)...	Bladder	At most 57.50 Gy dose at 0.03 cm³ volume
4	Plan dose: Cervix (12)...	Bladder	At most 75.00 % volume at 40.00 Gy dose
4	Plan dose: Cervix (12)...	Bladder	At most 85.00 % volume at 30.00 Gy dose
4	Plan dose: Cervix (12)...	Body	At most 61.53 Gy dose at 0.03 cm³ volume
4	Plan dose: Cervix (12)...	BowelBag	At most 57.50 Gy dose at 0.03 cm³ volume
4	Plan dose: Cervix (12)...	FemoralHead_L	At most 50.00 Gy dose at 0.03 cm³ volume
4	Plan dose: Cervix (12)...	FemoralHead_R	At most 50.00 Gy dose at 0.03 cm³ volume
4	Plan dose: Cervix (12)...	Kidney_L	At most 5.00 Gy average dose
4	Plan dose: Cervix (12)...	Kidney_L	At most 10.00 Gy average dose
4	Plan dose: Cervix (12)...	Kidney_R	At most 5.00 Gy average dose
4	Plan dose: Cervix (12)...	Kidney_R	At most 10.00 Gy average dose
4	Plan dose: Cervix (12)...	Rectum	At most 57.50 Gy dose at 0.03 cm³ volume
4	Plan dose: Cervix (12)...	Rectum	At most 85.00 % volume at 40.00 Gy dose
4	Plan dose: Cervix (12)...	Rectum	At most 95.00 % volume at 30.00 Gy dose
5	Plan dose: Cervix (12)...	BowelBag	At most 250.00 cm³ volume at 40.00 Gy dose
5	Plan dose: Cervix (12)...	BowelBag	At most 500.00 cm³ volume at 30.00 Gy dose
6	Plan dose: Cervix (12)...	xCTVp	At most 46.35 Gy dose at 0.03 cm³ volume
7	Plan dose: Cervix (12)...	xBladder-PTVn	At most 47.30 Gy dose at 0.03 cm³ volume
7	Plan dose: Cervix (12)...	xBody-PTVn	At most 48.20 Gy dose at 0.03 cm³ volume
7	Plan dose: Cervix (12)...	xBowelBag-PTVn	At most 47.30 Gy dose at 0.03 cm³ volume
7	Plan dose: Cervix (12)...	xRectum-PTVn	At most 47.30 Gy dose at 0.03 cm³ volume

Table A.2: The clinical goals of treatment planning for LACC with prescribes dose 57.5 Gy to boost volumes.

Priority	Dose	ROI/POI	Clinical goal	Value
1	Plan dose: Cervix (15)...	CTVn1_57.5	At least 98.00 % volume at 57.50 Gy dose	98.70 %
1	Plan dose: Cervix (15)...	CTVn2_57.5	At least 98.00 % volume at 57.50 Gy dose	98.84 %
1	Plan dose: Cervix (15)...	CTVn3_57.5	At least 98.00 % volume at 57.50 Gy dose	98.69 %
2	Plan dose: Cervix (15)...	SpinalCord	At most 48.00 Gy dose at 0.03 cm^3 volume	42.69 Gy
3	Plan dose: Cervix (15)...	CTV_45	At least 99.50 % volume at 42.75 Gy dose	99.54 %
3	Plan dose: Cervix (15)...	PTV_45	At least 98.00 % volume at 42.75 Gy dose	98.28 %
3	Plan dose: Cervix (15)...	PTVn_57.5	At least 98.00 % volume at 51.75 Gy dose	98.16 %
4	Plan dose: Cervix (15)...	Bladder	At most 57.50 Gy dose at 0.03 cm^3 volume	60.56 Gy
4	Plan dose: Cervix (15)...	Bladder	At most 75.00 % volume at 40.00 Gy dose	82.03 %
4	Plan dose: Cervix (15)...	Bladder	At most 85.00 % volume at 30.00 Gy dose	95.45 %
4	Plan dose: Cervix (15)...	Body	At most 61.53 Gy dose at 0.03 cm^3 volume	64.26 Gy
4	Plan dose: Cervix (15)...	BowelBag	At most 57.50 Gy dose at 0.03 cm^3 volume	63.43 Gy
4	Plan dose: Cervix (15)...	FemoralHead_L	At most 50.00 Gy dose at 0.03 cm^3 volume	50.18 Gy
4	Plan dose: Cervix (15)...	FemoralHead_R	At most 50.00 Gy dose at 0.03 cm^3 volume	46.62 Gy
4	Plan dose: Cervix (15)...	Kidney_L	At most 5.00 Gy average dose	5.45 Gy
4	Plan dose: Cervix (15)...	Kidney_L	At most 10.00 Gy average dose	5.45 Gy
4	Plan dose: Cervix (15)...	Kidney_R	At most 5.00 Gy average dose	5.49 Gy
4	Plan dose: Cervix (15)...	Kidney_R	At most 10.00 Gy average dose	5.49 Gy
4	Plan dose: Cervix (15)...	Rectum	At most 57.50 Gy dose at 0.03 cm^3 volume	48.73 Gy
4	Plan dose: Cervix (15)...	Rectum	At most 85.00 % volume at 40.00 Gy dose	96.50 %
4	Plan dose: Cervix (15)...	Rectum	At most 95.00 % volume at 30.00 Gy dose	100.00 %
5	Plan dose: Cervix (15)...	BowelBag	At most 250.00 cm^3 volume at 40.00 Gy dose	293.38 cm^3
5	Plan dose: Cervix (15)...	BowelBag	At most 500.00 cm^3 volume at 30.00 Gy dose	576.48 cm^3
6	Plan dose: Cervix (15)...	xCTVp	At most 46.35 Gy dose at 0.03 cm^3 volume	52.82 Gy
7	Plan dose: Cervix (15)...	xBladder-PTVn	At most 47.30 Gy dose at 0.03 cm^3 volume	60.56 Gy
7	Plan dose: Cervix (15)...	xBody-PTVn	At most 48.20 Gy dose at 0.03 cm^3 volume	60.56 Gy
7	Plan dose: Cervix (15)...	xBowelBag-PTVn	At most 47.30 Gy dose at 0.03 cm^3 volume	49.80 Gy
7	Plan dose: Cervix (15)...	xRectum-PTVn	At most 47.30 Gy dose at 0.03 cm^3 volume	48.33 Gy

Table A.3: The clinical goals of treatment planning for LACC with prescribes dose 55 Gy and 57.5 Gy to boost volumes.

B Objective Functions

Figure B.1 presents a set of objective functions used for automatic planning of LACC with VMAT.

Function	Constraint	Dose	ROI	Description	Robust	Weight
Physical composite objective						
Uniform dose		Plan	CTVn1_57.5	Uniform dose 58.70 Gy		50.00
Uniform dose		Plan	CTVn2_57.5	Uniform dose 58.70 Gy		50.00
Uniform dose		Plan	CTVn3_57.5	Uniform dose 58.70 Gy		50.00
Uniform dose		Plan	xCTV!_45	Uniform dose 45.00 Gy		50.00
Min dose		Plan	CTVn1_57.5	Min dose 57.60 Gy		19101.00
Min dose		Plan	CTVn2_57.5	Min dose 57.60 Gy		11324.00
Min dose		Plan	CTVn3_57.5	Min dose 57.60 Gy		7651.00
Min dose		Plan	PTVn_57.5	Min dose 51.75 Gy		54353.00
Max dose		Plan	PTVn_57.5	Max dose 61.50 Gy		600.00
Min dose		Plan	PTV_45	Min dose 42.90 Gy		489684.00
Max dose		Plan	xPTV!_45	Max dose 47.20 Gy		2000.00
Max dose		Plan	xCTVp	Max dose 46.50 Gy		50.00
Dose fall-off		Plan	Body	Dose fall-off [H]57.50 Gy [L]29.00 Gy, Low dose distance 2.00 cm		200.00
Max dose		Plan	Body	Max dose 61.00 Gy		400.00
Max EUD		Plan	Body	Max EUD 8.11 Gy, Parameter A 2		3.00
Max dose		Plan	SpinalCord_PRV	Max dose 45.00 Gy		1000.00
Max dose		Plan	CaudaEquina	Max dose 48.00 Gy		1000.00
Max DVH		Plan	xRectum-PTVn	Max DVH 35.00 Gy to 50.00% volume		50.00
Max DVH		Plan	xRectum-PTVn	Max DVH 42.00 Gy to 22.00% volume		252.00
Max EUD		Plan	Rectum	Max EUD 26.51 Gy, Parameter A 2		10.00
Max DVH		Plan	xBladder-PTVn	Max DVH 35.00 Gy to 50.00% volume		103.00
Max DVH		Plan	xBladder-PTVn	Max DVH 25.00 Gy to 50.00% volume		5.00
Max EUD		Plan	Bladder	Max EUD 25.30 Gy, Parameter A 2		10.00
Max DVH		Plan	xBowelBag-PTVn	Max DVH 35.00 Gy to 7.00% volume		1452.00
Max EUD		Plan	xBowelBag org	Max EUD 10.79 Gy, Parameter A 2		10.00
Max dose		Plan	BowelBag	Max dose 57.40 Gy		1500.00
Max dose		Plan	FemoralHead_L	Max dose 45.00 Gy		10.00
Max dose		Plan	FemoralHead_R	Max dose 45.00 Gy		10.00
Max EUD		Plan	Kidney_L	Max EUD 2.70 Gy, Parameter A 1		1.00
Max EUD		Plan	Kidney_R	Max EUD 2.89 Gy, Parameter A 1		1.00
Dose fall-off		Plan	xPTV_Ring0-1.5cm	Dose fall-off [H]55.00 Gy [L]30.00 Gy, Low dose distance 1.50 cm		150.00

Table B.1: A set of objective functions used in optimisation process for generating automatic plans for LACC with VMAT.

C Dose Statistics for Target Volume Coverage

Dose statistics for target volumes were extracted from RayStation with a Python script. The dose coverage to the target volumes are evaluated in terms of the volume receiving a given percentage of a prescribed dose, in percentage. E.g. clinical goal for the PTV_45 is that at least 98 % volumes receives 42.75 Gy, which corresponds to 95 % of the prescribed dose. The fulfilment of corresponding clinical goals are presented in Figure C.1-C.10.

An example of the Excel sheets used for analysing the dose statistics/clinical goals defined in Figure **??**. Note that clinical goals may vary between patients due to their diagnosis, .. case and personalized treatment. In the following figures, the data is color coded: green if the clinical goal is fulfilled, red if not.

Patient 1	**Volume receiving prescribed isodose [%]**					
Plan name	CTV_45	PTV_45	PTVn_57.5	CTVn1_57.5	CTVn2_57.5	CTVn3_57.5
Reference plan	99,96	98,85	98,24	98,71	99,07	99,01
Plan 1	99,66	98,34	98,86	98,61	98,67	98,12
Plan 2	99,52	98,37	98,04	98,98	99,08	98,21
Plan 3	99,61	98,34	98,19	98,94	99,17	99,24
Plan 4**	99,65	98,42	98,18	99,13	99,42	98,91
Plan 5**	99,52	98,31	99,28	98,52	98,81	98,91
Plan 6	99,43	98,30	98,13	99,02	99,11	99,28
Plan 7	99,65	98,50	97,96	99,34	99,45	99,55
Plan 8	99,62	98,36	98,18	99,43	99,50	98,10
Plan 10 min	99,74	98,43	97,12	99,82	99,99	99,97
Plan 11**	99,48	98,10	98,25	98,43	98,85	98,82
Plan 12	99,55	98,16	97,77	98,39	99,23	98,33
Plan 13	99,39	98,22	98,17	99,34	99,33	99,68
Plan 14	99,61	98,14	97,78	97,81	99,34	97,76
Plan 15	99,54	98,28	98,16	98,70	98,84	98,69
Plan 16	99,38	98,18	97,98	98,53	98,97	98,82
Plan 17	99,58	98,41	97,96	98,78	99,37	99,06
Plan 18**	99,70	98,54	97,72	99,30	98,97	99,15
Plan 20 min	99,76	98,50	97,05	98,34	98,08	98,56

Table C.1: Clinical goals for target volumes for patient 1.

Plan name	**Volume receiving prescribed isodose [%]**							
	CTV_45	PTV_45	PTVn_57.5	CTVn1_57.5	CTVn2_57.5	CTVn3_57.5	CTVn4_57.5	CTVn5_57.5
Reference plan	99,94	98,83	98,45	99,10	99,08	99,34	99,63	98,72
Plan 1**	99,95	98,40	98,86	99,01	99,57	99,54	99,42	100,00
Plan 2	99,70	98,17	98,68	99,67	99,50	99,45	99,46	98,54
Plan 3	99,54	98,08	98,48	99,84	99,36	99,75	99,39	99,45
Plan 4	99,68	98,14	98,66	99,52	99,29	99,51	99,69	99,75
Plan 5	99,91	98,46	98,77	98,99	98,65	98,76	99,76	99,65
Plan 6	99,51	98,17	98,47	99,57	99,55	99,50	99,02	98,78
Plan 7	99,28	98,17	98,26	99,66	99,58	99,65	99,49	98,20
Plan 8**	99,36	98,15	98,30	99,46	99,49	99,19	99,29	98,55
Plan 10 min	99,86	98,15	98,74	99,71	98,40	99,95	99,98	99,92
Plan 11**	99,88	98,51	98,93	98,62	99,44	99,46	99,91	99,75
Plan 12	99,46	98,10	99,00	99,30	98,91	99,69	99,16	99,97
Plan 13	99,26	97,96	98,92	99,73	98,89	99,30	99,33	99,91
Plan 14	99,54	98,06	99,23	100,00	99,46	99,87	99,26	99,84
Plan 15	99,74	98,45	98,82	98,79	99,57	99,43	99,72	99,82
Plan 16	99,21	97,96	98,67	99,37	98,69	98,40	98,70	99,13
Plan 17	98,92	97,85	98,55	99,34	99,68	98,69	99,37	97,47
Plan 18**	99,37	98,22	98,28	98,73	98,80	98,76	98,14	98,02
Plan 20 min	99,68	98,03	98,80	99,85	99,50	98,74	99,48	99,60

Table C.2: Clinical goals for target volumes for patient 2.

Patient 3	**Volume receiving prescribed isodose [%]**							
Plan name	CTV_45	PTV_45	PTVn_55	PTVn_57.5	CTVn1_57.5	CTVn2_57.5	CTVn1_55	CTVn2_55
Reference plan	99,92	98,78	98,52	98,20	99,10	99,72	98,64	99,04
Plan 1**	99,66	98,38	99,62	99,30	99,69	99,25	99,24	99,67
Plan 2	99,58	98,24	98,18	98,46	98,14	99,07	97,62	98,79
Plan 3	99,74	98,33	98,25	98,35	98,00	99,31	97,96	99,29
Plan 4	99,65	98,48	98,28	98,46	99,14	99,09	98,13	99,44
Plan 5	99,58	98,38	99,91	99,24	99,58	98,53	99,20	99,87
Plan 6	99,65	98,33	98,50	98,48	98,80	99,00	98,34	98,79
Plan 7	99,72	98,54	98,43	98,31	97,96	99,07	99,01	99,01
Plan 8**	99,72	98,61	98,56	98,28	99,06	99,53	98,26	98,94
Plan 10 min	99,52	98,24	98,63	98,48	99,11	100,00	99,96	99,93
Plan 11**	99,53	98,30	99,32	99,19	99,50	99,09	98,82	98,56
Plan 12	99,57	98,22	98,47	98,88	98,16	99,07	98,29	98,26
Plan 13	99,50	98,25	98,44	98,43	99,21	99,34	98,02	99,10
Plan 14**	99,74	98,39	98,52	98,79	99,55	99,48	98,16	99,09
Plan 15	99,46	98,35	99,38	98,29	99,15	99,02	98,45	98,03
Plan 16	99,37	98,16	98,36	98,86	98,40	98,20	97,39	98,57
Plan 17	99,66	98,43	98,36	98,37	98,78	99,26	98,96	98,25
Plan 18	99,73	98,59	98,32	98,48	98,90	98,57	98,54	98,42
Plan 20 min	99,71	98,15	98,62	98,42	99,36	99,99	98,79	96,94

Table C.3: Clinical goals for target volumes for patient 3.

Patient 4	Volume receiving prescribed isodose [%]					
Plan name	CTV_45	PTV_45	PTVn_55	CTVn1_55	CTVn2_55	CTVn3_55
Reference plan	99,83	98,75	98,52	99,22	99,11	99,01
Plan 1**	99,86	98,26	99,64	99,10	99,70	99,96
Plan 2	99,64	97,98	98,55	98,50	99,46	96,70
Plan 3	99,54	97,96	98,51	98,51	99,38	99,31
Plan 4**	99,41	97,99	98,67	99,48	99,67	99,02
Plan 5	99,77	98,23	99,56	98,66	99,03	99,66
Plan 6	99,46	98,06	98,55	98,44	99,46	99,51
Plan 7	99,41	98,25	98,21	99,18	98,90	99,19
Plan 8	99,20	98,24	98,40	99,50	98,27	96,57
Plan 10 min	99,88	98,09	98,65	100,00	100,00	99,26
Plan 11**	99,77	98,09	99,39	99,55	99,53	99,06
Plan 12	99,67	97,95	98,77	99,54	99,82	96,68
Plan 13	99,75	98,05	98,83	98,77	99,89	98,89
Plan 14**	99,88	98,01	98,88	99,36	99,96	97,44
Plan 15	99,67	98,11	99,24	99,25	98,98	95,96
Plan 16	99,58	98,19	98,53	98,59	98,89	98,51
Plan 17	99,61	98,14	98,62	98,88	99,20	98,21
Plan 18	99,49	97,89	98,75	99,73	99,53	99,58
Plan 20 min	100,00	98,15	99,22	99,95	99,90	99,93

Table C.4: Clinical goals for target volumes for patient 4.

Patient 5	Volume receiving prescribed isodose [%]									
Plan name	CTV_45	PTV_45	PTVn_55	CTVn1_55	CTVn2_55	CTVn3_55	CTVn4_55	PTVn_57.5	CTVn1_57.5	CTVn2_57.5
Reference plan	99,95	98,88	98,42	99,36	98,88	98,73	99,16	98,2	99,18	99,59
Plan 1**	99,47	98,24	99,65	99	99	98,42	98,85	98,23	99,16	99,42
Plan 2	99,51	98,22	98,14	98,97	98,48	98,98	98,58	98,29	98,62	99,49
Plan 3	99,48	98,24	98,33	99,25	99,24	99,65	98,85	98,35	99,85	99,85
Plan 4**	99,61	98,38	98,62	99,61	99,58	99,72	98,97	98,64	99,91	99,98
Plan 5	99,43	98,45	99,55	98,57	99,22	98,14	98,84	98,55	98,91	99,32
Plan 6	99,68	98,5	98,14	98,8	98,91	99,06	98,86	98,27	98,64	99,58
Plan 7	99,68	98,36	98,38	99,27	99,27	99,03	98,93	98,34	99,21	99,28
Plan 8	99,85	98,46	98,42	99,35	99,34	99,44	99,44	98,28	99,52	99,09
Plan 10 min	99,95	98,42	98,38	99,9	99,94	100	100	98,57	100	98,8
Plan 11**	99,31	98,12	99,47	98,69	99,07	97,97	98,39	98,57	98,53	99,16
Plan 12	99,56	98,36	98,64	98,78	99,05	98,28	98,37	98,37	98,09	99,85
Plan 13	99,6	98,26	98,34	99,49	98,58	98,43	99,17	98,41	98,55	99,6
Plan 14**	99,63	98,3	98,45	99,03	99,23	98,21	99,08	98,54	98,99	99,49
Plan 15	99,43	98,3	99	98,57	98,85	98,04	97,62	98,48	98,39	99,48
Plan 16	99,55	98,26	98,44	99,08	98,91	98,76	98,31	98,23	98,25	99,69
Plan 17	99,59	98,34	98,35	99,58	98,84	98,72	99,12	98,36	98,69	99,19
Plan 18	99,78	98,5	98,25	99,33	99,14	98,67	98,71	98,15	97,24	99,02
Plan 20 min	99,57	98,19	97,45	97,86	97,77	98,42	95,68	98,4	99,97	98,99

Table C.5: Clinical goals for target volumes for patient 5.

Patient 6	Volume receiving prescribed isodose [%]					
Plan name	CTV_45	PTV_45	PTVn_57.5	CTVn1_57.5	CTVn2_57.5	CTVn3_57.5
Reference plan	99,98	98,77	98,05	98,50	98,62	99,02
Plan 1**	99,52	98,28	98,34	98,97	98,42	99,16
Plan 2	99,69	98,43	98,27	99,24	99,00	99,23
Plan 3	99,65	98,35	98,39	99,74	99,30	99,40
Plan 4**	99,76	98,48	98,80	100,00	100,00	99,65
Plan 5	99,46	98,30	98,45	98,64	98,32	98,87
Plan 6	99,77	98,50	98,32	99,36	99,10	99,21
Plan 7	99,70	98,43	98,37	99,10	98,72	99,31
Plan 8	99,71	98,46	98,44	99,54	99,15	99,46
Plan 10 min	99,93	98,41	98,22	98,10	99,72	99,12
Plan 11	99,30	98,10	98,41	99,03	98,40	99,06
Plan 12	99,39	98,19	98,15	99,09	98,77	98,92
Plan 13	99,52	98,32	98,19	98,78	99,13	98,92
Plan 14	99,69	98,41	98,45	99,33	98,46	99,58
Plan 15**	99,27	98,22	98,19	98,86	98,49	98,91
Plan 16	99,36	98,18	97,98	98,71	98,82	99,06
Plan 17	99,52	98,32	98,19	98,78	99,13	98,92
Plan 18**	99,65	98,36	98,02	98,74	99,14	98,74
Plan 20 min	99,73	98,09	98,06	97,74	94,39	97,63

Table C.6: Clinical goals for target volumes for patient 6.

Patient 7	Volume receiving prescribed isodose [%]				
Plan name	CTV_45	PTV_45	PTVn_57.5	CTVn1_57.5	CTVn2_57.5
Reference plan	99,85	98,80	98,32	98,82	98,98
Plan 1	99,75	98,32	99,64	98,95	98,92
Plan 2	99,77	98,34	98,30	99,39	99,14
Plan 3	99,85	98,34	98,38	99,02	99,05
Plan 4**	99,77	98,25	98,35	99,13	99,06
Plan 5**	99,69	98,36	99,63	99,14	99,06
Plan 6	99,75	98,43	98,34	99,29	99,25
Plan 7	99,69	98,32	98,10	99,14	98,71
Plan 8	99,73	98,36	98,24	99,09	98,95
Plan 10 min	99,90	98,34	98,67	99,87	99,65
Plan 11**	99,69	98,32	99,16	99,53	98,57
Plan 12	99,62	98,16	98,45	98,88	98,91
Plan 13	99,68	98,17	98,44	98,82	98,51
Plan 14**	99,79	98,27	98,49	98,37	98,85
Plan 15	99,64	98,31	99,09	99,28	99,07
Plan 16	99,71	98,42	98,54	98,95	98,73
Plan 17	99,76	98,33	98,21	98,74	98,71
Plan 18	99,75	98,45	98,40	98,87	99,15
Plan 20 min	99,90	98,37	98,74	99,07	99,28

Table C.7: Clinical goals for target volumes for patient 7.

Patient 8	Volume receiving prescribed isodose [%]						
Plan name	CTV_45	PTV_45	PTVn_55	CTVn1_55	CTVn2_55	PTVn_57.5	CTVn1_57.5
Reference plan	99,93	98,73	98,53	98,60	98,75	98,14	98,30
Plan 1**	99,54	98,38	98,35	98,10	98,51	98,51	98,77
Plan 2	99,35	98,15	98,50	99,09	98,91	98,19	99,43
Plan 3	99,47	98,33	98,64	99,07	99,14	98,35	99,50
Plan 4	99,55	98,30	98,54	99,43	99,12	98,10	99,31
Plan 5	99,27	98,25	98,60	98,47	98,24	98,59	99,39
Plan 6	99,43	98,30	98,56	99,23	98,84	98,33	99,11
Plan 7**	99,54	98,51	98,73	99,19	98,98	98,25	99,21
Plan 8	99,54	98,59	98,66	99,20	99,00	98,50	97,93
Plan 10 min	99,94	98,13	99,17	99,90	99,77	99,24	99,68
Plan 11**	99,13	98,11	99,07	99,60	99,22	98,32	98,99
Plan 12	98,99	98,06	98,47	98,54	99,01	97,97	99,27
Plan 13	99,31	98,23	98,60	98,58	98,85	98,17	98,87
Plan 14	99,52	98,21	98,64	99,00	97,83	98,08	99,14
Plan 15	99,03	98,03	98,88	99,27	99,18	98,35	99,14
Plan 16	99,13	98,14	98,66	99,03	99,02	98,55	99,34
Plan 17**	99,36	98,34	98,53	98,81	98,82	98,12	98,87
Plan 18	99,37	98,33	98,66	99,15	98,34	98,54	99,25
Plan 20 min	100,00	97,91	99,22	99,79	100,00	99,92	99,72

Table C.8: Clinical goals for target volumes for patient 8.

Patient 9	**Volume receiving prescribed isodose [%]**			
Plan name	CTV_45	PTV_45	PTVn_57.5	CTVn1_57.5
Reference plan	99,99	98,96	98,26	98,01
Plan 1	99,86	98,17	100,00	100,00
Plan 2	99,53	97,94	98,34	98,60
Plan 3	99,42	97,97	97,87	98,55
Plan 4**	99,54	98,21	98,32	99,94
Plan 5**	99,86	98,30	100,00	100,00
Plan 6	99,52	98,11	97,89	97,68
Plan 7	99,59	98,26	98,15	98,42
Plan 8	99,66	98,22	98,12	99,36
Plan 10 min	99,73	98,28	98,67	99,87
Plan 11**	99,85	97,85	100,00	100,00
Plan 12	99,72	97,86	99,74	99,99
Plan 13	99,73	97,81	98,97	99,32
Plan 14	99,69	97,83	98,58	99,48
Plan 15	99,93	97,99	99,96	100,00
Plan 16	99,62	97,66	99,35	99,71
Plan 17	99,46	97,68	98,46	99,63
Plan 18**	99,78	98,03	98,26	99,42
Plan 20 min	99,96	98,29	99,03	99,82

Table C.9: Clinical goals for target volumes for patient 9.

Patient 10	Volume receiving prescribed isodose [%]				
Plan name	CTV_45	PTV_45	PTVn_57.5	CTVn1_57.5	CTVn2_57.5
Reference plan	99,72	98,81	98,19	99,14	99,45
Plan 1	99,47	98,08	98,39	99,06	98,90
Plan 2	99,85	98,49	99,35	99,90	99,31
Plan 3	99,40	98,14	98,10	98,94	98,74
Plan 4	99,27	98,05	98,40	99,02	98,32
Plan 5**	99,80	98,42	99,68	99,40	98,58
Plan 6	99,37	98,07	98,17	98,86	98,52
Plan 7	99,41	98,21	98,23	98,63	98,00
Plan 8**	99,57	98,56	98,26	99,32	99,09
Plan 10 min	99,70	98,23	99,40	100,00	99,98
Plan 11**	99,69	98,20	99,51	99,80	98,48
Plan 12	99,45	98,05	98,93	99,84	99,18
Plan 13	99,58	98,22	98,59	99,58	97,64
Plan 14	99,57	98,17	98,25	99,49	98,61
Plan 15	99,66	98,15	99,62	99,44	97,28
Plan 16	99,37	98,11	98,51	99,31	98,25
Plan 17**	99,57	98,30	98,44	99,10	98,76
Plan 18	99,58	98,42	98,17	98,52	96,79
Plan 20 min	99,73	98,25	98,13	98,27	93,61

Table C.10: Clinical goals for target volumes for patient 10.

D Automatic Planning Script

The automatic planning script that was used on LACC patients in this master's project is available on request to Marit Funderud at the RT department at St. Olavs Hospital.

E Access to Treatment Plans

All treatment plans that were made for the 10 LACC patients in this master's project is available for review on request to Josefine Ståhl-Kornerup at the RT department at St. Olavs Hospital.

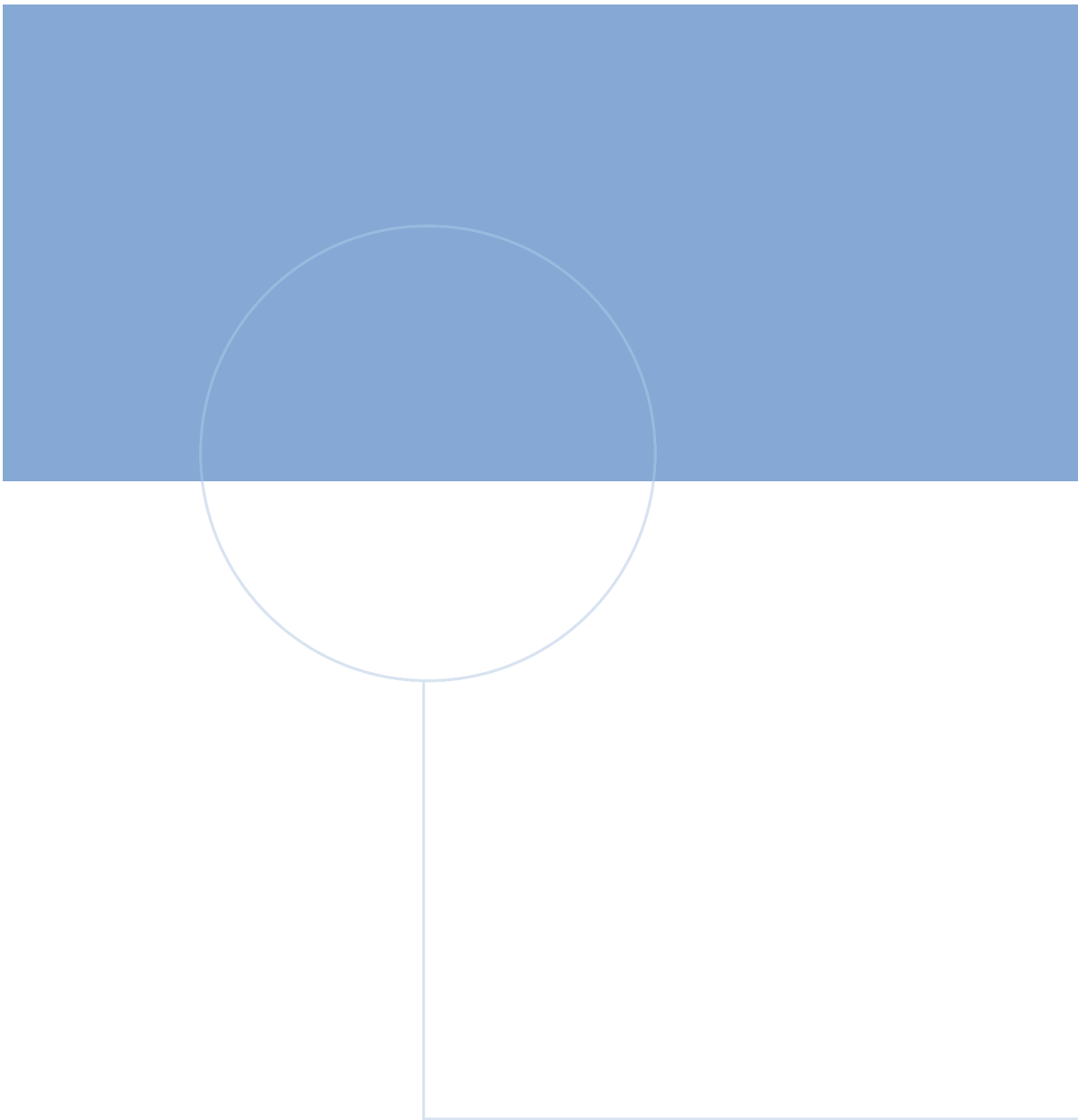

NTNU
Norwegian University of
Science and Technology

ST. OLAVS HOSPITAL
UNIVERSITETSSYKEHUSET I TRONDHEIM